

Involvement of mitogen activated kinase kinase 7 intracellular signalling pathway in Sunitinib-induced cardiotoxicity

Samantha Louise Cooper, Hardip Sandhu, Afthab Hussain, Christopher Mee and Helen Maddock

Accepted author manuscript deposited in Coventry University Repository

Original citation:

Cooper, S.L; Sandhu, H; Hussain, A; Mee, C. and Maddock, H. (2018) Involvement of mitogen activated kinase kinase 7 intracellular signalling pathway in Sunitinib-induced cardiotoxicity *Toxicology* (394) February, 72-83. DOI: 10.1016/j.tox.2017.12.005

<http://dx.doi.org/10.1016/j.tox.2017.12.005>

Elsevier

CC BY-NC-ND

Copyright © and Moral Rights are retained by the author(s) and/ or other copyright owners. A copy can be downloaded for personal non-commercial research or study, without prior permission or charge. This item cannot be reproduced or quoted extensively from without first obtaining permission in writing from the copyright holder(s). The content must not be changed in any way or sold commercially in any format or medium without the formal permission of the copyright holders.

1 **Involvement of mitogen activated kinase kinase 7 intracellular signalling pathway in**

2 **Sunitinib-induced cardiotoxicity**

3

4 Samantha Louise Cooper^{a,¶}, Hardip Sandhu^{a,¶}, Afthab Hussain^a, Christopher Mee^a, Helen
5 Maddock^{a,*}

6 ¶ shared first authorship

7

8 * Corresponding author: Prof. Helen Maddock

9 E-mail: helen.maddock@coventry.ac.uk

10 Phone: +44 2477 658 710

11

12 E-mail list:

13 Dr Samantha Louise Cooper: cooper87@uni.coventry.ac.uk

14 Dr Hardip Sandhu: hardip.sandhu@coventry.ac.uk

15 Dr Afthab Hussain: afthab.hussain@coventry.ac.uk

16 Dr Christopher Mee: christopher.mee@coventry.ac.uk

17

18 ^a Faculty Research Centre for Sport, Exercise and Life Sciences, Faculty of Health and Life
19 Sciences, Science & Health Building, 20 Whitefriars Street, Coventry, CV1 2DS, United
20 Kingdom

21

22 **Abbreviations:**

23 ASK1, apoptosis signal-regulating kinase 1; ASK2, apoptosis signal-regulating kinase 2;

24 DMSO, dimethyl sulphoxide; hERG, human ether-a-go-go-related gene; JNK, c-Jun N-

25 terminal kinase; MKK7, mitogen activated kinase kinase 7; MTT, 3-(4,5-dimethylthiazol-2-yl)-

26 2,5-diphenyltetrazolium bromide; NQDI-1, 2,7-dihydro-2,7-dioxo-3*H*-naphtho[1,2,3-

27 *de*]quinoline-1-carboxylic acid ethyl ester; TTC, 2,3,5-Triphenyl-2*H*-tetrazolium chloride.

28 **Abstract**

29 The tyrosine kinase inhibitor Sunitinib is used to treat cancer and is linked to severe adverse
30 cardiovascular events. Mitogen activated kinase kinase 7 (MKK7) is involved in the
31 development of cardiac injury and is a component of the c-Jun N-terminal kinase (JNK)
32 signal transduction pathway. Apoptosis signal-regulating kinase 1 (ASK1) is the upstream
33 activator of MKK7 and is specifically inhibited by 2,7-dihydro-2,7-dioxo-3*H*-naphtho[1,2,3-
34 *de*]quinoline-1-carboxylic acid ethyl ester (NQDI-1). This study investigates the role of ASK1,
35 MKK7 and JNK during Sunitinib-induced cardiotoxicity.

36
37 Infarct size were measured in isolated male Sprague-Dawley rat Langendorff perfused
38 hearts treated for 125 min with Sunitinib in the presence and absence of NQDI-1. Left
39 ventricular cardiac tissue samples were analysed by qRT-PCR for MKK7 mRNA expression
40 and cardiotoxicity associated microRNAs (miR-1, miR-27a, miR-133a and miR-133b) or
41 Western blot analysis to measure ASK1/MKK7/JNK phosphorylation.

42
43 Administration of Sunitinib (1 μ M) during Langendorff perfusion resulted in increased infarct
44 size, increased miR-133a expression, and decreased phosphorylation of the
45 ASK1/MKK7/JNK pathway compared to control. Co-administration of NQDI-1 (2.5 μ M)
46 attenuated the increased Sunitinib-induced infarct size, reversed miR-133a expression and
47 restored phosphorylated levels of ASK1/MKK7/JNK. These findings suggest that the
48 ASK1/MKK7/JNK intracellular signalling pathway is important in Sunitinib-induced
49 cardiotoxicity. The anti-cancer properties of Sunitinib were also assessed using the 3-(4,5-
50 dimethylthiazol-2-yl)-2,5-diphenyltetrazolium bromide (MTT) cell viability assay. Sunitinib
51 significantly decreased the cell viability of human acute myeloid leukemia 60 cell line (HL60).
52
53 The combination of Sunitinib (1 nM - 10 μ M) with NQDI-1 (2.5 μ M) enhanced the cancer-
54 fighting properties of Sunitinib. Investigations into the ASK1/MKK7/JNK transduction
55 pathway could lead to development of cardioprotective adjunct therapy, which could prevent
Sunitinib-induced cardiac injury.

56

57 **Keywords:**

- 58 – drug-induced cardiotoxicity
- 59 – tyrosine kinase inhibitor
- 60 – Sunitinib
- 61 – mitogen activated kinase kinase 7
- 62 – novel adjunct therapy
- 63 – ASK1 inhibitor 2,7-dihydro-2,7-dioxo-3*H*-naphtho[1,2,3-*de*]quinoline-1-
- 64 carboxylic acid ethyl ester

65

66 **1. Introduction**

67 The tyrosine kinase inhibitor Sunitinib is used in the treatment of renal cell carcinoma and in
68 gastrointestinal stromal tumours (Faivre et al. 2007). Sunitinib prevents tumour cell survival
69 and angiogenesis by inhibiting a variety of growth factor and cytokine receptors, including
70 platelet derived growth factor receptors, vascular endothelial growth factor receptors and
71 proto-oncogenes c-Kit and RET. However, Sunitinib unfortunately is also associated with a
72 lack of kinase selectivity resulting in the cardiotoxic adverse effects (Force et al. 2007). In
73 the clinic, Sunitinib causes QT prolongation (Bello et al. 2009), left ventricular dysfunction
74 (Shah and Morganroth 2015) and heart failure (Ewer et al. 2014). These findings are
75 consistent with many other successful chemotherapy agents linked with severe drug-induced
76 cardiotoxicity (Hahn et al. 2014), including electrophysiological changes and left ventricular
77 dysfunction which can cause heart failure in some patients (Aggarwal et al. 2013).
78 Intracellular studies using animals have revealed that Sunitinib causes mitochondrial injury
79 and cardiomyocyte apoptosis through an increase in caspase-9 and cytochrome C release in
80 both mice and in cultured rat cardiomyocytes (Chu et al. 2007). Other indicators of
81 apoptosis, such as an increase in caspase-3/7, have also been detected after Sunitinib
82 treatment in rat myocytes (Hasinoff et al. 2008).

83

84 MKK7 is a member of the mitogen-activated protein kinase kinase super family, which allows
85 the cell to respond to exogenous and endogenous stimuli (Foltz et al. 1998), and furthermore
86 MKK7 has shown to demonstrate a key role in protecting the heart from hypertrophic
87 remodelling, which occurs via cardiomyocyte apoptosis and heart failure (Liu et al. 2011).

88 The MKK7 activation of JNK results in many cellular processes including: proliferation,
89 differentiation and apoptosis (Chang and Karin 2001; Schramek et al. 2011; Sundarajan et
90 al. 2003), and JNK signalling is vital for the maintenance and organisation of the
91 cytoskeleton and sarcomere structure in cardiomyocytes (Windak et al. 2013). Interestingly,
92 Sunitinib is an ATP analogue and competitively inhibits the ATP binding domain of its target
93 proteins (Roskoski 2007; Shukla et al. 2009). MKK7 also contains a highly conserved ATP
94 binding domain (Song et al. 2013). It is possible that Sunitinib binds as a ligand in the MKK7
95 ATP binding pocket, and thereby Sunitinib inhibits the MKK7/JNK transduction pathway, and
96 as a result this could potentially cause myocardial injury. It is important to determine the
97 relationship between MKK7 expression and Sunitinib induced cardiotoxicity by measuring
98 the alteration of MKK7 mRNA and phosphorylated MKK7 levels in the presence of Sunitinib.
99 Unravelling the relationship between Sunitinib and MKK7 could lead to a greater
100 understanding of its off-target mechanism of action and lead to the improvement in the
101 development of future drug discovery programmes or novel cardioprotective adjunct
102 therapies.

103

104 Short non-coding RNA microRNAs carry out the negative regulation of mRNA transcripts by
105 repressing translation (Bagga et al. 2005). Specific microRNAs expression patterns have
106 been linked to cardiomyocyte differentiation and in response to stress (Babiarz et al. 2012)
107 and have also been shown to be differentially expressed during the development of heart
108 failure (Thum et al. 2007). The microRNAs miR-1, miR-27a, miR-133a and miR-133b
109 produce differential expression patterns during the progression of heart failure (Akat et al.

110 2014; Tijssen et al. 2012). It is important to identify microRNA expression profiles in response
111 to drug-induced cardiotoxicity as similar patterns in microRNA expression to those identified
112 during heart failure may indicate the early onset of cardiotoxicity at a molecular level.

113
114 As MKK7 has no direct inhibitor, we have chosen to look at the upstream kinase ASK1
115 linked to MKK7 activation (Ichijo et al. 1997). ASK1 is activated in response to oxidative
116 stress-induced cardiac vascular endothelial growth factor suppression in the heart (Nako et
117 al. 2012). Izumiya et al. 2003 used ASK1 deficient transgenic mice to assess the role of
118 ASK1 in angiotensin II induced hypertension and cardiac hypertrophy. Both the wild type and
119 ASK1 deficient mice developed hypertension when stimulated with angiotensin II, however,
120 the ASK1 deficient mice lacked cardiac hypertrophy and remodelling and activation of ASK1,
121 p38 and JNK was severely attenuated, thus emphasising the importance of ASK1 in cardiac
122 hypertrophy and remodelling signalling (Izumiya et al. 2003). ASK1 is selectively inhibited by
123 NQDI-1 with high specificity with a K_i of 500nM and IC_{50} of 3 μ M (Volynets et al. 2011),
124 however, as this is a relatively new drug, a complete pharmacological profile has not yet
125 been fully characterised. ASK1 inhibition has previously been shown to offer protection
126 against ischemia reperfusion injury (Toldo et al. 2012) and has also been shown to suppress
127 the progression of ventricular remodelling and fibrosis in hamsters expressing severe
128 cardiomyopathy phenotypes (Hikoso et al. 2007). These findings highlight the potential of
129 NQDI-1 as a valuable asset to inhibit cardiac injury via the ASK1/MKK7/JNK pathway.

130
131 This novel study investigated the involvement of the ASK1/MKK7/JNK pathway in the
132 Sunitinib-induced cardiotoxicity via the assessment of cardiac function and infarct in
133 conjunction with relevant intracellular signalling mediators. Furthermore, we assessed the
134 anti-cancer properties of Sunitinib and determined whether co-administration of Sunitinib
135 with NQDI-1 affected the anti-cancer/apoptotic effect of Sunitinib in HL60 cells.

136

137 **2. Materials and Methods**

138 **2.1. Main reagents and kits**

139 Sunitinib malate and NQDI-1 were purchased from Sigma Aldrich (UK). Both drugs were
140 dissolved in dimethyl sulphoxide (DMSO) and stored at -20 °C. Krebs perfusate salts were
141 from either VWR International (UK) or Fisher Scientific (UK). Total ASK1 (Catalogue no
142 ab131506) was purchased from Abcam (UK). Phospho-ASK1 (Thr 845) (Catalogue no
143 3765S), Phospho-MKK7 (Ser271/Thr275) (Catalogue no 4171S), Total MKK7 (Catalogue no
144 4172S), Phospho-SAPK/JNK (Thr183/Tyr185) (Catalogue no 9251), Total SAPK/JNK rabbit
145 mAb antibody (Catalogue no 9252), anti-rabbit IgG, HRP-linked antibody and anti-biotin,
146 HRP-linked antibody were purchased from Cell signalling technologies (UK). All the
147 primary antibodies were from a rabbit host, and MKK7 and JNK were monoclonal antibodies,
148 whereas ASK1 was polyclonal (all antibodies were validated by the manufacturers). The
149 Ambion MicroPoly(A)Puris kit, Ambion mirVana miRNA Isolation Kit and Reverse
150 Transcription Kit were from Life Technologies (USA). The mRNA primers and the Applied
151 Biosystems primers assays (U6, rno-miR-1, hsa-miR-27a, hsa-miR-133a, and hsa-miR-
152 133b) were purchased from Invitrogen (UK). The iTaq Universal SYBR Green Supermix was
153 purchased from BioRad (UK). The HL60 cell line were obtained from European Collection of
154 Cell Culture (UK) (catalogue no. 98070106).

156 **2.2. Animals**

157 Adult male Sprague-Dawley rats (300-350 g in body weight); were purchased from Charles
158 River UK Ltd (UK) and housed suitably. They received humane care and had free access to
159 standard diet according to the Guide for the Care and Use of Laboratory Animals published
160 by the US National Institute of Health (NIH Publication No. 85-23, revised 1996). Animals
161 were selected at random for all treatment groups and the collected tissue was blinded for
162 infarct size assessment. The experiments were performed following approval of the protocol
163 by the Coventry University Ethics Committee. All efforts were made to minimise animal
164 suffering and to reduce the number of animals used in the experiments. Rats were sacrificed

165 by cervical dislocation (Schedule 1 Home Office procedure). A total of 80 animals were used
166 for this study and the data from 68 rats were included, while data from 12 rats were excluded
167 from analysis due to the established haemodynamic exclusion criteria. A total of 16 animals
168 were included for Langendorff perfusion experiments per main groups (Control, Sunitinib,
169 Sunitinib+NQDI-1, and NQDI-1, where 6 of the animals were used for measurement of the
170 area of infarct and the area of risk and the left ventricular tissue from another 10 animals
171 was used for real time PCR and Western blot analysis). Furthermore, an additional 4
172 animals were used for Langendorff perfusion experiments with Sorbitol as a positive control
173 for p-MKK7 Western blot analysis. No animals were culled due to ill health.

2.3. Langendorff perfusion model

176 The hearts were rapidly excised after the rats were culled and placed into ice-cold Krebs
177 Henseleit buffer (118.5 mM NaCl, 25 mM NaHCO₃, 4.8 mM KCl, 1.2 mM MgSO₄, 1.2 mM
178 KH₂PO₄, 1.7 mM CaCl₂, and 12 mM glucose, pH7.4). The hearts were mounted onto the
179 Langendorff system and retrogradely perfused with Krebs Henseleit buffer. The pH of the
180 Krebs Henseleit buffer was maintained at 7.4 by gassing continuously with 95 % O₂ and 5 %
181 CO₂ and maintained at 37 ± 0.5 °C using a water-jacketed organ chamber. Each
182 Langendorff experiment was carried out for 145 minutes: a 20 minute stabilisation period
183 and 125 minutes of drug or vehicle perfusion in normoxic conditions. Hearts were included in
184 the study with a CF between 3.5-12.0 ml/g (weight of the rat heart) during the stabilisation
185 period. Sunitinib malate (1 µM) was administered throughout the perfusion period in the
186 presence or absence of NQDI-1 (2.5 µM).

187
188 The clinically relevant dose of 1 µM Sunitinib was chosen in line with previous studies by
189 (Henderson et al. 2013). Additionally, it has been reported that the plasma concentration of
190 Sunitinib has a C_{max} in the range of 0.5–1.4µM (Doherty et al. 2013). While, the dose of 2.5
191 µM NQDI-1 was chosen following a thorough literature review (Eaton et al. 2014; Song et al.

192 2015; Volynets et al. 2011). NQDI-1 is not yet used in the clinic, therefore a clinically relevant
1
2 193 dose has not been reported.

3
4 194
5
6 195 Langendorff perfused hearts treated with vehicle were analysed as the control group. The
7
8 196 hearts were then weighed and either stored at -20 °C for 2,3,5-triphenyl-2H-tetrazolium
9
10 197 chloride (TTC) staining or the left ventricular tissue was dissected free and immersed in
11
12 198 RNAlater from Ambion (USA) for qRT-PCR or snap frozen by liquid nitrogen for Western blot
13
14 199 analysis.

15
16
17
18 200

19 201 **2.4. Infarct size analysis**

22 202 Frozen whole hearts were sliced into approximately 2 mm thick transverse sections and
23
24 203 incubated in 0.1 % TTC solution in phosphate buffer (2 ml of 100 mM NaH₂PO₄·2H₂O and 8
25
26 204 ml of 100 mM NaH₂PO₄) at 37 °C for 15 minutes and fixed in 10% formaldehyde (Fisher
27
28 205 Scientific, UK) for 4 hours. The risk zone and infarct areas were traced onto acetate sheets.
29
30 206 The tissue at risk stained red and infarct tissue appeared pale. The acetate sheet was
31
32 207 scanned and ImageTool from UTHSCSA (USA) software was used to measure the area of
33
34 208 infarct and the area of risk. A ratio of infarct to risk size was calculated as a percentage for
35
36 209 each slice. An average was taken of all of the slices from each heart to give the percentage
37
38 210 infarct size of the whole heart. The mean of infarct to risk ratio for each treatment group and
39
40 211 the mean ± SEM was plotted as a bar chart. The infarct size determination was randomised
41
42 212 and blinded.

43
44
45
46
47 213

48 214 **2.5. Analysis of microRNA expression profiles**

50
51 215 The microRNA was isolated from left ventricular tissue using the *mirVana*[™] miRNA Isolation
52
53 216 Kit from Ambion (UK). The microRNA quantity and quality was measured by NanoDrop from
54
55 217 Nanoid Technology (USA). A total of 500 ng microRNA was reverse transcribed into cDNA
56
57 218 using primers specific for housekeeping reference RNA U6 snRNA and target microRNAs:
58
59 219 hsa-miR-155, hsa-miR-15a, hsa-miR-16-1, rno-miR-1, hsa-miR-27a, hsa-miR-133a or hsa-

220 miR-133b (please note all human hsa-miR assays are compatible with rat samples) from
221 Applied Biosystems (USA) using the MicroRNA Reverse Transcription Kit from Applied
222 Biosystems (USA) according to the manufacturer's instructions. The reverse transcription
223 quantitative PCR reaction was performed with the following setup: 16 °C for 30 min, 42°C for
224 30 min and 85 °C for 5 min and ∞ at 4°C. The qRT-PCR was performed using the TaqMan
225 Universal PCR Master Mix II (no UNG) from Applied Biosystems (USA) protocol on the 7500
226 HT Real Time PCR sequence detection system from Applied Biosystems (USA). A 20µl
227 reaction mixture containing 100 ng cDNA, specific primer assays mentioned above from
228 Applied Biosystems (USA) and the TaqMan Universal PCR Master Mix was used in the qRT-
229 PCR reaction in triplicates. A non-template control was included in all experiments. The real
230 time PCR reaction was performed using the program: 1) 2 minutes at 50°C, 2) 10 minutes at
231 95°C, 3) 15 seconds at 95°C, 4) 1 minute at 60°C. Steps 3) and 4) were repeated 40 times.

232
233 Analysis of qRT-PCR data of microRNAs were performed using the Ct values for U6 snRNA
234 as reference for the comparison of the relative amount of microRNAs (rno-miR-1, hsa-miR-
235 27a, hsa-miR-133a and hsa-miR-133b). The values of each of the microRNAs were
236 calculated to compare their ratios. The formula used was $X_0/R_0=2^{CTR-CTX}$, where X_0 is the
237 original amount of target microRNA, R_0 is the original amount of U6 snRNA, CTR is the CT
238 value for U6 snRNA, and CTX is the CT value for the target microRNAs (rno-miR-1, hsa-
239 miR-27a, hsa-miR-133a and hsa-miR-133b) (Sandhu et al. 2010). Averages of the Ct values
240 for each sample group (Control and Sunitinib treated hearts) and each individual primer set
241 were calculated, and bar charts were plotted with mean ± SEM. The mean of the control
242 group was set as 1 for all microRNAs.

243

244 **2.6. Measurement of MKK7 mRNA expression**

245 Total mRNA was extracted from left ventricular tissue using The Ambion MicroPoly(A)Purist
246 kit from Ambion (USA). Extracted mRNA was processed directly to cDNA by reverse
247 transcription using Reverse Transcription Kit from Applied Biosystems (USA) with the

248 respective primers for MKK7 (MKK7 forward primer: CCCCGTAAAATCACAAAGAAAATCC
249 and MKK7 reverse primer: GGCGGACACACACTCATAAACAGA) and GAPDH (GAPDH
250 Forward primer: GAACGGGAAGCTCACTGG and GAPDH Reverse primer:
251 GCCTGCTTCACCACCTTCT) according to the instructions from the manufacturer Invitrogen
252 (UK). The reverse transcription PCR reaction was performed with the following setup: 16 °C
253 for 30 minutes, 42°C for 30 minutes and 85 °C for 5 minutes. The qRT-PCR reactions were
254 performed with the iTaq Universal SYBR Green Supermix from BioRad (UK), GAPDH and
255 MKK7 mRNA primer sets on the 7500 HT Real Time PCR machine from Applied Biosystems
256 (USA) using the program: 1) 2 minutes at 50°C, 2) 10 minutes at 95°C, 3) 15 seconds at
257 95°C, 4) 1 minute at 60°C. Steps 3) and 4) were repeated 40 times.

259 Analysis of qRT-PCR data of MKK7 mRNA were performed using the Ct values for GAPDH
260 mRNA as reference for the comparison of the relative amount of MKK7 mRNA. The value of
261 mRNA was calculated to compare the ratios using the formula $X_0/R_0=2^{CTR-CTX}$, where X_0 is
262 the original amount of target mRNA, R_0 is the original amount of GAPDH mRNA, CTR is the
263 CT value for GAPDH mRNA, and CTX is the CT value for the MKK7 mRNA (Sandhu et al.
264 2010). Averages of the Ct values for each sample group (control and Sunitinib treated
265 hearts) and each individual primer set were calculated, and bar charts were plotted with
266 mean \pm SEM. The mean of the control group was set as 1 for the MKK7 mRNA.

2.7. Western blot detection of ASK1, MKK7 and JNK

269 A total 45-55 mg of the frozen left ventricular tissue was lysed in lysis buffer (NaCl 0.1 M,
270 Tris base 10 μ M, EDTA 1 mM, sodium pyrophosphate 2 mM, NaF 2 mM, β -glycaophosphate
271 2 mM, 4-(2-Aminoethyl) benzenesulfonyl fluoride hydrochloride (0.1 mg/ml, 1/1.5 of protease
272 cocktail tablet) using a IKA Overtechnical T25homogeniser at 11,000 RPM. The
273 supernatants were measured for protein content using NanoDrop from Nanoid Technology
274 (USA). Then 80 μ g of protein was loaded to 4–15 % Mini-Protean TGX Gel from BioRad
275 (UK) and separated at 200 V for 60 minutes. After separation, the proteins were transferred

1
2
3
4
5
6
7
8
9
10
11
12
13
14
15
16
17
18
19
20
21
22
23
24
25
26
27
28
29
30
31
32
33
34
35
36
37
38
39
40
41
42
43
44
45
46
47
48
49
50
51
52
53
54
55
56
57
58
59
60
61
62
63
64
65

276 to the Bond-P polyvinylidene difluoride membrane from BioRad (UK) by using the Trans-Blot
277 Turbo transfer system from BioRad (UK) and probed for the phosphorylated forms
278 Phospho(Thr⁸⁴⁵)-ASK1 (p-ASK1), Phospho(Ser²⁷¹/Thr²⁷⁵)-MKK7 (p-MKK7) and
279 Phospho(Thr¹⁸³/Tyr¹⁸⁵) -SAPK/JNK (p-JNK), and total forms of ASK1(Thr⁸⁴⁵),
280 MKK7(Ser²⁷¹/Thr²⁷⁵) and JNK(Thr¹⁸³/Tyr¹⁸⁵). The p-MKK7 and p-JNK blots were stripped by
281 boiling and the PVDF membrane was used for total MKK7 and total JNK analysis,
282 respectively. According to recommendations from Cell signalling technologies (UK) total
283 ASK1 analysis had to be performed on a separate Western blot, as the stripping procedure
284 would remove total ASK1 protein. The relative changes in the p-ASK1, p-MKK7 and p-JNK
285 protein levels were measured and corrected for differences in protein loading as established
286 by probing for total ASK1, MKK7 and JNK respectively.

287
288 For Western blot analysis phosphorylated antibody levels were normalised to total antibody
289 levels in order to correlate for unequal loading of protein and differential blot transfer and to
290 identify the level of active vs inactive protein levels. Results were expressed as a percentage
291 of the density of phosphorylated protein relative to the density of total protein using Image
292 Lab 4.1 from BioRad (UK). The phosphorylated antibody levels determination was
293 randomised and blinded.

294 295 **2.8. MTT assay assessment of HL60 cell viability in the presence of Sunitinib with and** 296 **without NQDI-1**

297 The HL60 cell line were maintained in in RPMI 1640 medium supplemented with L-
298 Glutamine (2 mM) and 10 % heat-inactivated fetal bovine serum and antibiotics mix at 37 °C
299 in a humidified incubator under 5 % CO₂/95 % air. Cells were split in a 1:5 ratio every 2-3
300 days. Cells were incubated with Control, increasing concentrations of Sunitinib (1nM – 10
301 µM), Sunitinib (0.1 – 10 µM) + NQDI-1 (2.5 µM), or increasing concentrations of NQDI-1
302 (0.2-200 µM) for 24 h. Both Sunitinib and NQDI-1 were dissolved in DMSO. The DMSO
303 concentration was < 0.05 % (v/v) during the *in vitro* studies.

304

1
2 305 Cells were plated at a cell density of 10^5 cells/ml in 96-well plates and the above indicated
3
4 306 concentration of the drug was added. The plate was then incubated at 37°C for 24hrs. After
5
6 307 drug incubation, 50 μ l of MTT solution (5 mg MTT/ml H₂O) was added and the cells were
7
8 308 incubated for a further 24 h. Next, 50 μ l of DMSO was added to each well and mixed by
9
10
11 309 pipetting to release reduced MTT crystals from the cells. Relative cell viability was obtained
12
13 310 by scanning with an ELISA reader (Anthos Labtech AR 2001 Multiplate Reader, *Anthos*
14
15 311 *Labtec* Instruments, Austria) with a 490 nm filter. Results were expressed as a percentage of
16
17 312 viable cells relative to untreated cells/control. Experiments were performed in triplicates and
18
19 313 repeated ≥ 3 times.
20
21

22 314

24 315 **2.9. Statistical analysis**

26 316 Results are presented as mean \pm standard error of the mean (SEM). Significance of all data
27
28 317 sets was measured by one-way ANOVA analysis with the Tukey post hoc test using the
29
30 318 Matlab prism program. The following groups were compared during ANOVA analysis:
31
32 319 Control versus Sunitinib, Control versus Sunitinib and NQDI-1, Control versus NQDI-1 (all
33
34 320 statistically significant data compared to control marked with *), and Sunitinib versus
35
36 321 Sunitinib and NQDI-1 (all statistically significant data compared to Sunitinib marked with #).
37
38 322 For MKK7 mRNA some data was evaluated by using student's t-test. P-values <0.05 were
39
40 323 considered statistically significant.
41
42 324

43 324

46 325 **3. Results**

48 326 **3.1. Sunitinib treatment induces cardiac injury**

50
51 327 The effect of Sunitinib (1 μ M) administration on myocardial infarction development was
52
53 328 investigated by TTC staining. The hearts were stabilised for a period of 20 minutes, followed
54
55 329 by 125 minutes of drug perfusion. Administration of Sunitinib (1 μ M) for 125 minutes resulted
56
57
58 330 in a significant increase in infarct size compared with non-treated controls (Control: $7.81 \pm$
59
60 331 1.16 %; Sunitinib: 41.02 ± 1.23 %, $p < 0.001$) (Fig 1). This demonstrated that Sunitinib
61
62
63
64
65

332 treatment of the Langendorff perfused hearts results in a drastic increase in cardiac injury.

333 The infarct was globally distributed in all groups investigated in this study (i.e. Control,

334 Sunitinib ± NQDI-1, and NQDI-1).

335

336 **3.2. Sunitinib and NQDI-1 co-treatment alleviate cardiac injury**

337 The effect of ASK1 inhibition by NQDI-1 on cardiac function and infarction was investigated.

338 Co-administration of Sunitinib (1 µM) with NQDI-1 (2.5 µM) significantly decreased infarct

339 size compared to Sunitinib treated hearts (Sunitinib: 41.02 ± 1.23 %; Sunitinib + NQDI-1:

340 17.54 ± 2.97 %, $p < 0.001$). However, administration of NQDI-1 alone for 125 minutes of

341 perfusion significantly increased infarct size compared with control hearts (Control: $7.81 \pm$

342 1.16 %; NQDI-1: 16.68 ± 2.66 %, $p < 0.05$) (Fig 1).

343

344 **3.3. Sunitinib treatment modulates expression of microRNAs involved in cardiac**

345 **injury**

346 The expression of cardiac injury specific microRNAs during Sunitinib-induced cardiotoxicity

347 was determined by qRT-PCR assessment. The microRNAs miR-1, miR-27a, miR-133a and

348 miR-133b have been shown to produce differential expression patterns during the

349 progression of heart failure. The ratio of target microRNA normalised to U6 was set to 1 in

350 the control group for easier comparison of microRNA ratio values between the various drug

351 therapy groups. There was a significant increase in miR-133a when hearts were perfused

352 with Sunitinib (1 µM) compared to control hearts (Ratio of target microRNA normalised to U6

353 in Sunitinib treated hearts: miR-133a: 535.78 ± 61.27 , $p < 0.001$). Co-administration of NQDI-

354 1 (2.5 µM) along with Sunitinib reversed this miR-133a expression trend by decreasing the

355 miR-133a expression when compared to Sunitinib perfused hearts (Ratio of target microRNA

356 normalised to U6 in Sunitinib and NQDI-1 treated hearts: miR-133a: 52.76 ± 28.30 ,

357 $p < 0.001$). Hearts perfused with NQDI-1 alone showed an increase in miR-1, miR-27a and

358 miR-133b expression compared to control hearts (Ratio of target microRNA normalised to

359 U6 in NQDI-1 treated hearts: miR-1: 32.33 ± 16.47 , $p < 0.01$; miR-27a: 11.27 ± 2.86 , $p < 0.001$;

360 miR-133b: 167.85 ± 58.13 , $p < 0.001$). The expression of miR-1, miR-27a, miR-133a and
361 miR-133b was increased in the Sunitinib and NQDI-1 co-treated hearts when compared to
362 Sunitinib perfused hearts (miR-1: $p < 0.05$; miR-27a: $p < 0.001$; miR-133a: $p < 0.001$; miR-133b:
363 $p < 0.05$). (Fig 2 A-D).

364
365 The results from the microRNA qRT-PCR analysis show there is a similar expression pattern
366 for miR-1, miR-27 and miR-133b, while miR-133a has its own pattern. This indicates that the
367 cardiac injury induced by Sunitinib, which is alleviated by the ASK1 inhibitor NQDI-1, triggers
368 a complex alteration of these cardiac injury microRNAs. Further studies looking at the
369 altered expression profiles for these cardiac injury microRNAs have to be undertaken in
370 order to clarify the expression patterns.

371

372 **3.4. MKK7 mRNA expression profile is altered by ASK1 inhibitor NQDI-1**

373 As MKK7 contains an ATP binding domain (Song et al. 2013) and Sunitinib is an ATP
374 analogue and competitively inhibits the ATP binding domain of its target proteins (Roskoski
375 2007; Shukla et al. 2009). We therefore wanted to investigate the interaction between
376 Sunitinib and MKK7, and question whether Sunitinib could bind as a ligand in the ATP
377 binding pocket of MKK7. This would determine if Sunitinib might potentially have an
378 inhibitory effect on the MKK7/JNK pathway. The relationship between MKK7 expression and
379 Sunitinib-induced cardiotoxicity was assessed on transcriptional level by MKK7 mRNA qRT-
380 PCR analysis on Sunitinib (1 μ M) perfused hearts, and the interaction by ASK1 specific
381 inhibitor NQDI-1 was detected to highlight if any interaction between ASK1/MKK7 and
382 Sunitinib-induced alteration of MKK7 transcription due to cardiac injury was observed to
383 impact on mRNA levels. The ratio of MKK7 mRNA normalised to GAPDH was set to 1 in the
384 control group for easier comparison of GAPDH normalised MKK7 mRNA values between the
385 various drug therapy groups. The qRT-PCR analysis of MKK7 mRNA revealed that co-
386 administration of NQDI-1 with Sunitinib caused a significant increase in MKK7 mRNA
387 expression compared to Sunitinib treatment alone ($p < 0.01$) (Ratio of MKK7 mRNA

388 normalised to GAPDH. Sunitinib: 0.12 ± 0.03 ; Sunitinib + NQDI-1: 1.18 ± 0.65) (Fig 3). The
389 decrease in MKK7 mRNA observed in the Sunitinib (1 μ M) perfused hearts compared to
390 control hearts was not significant, but a clear trend was observed. If the data from groups
391 control and Sunitinib were compared using a Student's t-test the decline in MKK7 mRNA in
392 Sunitinib treated hearts was statistically significant with $p=0.0043$.

393
394 These MKK7 mRNA qRT-PCR results clearly demonstrate that Sunitinib treatment shows a
395 tendency to decrease the MKK7 mRNA, and co-administration of ASK1 specific inhibitor
396 NQDI-1 restores the MKK7 mRNA level observed in control treated heart. This could indicate
397 a complex regulation system where Sunitinib-induced cardiac injury is directly linked with the
398 ability of Sunitinib to reduce MKK7 expression at transcriptional level, which is counteracted
399 by the ASK1 specific inhibitor NQDI-1.

400

401 **3.5. ASK1/MKK7/JNK pathway is involved in Sunitinib-induced cardiotoxicity**

402 As explained in the previous MKK7 mRNA results section we wanted to investigate the
403 interaction between Sunitinib and MKK7, as they both interact via the ATP binding pocket.
404 The key question being if Sunitinib can bind as a ligand in the ATP binding pocket of MKK7
405 and if Sunitinib is able to block the MKK7/JNK pathway. Here we investigate the role of
406 cardiotoxic Sunitinib therapy on the ASK1/MKK7/JNK pathway phosphorylation and how the
407 interaction with the cardioprotective ASK1 specific agent NQDI-1 affects the
408 ASK1/MKK7/JNK pathway phosphorylation. Following Langendorff perfusion of Sunitinib and
409 NQDI-1, p-ASK1, p-MKK7 and p-JNK levels were measured in the left ventricular tissue of
410 the hearts by Western blot analysis.

411

412 Western blot analysis showed that Sunitinib treatment decreased p-ASK1, p-MKK7 and p-
413 JNK levels significantly when compared to control (density of phosphorylated protein
414 normalised to total protein: *p-ASK1*: Control: 389.43 ± 4.18 and Sunitinib: 16.47 ± 3.56 ,
415 $p<0.001$; *p-MKK7*: Control: 55.60 ± 4.86 and Sunitinib: 23.66 ± 4.53 , $p<0.001$; *p-JNK*:

1
2
3
4
5
6
7
8
9
10
11
12
13
14
15
16
17
18
19
20
21
22
23
24
25
26
27
28
29
30
31
32
33
34
35
36
37
38
39
40
41
42
43
44
45
46
47
48
49
50
51
52
53
54
55
56
57
58
59
60
61
62
63
64
65

416 Control: 43.66 ± 2.82 and Sunitinib: 22.52 ± 2.74 , $p < 0.001$). Co-administration with NQDI-1
417 increased the p-ASK1, p-MKK7 and p-JNK levels, and these were statistically significantly
418 elevated when compared to heart treated with Sunitinib monotherapy (density of
419 phosphorylated protein normalised to total protein: *p-ASK1*: Sunitinib + NQDI-1: $51.17 \pm$
420 3.66 , $p < 0.001$; *p-MKK7*: Sunitinib + NQDI-1: 38.11 ± 1.87 , $p < 0.05$; *p-JNK*: 48.95 ± 2.76 ,
421 $p < 0.001$). The p-ASK1, p-MKK7 and p-JNK levels were decreased in NQDI-1 treated hearts
422 compared to control hearts (density of phosphorylated protein normalised to total protein: *p-*
423 *ASK1*: NQDI-1: 20.56 ± 1.99 , $p < 0.01$; *p-MKK7*: NQDI-1: 18.40 ± 2.98 , $p < 0.001$; *p-JNK*: 28.78
424 ± 3.03 , $p < 0.01$) (Fig 4A-C).

425
426 These Western blot results show that Sunitinib decreased the phosphorylation of the
427 ASK1/MKK7/JNK pathway. The fact that Sunitinib was able to show a strong tendency of
428 decreasing the MKK7 mRNA highlights that the decreased MKK7 phosphorylation is
429 regulated at the transcriptional level, which is then affecting the post-transcriptional MKK7
430 phosphorylation levels. However, interestingly the cardiotoxic Sunitinib is having an inhibiting
431 effect throughout all three parts of the ASK1/MKK7/JNK pathway. Co-administration of
432 NQDI-1 is counteracting the Sunitinib inhibiting effect on the phosphorylation level
433 throughout the ASK1/MKK7/JNK pathway. These results show a clear indication of Sunitinib
434 interacting with ASK1, MKK7 and JNK at post-translational level and MKK7 gene expression
435 at pre-transcriptional level.

436 437 **3.6. Cancer cell viability in response to Sunitinib with and without NQDI-1**

438 The effect of Sunitinib on cell viability was examined in HL60 cells. The HL60 cells were
439 treated with Sunitinib for 24 hrs and then the level of mitochondrial metabolic-activity
440 inhibition was measured with the MTT assay. Sunitinib showed a pronounced decrease in
441 metabolic activity and a dose-dependent decrease in cell viability (Fig 5A). In particular,
442 Sunitinib significantly reduces cell viability at 1 nM (82.62 ± 6.55 %, $p < 0.05$), 0.1 μ M ($85.94 \pm$
443 3.80 %, $p < 0.05$), 0.5 μ M (83.94 ± 3.86 %, $p < 0.05$), 1 μ M (77.28 ± 6.58 %, $p < 0.05$), 5 μ M

444 (58.61 ± 4.44 % p<0.001) and 10 µM (47.14 ± 6.77 %, p<0.001) concentrations of Sunitinib.

445 The IC₅₀ value was 6.16 µM. All the concentrations of Sunitinib in the absence and presence
446 of NQDI-1 used during this study produced significant reductions in HL60 cell viability
447 compared to vehicle treatment.

449 The co-administration of NQDI-1 (2.5 µM) to increasing concentrations of Sunitinib (1 nM -
450 10 µM) enhanced the inhibition of mitochondrial metabolism shown by Sunitinib (Fig 5A).

451 Specifically, co-treatment of Sunitinib with NQDI-1 reduced cell viability at 1 µM (59.58 ±
452 6.30 %, p<0.001), 5 µM (36.62 ± 6.52 %, p<0.001) and 10 µM (15.10 ± 2.31 %, p< 0.001)

453 concentrations of Sunitinib compared to Sunitinib alone. The IC₅₀ value for Sunitinib plus
454 NQDI-1 was 1.76 µM.

456 Interestingly, increasing concentrations of NQDI-1 alone (0.2-200 µM) only significantly
457 reduced cell viability at very high concentrations. Reductions in cell viability were significant
458 at 100 µM (55.44 ± 12.39 %, p<0.05), 200 µM (33.15± 9.67 %, p<0.001) (Fig 5B). The IC₅₀
459 value for NQDI-1 produced by the MTT assay was 130.8 µM.

4. Discussion

4.1. Involvement of ASK1/MKK7/JNK in Sunitinib-induced cardiotoxicity

463 The occurrence heart failure associated with anti-cancer treatment has been investigated
464 extensively (Khakoo et al. 2008), however, the underlying mechanism of cardiotoxicity is still
465 unclear. Determining cellular pathways involved in Sunitinib-induced cardiotoxicity could help
466 to develop therapies which could prevent the potential development of heart failure
467 associated with Sunitinib treatment.

469 Data presented in this study confirms that Sunitinib causes drug-induced myocardial injury
470 via an increase in infarct size (Fig 1). We observed that infarct size increased from ~ 8 % in
471 Control hearts to ~ 41 % in hearts perfused with Sunitinib. This observation is in accordance

1 472 with our previous study, where we investigated the involvement of A3 adenosine receptor
2 473 activation during Sunitinib induced cardiotoxicity in perfused rat hearts (Sandhu et al. 2017).
3
4 474 Also, the injury induced by Sunitinib administration is very similar to ischemia/reperfusion
5
6 475 injury rats investigated by the same Langendorff model (Gharanei et al. 2013). The Control
7
8 476 rat hearts do suffer from minor infarct injury during the brief period it takes from sacrificing
9
10 477 the animal and perfusing the heart with the Krebs buffer during the Langendorff model. This
11
12 478 insult accounts for the ~ 8 % infarct size we observe in Control hearts. A dose of 1 μ M
13
14 479 Sunitinib increased the infarct to ~ 41 % in perfused heart, and this steady state blood
15
16 480 concentration of Sunitinib has been found in patients treated with Sunitinib (Henderson et al.
17
18 481 2013). As the rat hearts are physically much smaller than human hearts, the rat hearts may
19
20 482 have been more sensitive to the adverse effect of Sunitinib administration at the clinically
21
22 483 relevant dose of 1 μ M.
23
24
25
26

27 484
28
29 485 Other animal studies investigating Sunitinib-induced cardiotoxicity were linked to a significant
30
31 486 decrease in left ventricular function (Henderson et al. 2013; Mooney et al. 2015), and
32
33 487 interestingly left ventricular dysfunction has also been identified in patients undergoing
34
35 488 Sunitinib chemotherapy (Di Lorenzo et al. 2009). Also, Sunitinib has also been associated
36
37 489 with electrophysiological disturbances and an increased pro-arrhythmic relative risk of
38
39 490 developing QTc interval prolongation (Ghatalia et al. 2015; Schmidinger et al. 2008).
40
41 491 Several studies show that Sunitinib could potentially block human ether-a-go-go-related
42
43 492 gene (hERG) potassium channels and cause irregular contractions (Doherty et al. 2013; Guo
44
45 493 et al. 2013). The *in vitro* study by *Thijs et al.* 2015 investigated the effect of Sunitinib on the
46
47 494 contractile force measured during normal pacing or after simulated ischemia on isolated
48
49 495 human atrial trabeculae from patients awaiting coronary artery bypass graft and/or aorta
50
51 496 valve replacement. They showed that treatment with 81.3 nM Sunitinib did not attenuate the
52
53 497 recovery in contractile force of atrial cardiomyocytes after simulated ischemia and
54
55 498 reperfusion compared to vehicle treated atrial cardiomyocytes, and thus they concluded that
56
57 499 the development of heart failure in patients treated with Sunitinib could not be explained by
58
59
60
61
62
63
64
65

1 500 an acute cardiotoxic Sunitinib stimulation of cardiomyocytes. However, it should be noted
2 501 that they used a 12-times lower Sunitinib dose compared to what we have used in this study,
3
4 502 and thus they might have not used a dose of Sunitinib in the toxic range (Thijs et al. 2015).
5
6 503
7
8 504 Modulation of ASK1 and its downstream targets MKK7 and JNK have been shown to play
9
10 505 important roles in regulating cardiomyocyte survival, apoptosis, hypertrophic remodeling and
11
12 506 intracellular signalling associated with heart failure (Mitchell et al. 2006). Therefore, we
13
14 507 hypothesised that successful modulation of the ASK1/MKK7/JNK pathway would produce an
15
16 508 effective cardioprotective treatment against Sunitinib induced cardiotoxicity.
17
18
19
20 509

21
22 510 As we were interested in the ASK1/MKK7/JNK signalling pathway we targeted ASK1 with
23
24 511 NQDI-1. Administration of the ASK1 specific inhibitor NQDI-1 resulted in abrogation of the
25
26 512 some cardiotoxic effects of Sunitinib. This study therefore, demonstrates the potentially
27
28 513 pivotal role that this kinase and the related pathway could play in protecting the heart from
29
30 514 Sunitinib induced cardiotoxicity. These observations are in accordance with other studies
31
32 515 that have also implicated the involvement of ASK1 in cardioprotection in other mammalian
33
34 516 models (Boehm 2015; Hao et al. 2016; He et al. 2003). Furthermore, inhibition of ASK1 with
35
36 517 thioredoxin results in reduction of infarct size compared to ischemic/reperfusion control
37
38 518 hearts (Gerczuk et al. 2012; Huang et al. 2015; Zhang et al. 2007).
39
40
41

42 519
43
44 520 ASK1 signalling pathway is facilitated through two main routes: either (i) MKK4/7 and JNK,
45
46 521 or (ii) MKK3/6 and p38 (Ichijo et al. 1997). As mentioned in the introduction the study by
47
48 522 Izumiya *et al.* 2003 showed the importance of ASK1 during angiotensin II induced
49
50 523 hypertension and cardiac hypertrophy in mice, as ASK1 knockout mice failed to develop
51
52 524 cardiac hypertrophy and remodelling through both JNK and p38 (Izumiya et al. 2003). In
53
54 525 another study by Yamaguchi *et al.* 2003 knockout of ASK1 in mice was also linked to
55
56 526 cardioprotection through the JNK pathway, as coronary artery ligation or thoracic transverse
57
58 527 aortic constriction in ASK1 deficient hearts showed no morphological or histological defects.
59
60
61

528 Both left ventricular end-diastolic and end-systolic ventricular dimensions were increased
1
2 529 less than wild-type mice, and the decreases in fractional shortening in both experimental
3
4 530 models were less when compared with wild-type mice (Yamaguchi et al. 2003). However, in
5
6 531 a study by Taniike *et al.* 2008 when ASK1 knockout mice were subjected to mechanical
7
8 532 stress it resulted in exaggerated heart growth and hypertrophy development through p38
9
10 533 pathway (Taniike et al. 2008). It is worth noting that attenuation of ASK1 by NQDI-1 during
11
12 534 normoxic conditions and Sunitinib treatment could have affected the MKK3/6 and p38
13
14 535 signalling pathway, which would have led to the conflicting results that we observe during
15
16 536 our study: there was a significant reduction in infarct size when Sunitinib was administered in
17
18 537 the presence of the ASK-1 inhibitor NQDI-1, however administration of NQDI-1 alone also
19
20 538 increased the infarct size. The increase in infarct size with NQDI-1 was not as profound as
21
22 539 the increase observed with Sunitinib (Fig 1).

23
24
25
26 540
27
28 541 NQDI-1 is a recently discovered highly specific ASK1 inhibitor. In the presence of 25 μ M
29
30 542 NQDI-1 the residual activity of ASK1 is reduced to 12.5 % using the γ -32P-ATP *in vitro*
31
32 543 kinase assay model. By using the same assay model Volynets and colleagues determined
33
34 544 the residual activity of the tyrosine protein kinase fibroblast growth factor receptor 1 (FGFR1)
35
36 545 which was measured to be 44 % after 25 μ M NQDI-1 exposure (Volynets et al. 2011).
37
38 546 FGFR1 as a key component involved in *in vivo* cardiomyocyte proliferation during early
39
40 547 stage heart development (Mima et al. 1995). Furthermore, FGFR1 is an essential regulator
41
42 548 of coronary vascular development through Hedgehog signalling activation, which in the adult
43
44 549 heart leads to increased coronary vessel density (Lavine et al. 2006). It is therefore possible
45
46 550 that NQDI-1 is blocking FGFR1 directly in the treated hearts of our study and thereby
47
48 551 exerting a slight increase in infarct size compared to the control.
49
50

51
52
53 552
54
55 553 In addition, NQDI-1's specificity towards other kinases has yet to be determined. In particular
56
57 554 its homologue apoptosis signal-regulating kinase 2 (ASK2) may potentially be inhibited by
58
59 555 NQDI-1 (Hattori et al. 2009). Both ASK1 and ASK2 is expressed in the heart (Iriyama et al.
60
61

2009). ASK2 is only stable and active when it forms a heteromeric complex with ASK1. ASK2 mediate its stress response from the stable ASK1-ASK2 heteromeric complex platform through both JNK and p38 and induce apoptosis. Furthermore, ASK1 and AS2 are able to activate each other, and thus ASK1 assists ASK2 with ASK2 regulatory mechanisms in addition to stabilising and activating ASK2 (Takeda et al. 2007). It is therefore very likely that NQDI-1 will affect the ASK2 mediated signalling. Several studies by the team of Kataoka have revealed the involvement of ASK2 during hypertension, cardiac hypertrophy and remodelling development. They have shown that ASK2 deficient mice have a significantly higher blood pressure and increased left ventricular weight then wild type mice, with an underlying analysis revealing that perivascular and interstitial myocardial fibrosis was increased (Kataoka 2008, 2009, 2010, 2011). Therefore, the relatively small adverse effect of NQDI-1 administration on producing an increased infarct size could also be caused by the NQDI-1 effect through attenuated ASK2 signalling.

Further studies are required to unravel the underlying mechanisms associated with the cardiac tissue injury and haemodynamic responses observed upon NQDI-1 stimuli to assess if p38, FGFR1, and/or ASK2 are involved. Also, other concentration of NQDI-1 treatment of hearts should be investigated, as lower concentrations of NQDI-1 most likely would cause less cardiac adverse effects.

4.2. Profiling of cardiotoxicity linked microRNAs

MicroRNAs have been shown to have important roles in tissue formation and function in response to injury and disease. The microRNAs miR-1, miR-27a, miR-133a and miR-133b have been shown to produce differential expression patterns during the progression of heart failure (Akat et al. 2014; Tijssen et al. 2012). Here we investigate the altered expression profiles of microRNAs miR-1, miR-27a, miR-133a and miR-133b after Sunitinib-induced cardiotoxicity with or without the ASK1 inhibitor NQDI-1 (Fig 2A-D). To the best of our knowledge there are no other studies showing a significant altered expression of miR-1,

1
2 584 miR-27a, miR-133a and miR-133b after Sunitinib treatment. A reduction in hERG potassium
3
4 585 channels expression causes the delayed myocyte repolarisation attributed to a long QT
5
6 586 interval and interestingly the 3' untranslated region of hERG potassium channel transcripts
7
8 587 have a partial complimentary miR-133a target site (Xiao et al. 2007). The current study
9
10 588 shows an increase in miR-133a expression following Sunitinib treatment, which was
11
12 589 attenuated with NQDI-1 co-administration (Fig 2C). This could imply that miR-133a
13
14 590 overexpression inhibits the hERG potassium channel, which would have a negative impact
15
16 591 on the electrophysiological response (Xu et al. 2007). Over expression of miR-133a has also
17
18 592 been shown to have negative effects on cardiomyocyte proliferation and survival (Liu et al.
19
20 593 2008), which corroborates the results from the current study.

21
22 594
23
24 595 In the heart miR-1 and miR-133 maintain the heart beat rhythm by regulating the cardiac
25
26 596 conduction system (Kim 2013). Furthermore, miR-1 and miR-133 are downregulated during
27
28 597 cardiac hypertrophy in both mouse and human models. *In vitro* studies have shown that the
29
30 598 overexpression of miR-133 inhibits cardiac hypertrophy, whereas inhibition of miR-133
31
32 599 induces more pronounced hypertrophy (Care et al. 2007). In addition, a decreased in cardiac
33
34 600 expression of miR-133b is sufficient to induce hypertrophic gene expression (Sucharov et al.
35
36 601 2008). In support of these studies our analysis shows that the miR-133b expression is
37
38 602 increased during NQDI-1 mono-therapy and co-administration of Sunitinib and NQDI-1 (Fig
39
40 603 2C), thus protecting the heart against hypotrophy/cardiac damage development, which is the
41
42 604 same pattern as we observe in the infarct to risk analysis.

43
44 605
45
46 606 The miR-27a expression has been observed to downregulate FOXO-1 protein, a
47
48 607 transcription factor which regulates genes involved in the apoptotic response, cell cycle, and
49
50 608 cellular metabolism (Guttilla and White 2009). Moreover, miR-27a is downregulated in
51
52 609 coronary sinus samples of heart failure patients (Marques et al. 2016). The increase in miR-
53
54 610 27a expression in our study during NQDI-1 mono-therapy and co-administration of Sunitinib
55
56
57
58
59
60
61
62
63
64
65

611 and NQDI-1 (Fig 2B) support the findings from these studies as the link increased miR-27
612 expression to reduced apoptosis, which is what we observe in the infarct to risk analysis.

613

614 **4.3. Sunitinib treatment suppresses the ASK1/MKK7/JNK pathway**

615 **4.3.1. ASK1**

616 Western blot assessment of Sunitinib treated hearts showed a significant decrease in p-
617 ASK1 when compared to control perfused hearts, and this decrease in p-ASK1 levels was
618 abrogated with NQDI-1 co-administration. However, in p-ASK1 levels from hearts subjected
619 to Sunitinib and NQDI-1 co-administration were compared to control hearts we did observe a
620 significant increase in p-ASK1. Furthermore, NQDI-1 treated hearts had significantly
621 decreased p-ASK1 levels when compared to control hearts (Fig 4A).

622

623 ASK1 has multiple phosphorylation sites. The Akt/protein kinase B complex binds to and
624 phosphorylates Ser⁸³ of ASK1, resulting in the inhibition of ASK1-mediated apoptosis (Kim et
625 al. 2001), the 14-3-3 interacts with phosphorylated Ser⁹⁶⁷ of ASK1 to block the function of
626 ASK1 (Zhang et al. 1999), protein phosphatase 5 dephosphorylates Thr⁸⁴⁵ within the
627 activation loop of ASK1 and thereby inhibits ASK1-mediated apoptosis (Morita et al. 2001),
628 while Ser¹⁰³⁴ phosphorylation suppresses ASK1 proapoptotic function (Fujii et al. 2004).
629 ASK1 undergoes auto-phosphorylation at the Thr⁸⁴⁵ (Tobiome et al. 2002). It is possible that
630 auto-phosphorylation increased when Sunitinib was combined with NQDI-1, which led to the
631 increased levels of p-ASK1 identified by western blot analysis. In its inactive form, ASK1 is
632 complexed with thioredoxin (Saitoh et al. 1998). It has been proposed that auto-
633 phosphorylation at Thr⁸⁴⁵ is increased in response to H₂O₂ treatment, due to H₂O₂ preventing
634 thioredoxin from complexing with ASK1. This suggests that ASK1 activation is due to
635 oxidative stress (Tobiome et al. 2002). An increase in p-ASK1 could indicate increased
636 levels of oxidative stress, which potentially reduced cardiac function and generated a level of
637 infarct when NQDI-1 was administered alone compared to control.

638

1
2 639 Attenuation of ASK1 by the specific inhibitor NQDI-1 produces a protective role in the heart
3
4 640 compared to Sunitinib treatment alone. In this study we have focused on the ASK1 Thr⁸⁴⁵
5
6 641 phosphorylation site, however, in future studies it would be interesting to investigate the
7
8 642 ASK1 Ser⁹⁶⁷ phosphorylation, as phosphorylation at this site has been linked to
9
10
11 643 cytoprotection (Kim et al. 2009). Another interesting aspect would be to identify if NQDI-1 is
12
13 644 able to inhibit the ASK1 homologue ASK2 as indicated by Nomura *et al.* 2013 (Nomura et al.
14
15 645 2013) and establish the K_i and IC₅₀ values are.

16
17
18 646

19
20 647 ASK1 is also a key mediator of apoptotic signalling (Hattori et al. 2009; Ichijo et al. 1997) and
21
22 648 the team of Huynh *et al.* 2011 investigated the expression of ASK1 in tumours lysates from
23
24 649 mice bearing 06-0606 tumours treated with 40 mg/kg/day Sunitinib for 11 days (Huynh et al.
25
26 650 2011). Their study showed a significant increase in total ASK1 levels after Sunitinib
27
28 651 treatment compared to vehicle treated 06-0606 tumour expressing mice, however, in our
29
30 652 study the expression of total ASK1 levels in left ventricular coronary tissue did not differ in
31
32 653 hearts perfused with Sunitinib compared to vehicle treated hearts.

33
34
35
36 654

37 38 655 **4.3.2. MKK7**

39
40
41 656 We assessed MKK7 expression level at both transcriptional and post-translational levels in
42
43 657 hearts treated with Sunitinib with and without the upstream ASK1 inhibitor NQDI-1. There
44
45 658 was a strong tendency for MKK7 mRNA expression to be decreased in Sunitinib perfused
46
47 659 hearts compared to control, but without significance. The expression of MKK7 mRNA was
48
49 660 increased significantly in Sunitinib and NQDI-1 co-treated hearts compared to Sunitinib
50
51 661 perfused hearts, and NQDI-1 solo treatment did not alter the MKK7 mRNA expression
52
53 662 compared to control hearts (Fig 3). The p-MKK7 level was significantly decreased in
54
55 663 Sunitinib treated hearts when compared to control, and the p-MKK7 decrease is attenuated
56
57 664 by NQDI-1 co-administration. The p-MKK7 levels are significantly decreased in Sunitinib and
58
59
60
61
62
63
64
65

665 NQDI-1 co-treatment and NQDI-1 solo-treatment hearts compared to control hearts (Fig 4B).

666 We believe that this is the first study to investigate the expression of MKK7 after Sunitinib
667 therapy.

668

669 MKK7 has a vital role in protecting the heart from hypertrophic remodelling and
670 cardiomyocytes apoptosis during stress and therefore the transition into heart failure
671 (Mitchell et al. 2006). Studies by Liu *et al.* 2011 revealed the importance of MKK7 by
672 demonstrating that deprivation of MKK7 in cardiomyocytes provokes heart failure in mice
673 when exposed to pressure overload (Liu et al. 2011). In addition to this, it has been shown
674 that inhibition and specific knockout of MKK7 increases the sensitivity of hepatocytes to
675 tumour necrosis factor alpha-induced apoptosis (Jia et al. 2015). Treatment with Sunitinib in
676 rat hearts in the current study down regulates both mRNA and phosphorylated protein levels
677 of MKK7. These studies suggest an important role of MKK7 in the maintenance of heart
678 homeostasis and expression of associated genes are important during cardiac hypertrophy
679 and heart failure.

680

681 MKK7 contains an ATP binding domain which could be inhibited by the ATP analogue,
682 Sunitinib (Roskoski 2007; Shukla et al. 2009; Song et al. 2013). It is therefore possible that
683 Sunitinib has an inhibitory effect on the MKK7/JNK signal transduction pathway. With
684 reduced MKK7 activity demonstrating both an incline towards cardiomyocyte damage and a
685 reversal of anti-tumour effects of chemotherapy, it would be interesting to assess both the
686 changes in expression levels and levels of phosphorylated MKK7 during Sunitinib treatment
687 affecting the heart in future studies. It may therefore be possible to identify a link between
688 MKK7 expression and tyrosine kinase inhibitor-induced cardiotoxicity.

689

690 Co-treatment of Sunitinib and NQDI-1 increases the level of p-MKK7 to levels compared to
691 Sunitinib treated hearts, restoring them almost back to the p-MKK7 levels observed in
692 control hearts. This could suggest that phosphorylated MKK7 is required to maintain at a

1
2 694 stable level to prevent damage to the heart. To illustrate this upregulation of transforming
3 growth factor beta has been found in compensatory hypertrophy, myocardial remodelling
4 695 and heart failure (Rosenkranz 2004). However, if MKK7 is removed entirely from the JNK
5 pathway cardiomyocyte damage ensues (Liu et al. 2011). Tang *et al.* 2012 demonstrated
6 696 that by causing an upregulation of MKK7 in hepatoma cells with the treatment with Alpinetin
7 that by causing an upregulation of MKK7 in hepatoma cells with the treatment with Alpinetin
8 it was possible to arrest cells in the G₀/G₁ phase of the cell cycle. However, by inhibiting
9 697 MKK7 the anti-tumour effect of the delta-opioid receptor agonist cis-diammined
10 dichloridoplatinum was reversed (Tang et al. 2012). This suggests that by agonising MKK7 it
11 698 may be possible to both enhance anti-cancer properties of chemotherapy agents, as well as
12 limiting apoptosis as the cell cycle is arrested.
13 702

14 703

15 704 **4.3.3. JNK**

16 705 Administration of Sunitinib decreased the p-JNK levels significantly when compared to
17 706 control hearts, and this decrease was abrogated with NQDI-1 co-treatment. Treatment with
18 707 NQDI-1 however also decreased the p-MKK7 levels when compared to control perfused
19 708 hearts (Fig 4C).

20 709

21 710 Many JNK knock out models have been used to determine the role of JNK in the
22 711 development of cardiac dysfunction. Kaiser *et al.* 2005 demonstrated the importance of JNK
23 712 in ischemia-reperfusion injury. They showed that a reduction in JNK activity in the heart
24 713 resulted in a reduced level of cardiac injury and cellular apoptosis. The same study
25 714 demonstrated an increase in JNK activity by using mouse models overexpressing MKK7 in
26 715 the heart, and this caused a significant protection against ischemia-reperfusion injury (Kaiser
27 716 *et al.* 2005). This highlights the complexity of JNK signalling. In this study, a significant
28 717 decrease in JNK phosphorylation was identified when hearts were treated with Sunitinib. In
29 718 addition, NQDI-1 treatment had a tendency to increase in JNK phosphorylation. It has been
30 719 established that a reduction in JNK activation is associated with cardiac hypertrophy and
31 720 cardiovascular dysfunction (Pan et al. 2014). The reduction in JNK activation caused by the

1 721 treatment of Sunitinib could also explain the increased infarct size and irregularities found in
2 722 the haemodynamic data.

3
4 723

5
6 724 Our study contradicts some previous studies, for example Wang *et al.* 1998 investigated the
7
8 725 role of MKK7 in cardiac hypertrophy in neonatal myocytes (Wang et al. 1998). Transgenic
9
10 726 neonatal rat cardiomyocytes expressing wild type MKK7 and a constitutively active mutant of
11
12 727 MKK7 were created. This study demonstrated JNK specific activation by MKK7 and showed
13
14 728 the key role of the JNK pathway in cardiac hypertrophy as cells infected with the
15
16 729 constitutively active form of MKK7 adopted characteristic features of myocardial stress
17
18 730 (Wang et al. 1998).

19
20 731

21
22 732 The study by Fenton *et al.* 2010 looked at the expression of JNK in papillary cancer cells
23
24 733 with RET/PTC1 rearrangement treated with Sunitinib (Fenton et al. 2010). Sunitinib inhibited
25
26 734 proliferation of these RET/PTC1 subcloned papillary cancer cells, and furthermore inhibited
27
28 735 the JNK phosphorylation in the cytoplasm of the papillary cancer cells. In our study the
29
30 736 expression of p-JNK levels in left ventricular coronary tissue was also reduced in hearts
31
32 737 perfused with Sunitinib compared to vehicle treated hearts.

33
34 738

35
36 739 In summary, Sunitinib administration resulted in significant reduction in p-ASK1, p-MKK7 and
37
38 740 p-JNK levels, whilst NQDI-1 co-administration counteracted this increase. It is worth noting
39
40 741 that MKK7 is activated through phosphorylation at a special site at the C-terminal kinase
41
42 742 domain core called the "Domain for Versatile Docking" (DVD), which includes serine and
43
44 743 threonine sites (Wang et al. 2007). Sunitinib does not not discriminate between inhibition of
45
46 744 tyrosine kinases or serine-threonine kinases (Karaman et al. 2008). Therefore, Sunitinib
47
48 745 might potentially inhibiting serine-threonine kinases, however, it is much more likely that
49
50 746 Sunitinib inhibits tyrosine kinases as expected, resulting in the downstream inhibition of
51
52 747 ASK1, which then results in a downstream inhibition of MKK7 and JNK. However, more
53
54 748 detailed investigations into the pathway involvement are required to fully elucidate the
55
56
57
58
59
60
61

1
2 750 intracellular signalling pathways. In addition, the increase in p-ASK1, p-MKK7 and p-JNK
3 levels that we observe in the presence of both Sunitinib and NQDI-1, when compared to
4 751 Sunitinib perfused hearts, could be due to the fact that we only assessed the
5 phosphorylation of ASK1 at Thr⁸⁴⁵, however, it is possible that NQDI-1 blocks both Ser⁸³ and
6 752 Thr⁸⁴⁵ of ASK1, and further investigations of phosphorylation activity at both sides could
7 clarify this issue. This altered pattern in ASK1/MKK7/JNK pathway phosphorylation suggests
8 753 that Sunitinib has a direct effect on part of the ASK1/MKK7/JNK pathway.
9
10
11
12
13
14
15

16 756

18 757 **4.4. The anti-cancer properties of Sunitinib were enhanced by NQDI-1 treatment**

19
20
21 758 It is well established that Sunitinib achieves anti-tumour effects by inhibiting tyrosine kinases,
22 which have been over-expressed in cancer cells (Krause and Van Etten 2005). Sunitinib has
23 759 previously been shown to directly inhibit the survival and proliferation of a variety of cancer
24 cells, including leukaemia cells (Ilyas 2016).
25
26
27
28
29

30 762

31
32 763 We demonstrated a dose dependant decline in the cell viability of HL60 cells when treated
33 with Sunitinib (Fig 5A). This produced an IC₅₀ value of 6.16 µM. Our results are in line with
34 764 existing data on the anti-proliferative effect of Sunitinib on HL60 cells. Sunitinib has
35 previously been shown to reduce the level of HL60 cell survival in a dose dependant manor
36 765 using a cell-titre blue reagent proliferation assay. This produced an IC₅₀ value of 5.7 µM after
37 48 hrs of Sunitinib treatment (Ilyas 2016). Another group performed an MTT assay on a
38 766 variety of acute myelogenous leukaemia cell lines and found Sunitinib to have an IC₅₀ values
39 between 0.007-13 µM (Hu et al. 2008).
40
41
42
43
44
45
46
47
48
49

50 771

51
52 772 To investigate the anti-proliferative effect of inhibition of the MKK7 pathway, HL60 cells were
53 treated with Sunitinib in co-treatment with NQDI-1 and NQDI-1 alone (Fig 5A-B). NQDI-1 is a
54 773 selective inhibitor for ASK1, the upstream regulator of MKK7. Previous studies have shown
55 ASK1 to have a crucial role in a variety of organ systems. However, ASK1 has also been
56
57
58
59
60
61
62
63
64
65

1 776 shown to promote tumorigenesis in gastric cancer and promote the proliferation of cancer
2 777 cells in skin cancer (Hayakawa et al. 2012; Iriyama et al. 2009).

3
4 778
5
6 779 Inhibition of ASK1 with compound K811 has been shown to prevent cell proliferation in
7
8 780 gastric cancer cell lines and reduce the size of xenograft tumours (Hayakawa et al. 2012).

9
10 781 Recently, Luo et al. 2016, investigated the involvement of ASK1 during proliferation in
11
12 782 pancreatic tumour cell line PANC-1 (Luo et al. 2016). The knock-down of ASK1 in mice with
13
14 783 pancreatic tumours reduced tumour growth, suggesting that ASK1 has an important role in
15
16 784 pancreatic tumorigenesis. The same group also demonstrated a dose-dependent inhibition
17
18 785 of the PANC-1 cell line when cells were treated with NQDI-1 at concentrations of 10 and 30
19
20 786 μM . However, the inhibition of ASK1 did not increase levels of apoptosis.

21
22 787
23
24 788 We have shown that increasing concentrations of NQDI-1 (0.2-200 μM) significantly reduce
25
26 789 the level of viable HL60 cells at 100 and 200 μM . This could suggest that ASK1 is expressed
27
28 790 at different levels in different cell types as a higher concentration was required in HL60 cells
29
30 791 compared to PANC-1 cells. Interestingly, the increasing concentrations of Sunitinib with 2.5
31
32 792 μM NQDI-1 enhanced the level of Sunitinib induced a reduction in HL60 cell proliferation.
33
34 793 The reason for this is not yet clear and further investigation into this is required.

35
36 794
37
38 795 As mentioned before NQDI-1 blocks FGFR-1 (Volynets et al. 2011). In cancer cells FGFR1
39
40 796 inhibitors have shown to elicit direct anti-tumour effects. The FGFR-1 inhibitors being
41
42 797 investigated in clinical trials for their anti-tumour qualities effecting various cancer types
43
44 798 include AZD4547, BGJ398, Debio-1347 and dovitinib (Katoh 2016). The apoptotic effect of
45
46 799 NQDI-1 we are observing in HL60 cells can therefore be a direct consequence of FGFR-1
47
48 800 inhibition.

49
50 801
51
52 802 In conclusion, our study demonstrates the potential of NQDI-1 as a valuable asset to cardiac
53
54 803 injury through the ASK1/MKK7/JNK transduction pathway, which could potentially lead to

1 804 development of cardioprotective adjunct therapy during drug-induced cardiac injury. NQDI-1
2 805 was observed to be cardioprotective as it reduced the Sunitinib-induced infarct size, and
3
4 806 addition it increased the apoptotic effect of Sunitinib in HL60 cells. This could indicate that
5
6 807 NQDI-1 - or an optimised derivative - could potentially be used as cardioprotective adjunct
7
8 808 therapy in e.g. Sunitinib treated leukaemia patients, which would not only protect the
9
10
11 809 patients' hearts but also boost the anti-cancer abilities of Sunitinib.
12

13 810

15 811 **Funding**

17 812 This research did not receive any specific grant from funding agencies in the public,
18
19
20 813 commercial, or non-for-profit sectors.
21

22 814

24 815 **Conflict of interest**

26 816 All authors have no conflict of interest to declare.
27
28

29 817

31 818 **Acknowledgments**

33 819 The assistance and support from technicians at Coventry University Mr Mark Bodycote and
34
35 820 Mrs Bethan Grist is greatly appreciated.
36
37
38
39
40
41
42
43
44
45
46
47
48
49
50
51
52
53
54
55
56
57
58
59
60
61
62
63
64
65

821 **Figure legends**

1
2 822 **Figure 1: Infarct to whole heart ratio assessment.** The hearts were drug perfused with
3
4 823 Sunitinib and/or NQDI-1 for 125 min in an isolated Langendorff heart model. This establishes
5
6 824 that Sunitinib-induced cardiotoxicity is reduced by ASK1 inhibitor NQDI-1. Groups: Control,
7
8 825 Sunitinib (1 μ M), Sunitinib (1 μ M) and NQDI-1 (2.5 μ M), and NQDI-1 (2.5 μ M) (n=6 per
9
10 826 group). Groups were assessed for statistical significance at each time point using one-way
11
12 827 ANOVA. Control versus Sunitinib (***=P<0.001), Control versus Sunitinib+NQDI-1
13
14 828 (**=P<0.01), Control versus NQDI-1 (*=P<0.05), or Sunitinib vs Sunitinib+NQDI-1
15
16 829 (###=P<0.001).

17
18
19
20 830

21
22 831 **Figure 2: Cardiotoxicity linked microRNAs expression.** The effect of Sunitinib (1 μ M) and
23
24 832 the co-administration of ASK1 inhibitor, NQDI-1 (2.5 μ M), on the expression of cardiotoxicity
25
26 833 linked microRNAs following 125 minute drug perfusion in an isolated heart Langendorff
27
28 834 model. The qRT-PCR results are shown as the ratio of target microRNA normalised to U6
29
30 835 with control group microRNA ratio set as 1 of microRNAs A) miR-1, B) miR-27a, C) miR-
31
32 836 133a and D) miR-133b. The ratio of target microRNA normalised to U6 is presented on a log
33
34 837 scale. Groups: Control (n=6 for miR-1, miR-27a and miR-133a; n=5 for miR-133b), Sunitinib
35
36 838 (1 μ M) (n=6 for miR-1 and miR-27a; n=5 for miR-133a and miR-133b), Sunitinib (1 μ M) and
37
38 839 NQDI-1 (2.5 μ M) (n=6 for miR-1, miR-27a, miR-133a and miR-133b), and NQDI-1 (2.5 μ M)
39
40 840 (n=4 for miR-1, miR-27a, miR-133a and miR-133b). Groups were assessed for statistical
41
42 841 significance at each time point using one-way ANOVA. Control versus Sunitinib
43
44 842 (***=P<0.001), Control versus Sunitinib+NQDI-1 (*=P<0.05, **=P<0.01), Control versus
45
46 843 NQDI-1 (**=P<0.01, ***=P<0.001), or Sunitinib vs Sunitinib+NQDI-1 (#=p<0.05,
47
48 844 ###=P<0.001).

49
50
51
52 845

53
54
55 846 **Figure 3: MKK7 mRNA expression levels.** The qRT-PCR assessment of MKK7 mRNA
56
57 847 expression levels in an isolated heart Langendorff model. The qRT-PCR results are shown
58
59 848 as the ratio of MKK7 mRNA normalised to GAPDH with control group ratio set as 1. Groups:

1
2 850 Control (n=5), Sunitinib (1 μ M) (n=6), Sunitinib (1 μ M) and NQDI-1 (2.5 μ M) (n=3), and
3
4 851 NQDI-1 (2.5 μ M) (n=3). Groups were assessed for statistical significance at each time point
5
6 852 using one-way ANOVA. Control versus Sunitinib, Control versus Sunitinib+NQDI-1, Control
7
8
9 853 versus NQDI-1, or Sunitinib vs Sunitinib+NQDI-1 ($\#$ = p <0.05).

10
11 854 **Figure 4: ASK1/MKK7/JNK pathway western blot assessment.** A) p-ASK1, B) p-MKK7,
12
13 855 and C) p-JNK phosphorylation levels in an isolated heart Langendorff model. Sorbitol was
14
15 856 included as a positive control in p-MKK7 Western blot analysis (n=4). Groups: Control (n=6
16
17 857 for p-ASK1; n=4 for p-MKK7 and p-JNK), Sunitinib (1 μ M) (n=5 for p-ASK1; n=4 for p-MKK7
18
19 858 and p-JNK), Sunitinib (1 μ M) and NQDI-1 (2.5 μ M) (n=6 for p-ASK1; n=4 for p-MKK7 and p-
20
21 859 JNK) and NQDI-1 (2.5 μ M) (n=5 for p-ASK1; n=4 for p-MKK7 and p-JNK). Groups were
22
23 860 assessed for statistical significance at each time point using one-way ANOVA. Control
24
25 861 versus Sunitinib ($***$ = P <0.001), Control versus Sunitinib+NQDI-1 ($*$ = p <0.05), Control versus
26
27 862 NQDI-1 ($**$ = P <0.01; $***$ = P <0.001), or Sunitinib vs Sunitinib+NQDI-1 ($\#$ = p <0.05;
28
29 863 $###$ = P <0.001).

30
31 864
32
33
34
35 865 **Figure 5: HL60 cell viability.** HL60 cells (10^5 cells/ml) were incubated for 24 hours with
36
37 866 control or with increasing concentrations of A) Sunitinib (0.1 – 10 μ M) or Sunitinib (0.1 – 10
38
39 867 μ M) + NQDI-1 (2.5 μ M) or B) NQDI-1 (0.2 μ M – 200 μ M). Groups were assessed for
40
41 868 statistical significance at each time point using one-way ANOVA. Control versus Sunitinib
42
43 869 ($*$ = P <0.05 and $***$ = P <0.001), Control versus NQDI-1 ($*$ = P <0.05 and $***$ = P <0.001), or
44
45 870 Sunitinib vs Sunitinib+NQDI-1 ($###$ = p <0.001).

871 **References**

1 872

2 873 Aggarwal, S., Kamboj, J. and Arora, R. 2013. Chemotherapy-related cardiotoxicity. *Ther Adv*

3
4 874 *Cardiovasc Dis* 7, 87-98.

5
6
7 875 Akat, K.M., Moore-McGriff, D., Morozov, P., Brown, M., Gogakos, T., Correa Da Rosa, J.,

8
9 876 Mihailovic, A., Sauer, M., Ji, R., Ramarathnam, A., Totary-Jain, H., Williams, Z., Tuschl, T.

10
11 877 and Schulze, P.C. 2014. Comparative RNA-sequencing analysis of myocardial and

12
13 878 circulating small RNAs in human heart failure and their utility as biomarkers. *Proc Natl Acad*

14
15 879 *Sci U S A* 111, 11151-11156.

16
17
18 880 Babiarz, J.E., Ravon, M., Sridhar, S., Ravindran, P., Swanson, B., Bitter, H., Weiser, T.,

19
20 881 Chiao, E., Certa, U. and Kolaja, K.L. 2012. Determination of the human cardiomyocyte

21
22 882 mRNA and miRNA differentiation network by fine-scale profiling. *Stem Cells Dev* 21, 1956-

23
24 883 1965.

25
26
27 884 Bagga, S., Bracht, J., Hunter, S., Massirer, K., Holtz, J., Eachus, R. and Pasquinelli, A.E.

28
29 885 2005. Regulation by let-7 and lin-4 miRNAs results in target mRNA degradation. *Cell* 122,

30
31 886 553-563.

32
33
34 887 Bello, C.L., Mulay, M., Huang, X., Patyna, S., Dinolfo, M., Levine, S., Van Vugt, A., Toh, M.,

35
36 888 Baum, C. and Rosen, L. 2009. Electrocardiographic characterization of the QTc interval in

37
38 889 patients with advanced solid tumors: pharmacokinetic- pharmacodynamic evaluation of

39
40 890 sunitinib. *Clin Cancer Res* 15, 7045-7052.

41
42 891 Boehm, M., Kojonazarov, B., Ghofrani, H. A., Grimminger, F., Weissmann, N., Liles, J. T.,

43
44 892 Budas, G. R., Seeger, W., and Schermuly, R. T. . 2015. Effects of Apoptosis Signal-

45
46 893 Regulating Kinase 1 (ASK1) Inhibition in Experimental Pressure Overload-Induced Right

47
48 894 Ventricular Dysfunction. *European Respiratory Journal* 46, PA4913.

49
50
51 895 Care, A., Catalucci, D., Felicetti, F., Bonci, D., Addario, A., Gallo, P., Bang, M.L., Segnalini,

52
53 896 P., Gu, Y., Dalton, N.D., Elia, L., Latronico, M.V., Hoydal, M., Autore, C., Russo, M.A., Dorn,

54
55 897 G.W., Ellingsen, O., Ruiz-Lozano, P., Peterson, K.L., Croce, C.M., Peschle, C. and

56
57 898 Condorelli, G. 2007. MicroRNA-133 controls cardiac hypertrophy. *Nat. Med* 13, 613-618.

1 899 Chang, L. and Karin, M. 2001. Mammalian MAP kinase signalling cascades. *Nature* 410, 37-
2 900 40.
3
4 901 Chu, T.F., Rupnick, M.A., Kerkela, R., Dallabrida, S.M., Zurakowski, D., Nguyen, L., Woulfe,
5
6 902 K., Pravda, E., Cassiola, F., Desai, J., George, S., Morgan, J.A., Harris, D.M., Ismail, N.S.,
7
8 903 Chen, J.H., Schoen, F.J., Van den Abbeele, A.D., Demetri, G.D., Force, T. and Chen, M.H.
9
10 904 2007. Cardiotoxicity associated with tyrosine kinase inhibitor sunitinib. *Lancet* 370, 2011-
11
12 905 2019.
13
14 906 Di Lorenzo, G., Autorino, R., Bruni, G., Carteni, G., Ricevuto, E., Tudini, M., Ficorella, C.,
15
16 907 Romano, C., Aieta, M., Giordano, A., Giuliano, M., Gonnella, A., De Nunzio, C., Rizzo, M.,
17
18 908 Montesarchio, V., Ewer, M. and De Placido, S. 2009. Cardiovascular toxicity following
19
20 909 sunitinib therapy in metastatic renal cell carcinoma: a multicenter analysis. *Ann Oncol* 20,
21
22 910 1535-1542.
23
24 911 Doherty, K.R., Wappel, R.L., Talbert, D.R., Trusk, P.B., Moran, D.M., Kramer, J.W., Brown,
25
26 912 A.M., Shell, S.A. and Bacus, S. 2013. Multi-parameter in vitro toxicity testing of crizotinib,
27
28 913 sunitinib, erlotinib, and nilotinib in human cardiomyocytes. *Toxicol Appl Pharmacol* 272, 245-
29
30 914 255.
31
32 915 Eaton, G.J., Zhang, Q.S., Diallo, C., Matsuzawa, A., Ichijo, H., Steinbeck, M.J. and Freeman,
33
34 916 T.A. 2014. Inhibition of apoptosis signal-regulating kinase 1 enhances endochondral bone
35
36 917 formation by increasing chondrocyte survival. *Cell Death Dis* 5, e1522.
37
38 918 Ewer, M.S., Suter, T.M., Lenihan, D.J., Niculescu, L., Breazna, A., Demetri, G.D. and
39
40 919 Motzer, R.J. 2014. Cardiovascular events among 1090 cancer patients treated with sunitinib,
41
42 920 interferon, or placebo: a comprehensive adjudicated database analysis demonstrating
43
44 921 clinically meaningful reversibility of cardiac events. *Eur J Cancer* 50, 2162-2170.
45
46 922 Faivre, S., Demetri, G., Sargent, W. and Raymond, E. 2007. Molecular basis for sunitinib
47
48 923 efficacy and future clinical development. *Nat Rev Drug Discov* 6, 734-745.
49
50 924 Fenton, M.S., Marion, K.M., Salem, A.K., Hogen, R., Naeim, F. and Hershman, J.M. 2010.
51
52 925 Sunitinib inhibits MEK/ERK and SAPK/JNK pathways and increases sodium/iodide
53
54 926 symporter expression in papillary thyroid cancer. *Thyroid* 20, 965-974.
55
56
57
58
59
60
61
62
63
64
65

1 927 Foltz, I.N., Gerl, R.E., Wieler, J.S., Luckach, M., Salmon, R.A. and Schrader, J.W. 1998.
2 928 Human mitogen-activated protein kinase kinase 7 (MKK7) is a highly conserved c-Jun N-
3
4 929 terminal kinase/stress-activated protein kinase (JNK/SAPK) activated by environmental
5
6 930 stresses and physiological stimuli. *J Biol Chem* 273, 9344-9351.
7
8 931 Force, T., Krause, D.S. and Van Etten, R.A. 2007. Molecular mechanisms of cardiotoxicity of
9
10 932 tyrosine kinase inhibition. *Nat. Rev. Cancer* 7, 332-344.
11
12 933 Fujii, K., Goldman, E.H., Park, H.R., Zhang, L., Chen, J. and Fu, H. 2004. Negative control of
13
14 934 apoptosis signal-regulating kinase 1 through phosphorylation of Ser-1034. *Oncogene* 23,
15
16 935 5099-5104.
17
18 936 Gerczuk, P.Z., Breckenridge, D.G., Liles, J.T., Budas, G.R., Shryock, J.C., Belardinelli, L.,
19
20 937 Kloner, R.A. and Dai, W. 2012. An apoptosis signal-regulating kinase 1 inhibitor reduces
21
22 938 cardiomyocyte apoptosis and infarct size in a rat ischemia-reperfusion model. *J Cardiovasc*
23
24 939 *Pharmacol* 60, 276-282.
25
26 940 Gharanei, M., Hussain, A., Janneh, O. and Maddock, H. 2013. Attenuation of doxorubicin-
27
28 941 induced cardiotoxicity by mdivi-1: a mitochondrial division/mitophagy inhibitor. *PLoS One* 8,
29
30 942 e77713.
31
32 943 Ghatalia, P., Je, Y., Kaymakcalan, M.D., Sonpavde, G. and Choueiri, T.K. 2015. QTc interval
33
34 944 prolongation with vascular endothelial growth factor receptor tyrosine kinase inhibitors. *Br J*
35
36 945 *Cancer* 112, 296-305.
37
38 946 Guo, L., Coyle, L., Abrams, R.M., Kemper, R., Chiao, E.T. and Kolaja, K.L. 2013. Refining
39
40 947 the human iPSC-cardiomyocyte arrhythmic risk assessment model. *Toxicol Sci* 136, 581-
41
42 948 594.
43
44 949 Guttilla, I.K. and White, B.A. 2009. Coordinate regulation of FOXO1 by miR-27a, miR-96,
45
46 950 and miR-182 in breast cancer cells. *J Biol Chem* 284, 23204-23216.
47
48 951 Hahn, V.S., Lenihan, D.J. and Ky, B. 2014. Cancer therapy-induced cardiotoxicity: basic
49
50 952 mechanisms and potential cardioprotective therapies. *J Am Heart Assoc* 3, e000665.
51
52
53
54
55
56
57
58
59
60
61
62
63
64
65

1 953 Hao, H., Li, S., Tang, H., Liu, B., Cai, Y., Shi, C. and Xiao, X. 2016. NQDI-1, an inhibitor of
2 954 ASK1 attenuates acute perinatal hypoxic-ischemic cerebral injury by modulating cell death.
3
4 955 Mol Med Rep 13, 4585-4592.
5
6 956 Hasinoff, B.B., Patel, D. and O'Hara, K.A. 2008. Mechanisms of myocyte cytotoxicity
7
8 957 induced by the multiple receptor tyrosine kinase inhibitor sunitinib. Mol. Pharmacol 74, 1722-
9
10 958 1728.
11
12 959 Hattori, K., Naguro, I., Runchel, C. and Ichijo, H. 2009. The roles of ASK family proteins in
13
14 960 stress responses and diseases. Cell Commun Signal 7, 9.
15
16 961 Hayakawa, Y., Hirata, Y., Sakitani, K., Nakagawa, H., Nakata, W., Kinoshita, H., Takahashi,
17
18 962 R., Takeda, K., Ichijo, H., Maeda, S. and Koike, K. 2012. Apoptosis signal-regulating kinase-
19
20 963 1 inhibitor as a potent therapeutic drug for the treatment of gastric cancer. Cancer Sci 103,
21
22 964 2181-2185.
23
24 965 He, X., Liu, Y., Sharma, V., Dirksen, R.T., Waugh, R., Sheu, S.S. and Min, W. 2003. ASK1
25
26 966 associates with troponin T and induces troponin T phosphorylation and contractile
27
28 967 dysfunction in cardiomyocytes. Am J Pathol 163, 243-251.
29
30 968 Henderson, K.A., Borders, R.B., Ross, J.B., Huwar, T.B., Travis, C.O., Wood, B.J., Ma, Z.J.,
31
32 969 Hong, S.P., Vinci, T.M. and Roche, B.M. 2013. Effects of tyrosine kinase inhibitors on rat
33
34 970 isolated heart function and protein biomarkers indicative of toxicity. J. Pharmacol. Toxicol.
35
36 971 Methods 68, 150-159.
37
38 972 Hikoso, S., Ikeda, Y., Yamaguchi, O., Takeda, T., Higuchi, Y., Hirotani, S., Kashiwase, K.,
39
40 973 Yamada, M., Asahi, M., Matsumura, Y., Nishida, K., Matsuzaki, M., Hori, M. and Otsu, K.
41
42 974 2007. Progression of heart failure was suppressed by inhibition of apoptosis signal-
43
44 975 regulating kinase 1 via transc coronary gene transfer. J Am Coll Cardiol 50, 453-462.
45
46 976 Hu, S., Niu, H., Minkin, P., Orwick, S., Shimada, A., Inaba, H., Dahl, G.V., Rubnitz, J. and
47
48 977 Baker, S.D. 2008. Comparison of antitumor effects of multitargeted tyrosine kinase inhibitors
49
50 978 in acute myelogenous leukemia. Mol Cancer Ther 7, 1110-1120.
51
52 979 Huang, Q., Zhou, H.J., Zhang, H., Huang, Y., Hinojosa-Kirschenbaum, F., Fan, P., Yao, L.,
53
54 980 Belardinelli, L., Tellides, G., Giordano, F.J., Budas, G.R. and Min, W. 2015. Thioredoxin-2
55
56
57
58
59
60
61
62
63
64
65

1 981 inhibits mitochondrial reactive oxygen species generation and apoptosis stress kinase-1
2 982 activity to maintain cardiac function. *Circulation* 131, 1082-1097.
3
4 983 Huynh, H., Choo, S.P., Toh, H.C., Tai, W.M., Chung, A.Y., Chow, P.K., Ong, R. and Soo,
5
6 984 K.C. 2011. Comparing the efficacy of sunitinib with sorafenib in xenograft models of human
7
8 985 hepatocellular carcinoma: mechanistic explanation. *Curr Cancer Drug Targets* 11, 944-953.
9
10 986 Ichijo, H., Nishida, E., Irie, K., ten Dijke, P., Saitoh, M., Moriguchi, T., Takagi, M.,
11
12 987 Matsumoto, K., Miyazono, K. and Gotoh, Y. 1997. Induction of apoptosis by ASK1, a
13
14 988 mammalian MAPKKK that activates SAPK/JNK and p38 signaling pathways. *Science* 275,
15
16 989 90-94.
17
18 990 Ilyas, A.M., Ahmed, Y., Gari, M., Alqahtani, M. H., Kumosani, T. A., Al-Malki, A. L.,
19
20 991 Abualnaja, K. O., Albohairy, S. H., Chaudhary, A. G., and Ahmed, F. . 2016. Sunitinib
21
22 992 Reduces Acute Myeloid Leukemia Clonogenic Cells in Vitro and has Potent Inhibitory Effect
23
24 993 on Sorted AML ALDH Cells. . *Open Journal of Blood Diseases* 6, 9.
25
26 994 Iriyama, T., Takeda, K., Nakamura, H., Morimoto, Y., Kuroiwa, T., Mizukami, J., Umeda, T.,
27
28 995 Noguchi, T., Naguro, I., Nishitoh, H., Saegusa, K., Tobiume, K., Homma, T., Shimada, Y.,
29
30 996 Tsuda, H., Aiko, S., Imoto, I., Inazawa, J., Chida, K., Kamei, Y., Kozuma, S., Taketani, Y.,
31
32 997 Matsuzawa, A. and Ichijo, H. 2009. ASK1 and ASK2 differentially regulate the counteracting
33
34 998 roles of apoptosis and inflammation in tumorigenesis. *EMBO J* 28, 843-853.
35
36 999 Izumiya, Y., Kim, S., Izumi, Y., Yoshida, K., Yoshiyama, M., Matsuzawa, A., Ichijo, H. and
37
38 1000 Iwao, H. 2003. Apoptosis signal-regulating kinase 1 plays a pivotal role in angiotensin II-
39
40 1001 induced cardiac hypertrophy and remodeling. *Circ Res* 93, 874-883.
41
42 1002 Jia, B., Guo, M., Li, G., Yu, D., Zhang, X., Lan, K. and Deng, Q. 2015. Hepatitis B virus core
43
44 1003 protein sensitizes hepatocytes to tumor necrosis factor-induced apoptosis by suppression of
45
46 1004 the phosphorylation of mitogen-activated protein kinase kinase 7. *J Virol* 89, 2041-2051.
47
48 1005 Kaiser, R.A., Liang, Q., Bueno, O., Huang, Y., Lackey, T., Klevitsky, R., Hewett, T.E. and
49
50 1006 Molkentin, J.D. 2005. Genetic inhibition or activation of JNK1/2 protects the myocardium
51
52 1007 from ischemia-reperfusion-induced cell death in vivo. *J Biol Chem* 280, 32602-32608.
53
54
55
56
57
58
59
60
61
62
63
64
65

1008 Karaman, M.W., Herrgard, S., Treiber, D.K., Gallant, P., Atteridge, C.E., Campbell, B.T.,
1
2 1009 Chan, K.W., Ciceri, P., Davis, M.I., Edeen, P.T., Faraoni, R., Floyd, M., Hunt, J.P., Lockhart,
3
4 1010 D.J., Milanov, Z.V., Morrison, M.J., Pallares, G., Patel, H.K., Pritchard, S., Wodicka, L.M.
5
6 1011 and Zarrinkar, P.P. 2008. A quantitative analysis of kinase inhibitor selectivity. *Nat*
7
8 1012 *Biotechnol* 26, 127-132.
9
10
11 1013 Kataoka, K., Koibuchi, N., Toyama, K., Sueta, D., Dong, Y., Ogawa, H., Kim-Mitsuyama, S.
12
13 1014 2011. ASK2 is a Novel Factor Associated with Salt-Sensitive Hypertension. *Circulation* 124,
14
15 1015 A9386.
16
17 1016 Kataoka, K., Nakamura, T., Dong, Y., Fukuda, M., Nako, H., Toyama, K., Sueta, D., Ogawa,
18
19 1017 H., Kim-Mitsuyama, S. 2010. ASK2 Deficiency Causes Hypertension and Cardiac Fibrosis
20
21 1018 Independently of the Presence of ASK1 ~ Investigation with ASK1/2 Double Deficient Mice.
22
23 1019 *Circulation* 122, A13837.
24
25
26 1020 Kataoka, K., Nakamura, T., Fukuda, M., Nako, H., Dong, Y., Liu, R., Tokutomi, Y., Ogawa,
27
28 1021 H., Kim-Mitsuyama, S. 2009. Apoptosis Signal-Regulating Kinase (ASK) 2 Deficient Mice
29
30 1022 Have Salt-Resistant Hypertension With Cardiac Hypertrophy. *Circulation* 120, S1112.
31
32
33 1023 Kataoka, K., Tokutomi, Y., Yamamoto, E., Nakamura, T., Fukuda, M., Dong, Y., Ogawa, H.,
34
35 1024 Kim-Mitsuyama, S. 2008. ASK2 Deficient Mice Have Elevated Blood Pressures with Cardiac
36
37 1025 Hypertrophy and Remodeling. *Circulation* 118, S_384.
38
39
40 1026 Katoh, M. 2016. FGFR inhibitors: Effects on cancer cells, tumor microenvironment and
41
42 1027 whole-body homeostasis (Review). *Int J Mol Med* 38, 3-15.
43
44 1028 Khakoo, A.Y., Kassiotis, C.M., Tannir, N., Plana, J.C., Halushka, M., Bickford, C., Trent, J.,
45
46 1029 Champion, J.C., Durand, J.B. and Lenihan, D.J. 2008. Heart failure associated with sunitinib
47
48 1030 malate: a multitargeted receptor tyrosine kinase inhibitor. *Cancer* 112, 2500-2508.
49
50
51 1031 Kim, A.H., Khursigara, G., Sun, X., Franke, T.F. and Chao, M.V. 2001. Akt phosphorylates
52
53 1032 and negatively regulates apoptosis signal-regulating kinase 1. *Mol Cell Biol* 21, 893-901.
54
55 1033 Kim, G.H. 2013. MicroRNA regulation of cardiac conduction and arrhythmias. *Transl Res*
56
57 1034 161, 381-392.
58
59
60
61
62
63
64
65

1035 Kim, I., Shu, C.W., Xu, W., Shiau, C.W., Grant, D., Vasile, S., Cosford, N.D. and Reed, J.C.
1
2 1036 2009. Chemical biology investigation of cell death pathways activated by endoplasmic
3
4 1037 reticulum stress reveals cytoprotective modulators of ASK1. *J Biol Chem* 284, 1593-1603.
5
6 1038 Krause, D.S. and Van Etten, R.A. 2005. Tyrosine kinases as targets for cancer therapy. *N.*
7
8 1039 *Engl. J Med* 353, 172-187.
9
10
11 1040 Lavine, K.J., White, A.C., Park, C., Smith, C.S., Choi, K., Long, F., Hui, C.C. and Ornitz,
12
13 1041 D.M. 2006. Fibroblast growth factor signals regulate a wave of Hedgehog activation that is
14
15 1042 essential for coronary vascular development. *Genes Dev* 20, 1651-1666.
16
17 1043 Liu, N., Bezprozvannaya, S., Williams, A.H., Qi, X., Richardson, J.A., Bassel-Duby, R. and
18
19 1044 Olson, E.N. 2008. microRNA-133a regulates cardiomyocyte proliferation and suppresses
20
21 1045 smooth muscle gene expression in the heart. *Genes Dev* 22, 3242-3254.
22
23
24 1046 Liu, W., Zi, M., Chi, H., Jin, J., Prehar, S., Neyses, L., Cartwright, E.J., Flavell, R.A., Davis,
25
26 1047 R.J. and Wang, X. 2011. Deprivation of MKK7 in cardiomyocytes provokes heart failure in
27
28 1048 mice when exposed to pressure overload. *J Mol Cell Cardiol* 50, 702-711.
29
30
31 1049 Luo, Y., Gao, S., Hao, Z., Yang, Y., Xie, S., Li, D., Liu, M. and Zhou, J. 2016. Apoptosis
32
33 1050 signal-regulating kinase 1 exhibits oncogenic activity in pancreatic cancer. *Oncotarget* 7,
34
35 1051 75155-75164.
36
37
38 1052 Marques, F.Z., Vizi, D., Khammy, O., Mariani, J.A. and Kaye, D.M. 2016. The transcardiac
39
40 1053 gradient of cardio-microRNAs in the failing heart. *Eur J Heart Fail* 18, 1000-1008.
41
42 1054 Mima, T., Ueno, H., Fischman, D.A., Williams, L.T. and Mikawa, T. 1995. Fibroblast growth
43
44 1055 factor receptor is required for in vivo cardiac myocyte proliferation at early embryonic stages
45
46 1056 of heart development. *Proc Natl Acad Sci U S A* 92, 467-471.
47
48
49 1057 Mitchell, S., Ota, A., Foster, W., Zhang, B., Fang, Z., Patel, S., Nelson, S.F., Horvath, S. and
50
51 1058 Wang, Y. 2006. Distinct gene expression profiles in adult mouse heart following targeted
52
53 1059 MAP kinase activation. *Physiol Genomics* 25, 50-59.
54
55
56 1060 Mooney, L., Skinner, M., Coker, S.J. and Currie, S. 2015. Effects of acute and chronic
57
58 1061 sunitinib treatment on cardiac function and calcium/calmodulin-dependent protein kinase II.
59
60 1062 *Br J Pharmacol* 172, 4342-4354.
61
62
63
64
65

1063 Morita, K., Saitoh, M., Tobiume, K., Matsuura, H., Enomoto, S., Nishitoh, H. and Ichijo, H.
1
2 1064 2001. Negative feedback regulation of ASK1 by protein phosphatase 5 (PP5) in response to
3
4 1065 oxidative stress. *EMBO J* 20, 6028-6036.
5
6 1066 Nako, H., Kataoka, K., Koibuchi, N., Dong, Y.F., Toyama, K., Yamamoto, E., Yasuda, O.,
7
8 1067 Ichijo, H., Ogawa, H. and Kim-Mitsuyama, S. 2012. Novel mechanism of angiotensin II-
9
10 1068 induced cardiac injury in hypertensive rats: the critical role of ASK1 and VEGF. *Hypertens*
11
12 1069 *Res* 35, 194-200.
13
14 1070 Nomura, K., Lee, M., Banks, C., Lee, G. and Morris, B.J. 2013. An ASK1-p38 signalling
15
16 1071 pathway mediates hydrogen peroxide-induced toxicity in NG108-15 neuronal cells. *Neurosci*
17
18 1072 *Lett* 549, 163-167.
19
20 1073 Pan, Y., Wang, Y., Zhao, Y., Peng, K., Li, W., Wang, Y., Zhang, J., Zhou, S., Liu, Q., Li, X.,
21
22 1074 Cai, L. and Liang, G. 2014. Inhibition of JNK phosphorylation by a novel curcumin analog
23
24 1075 prevents high glucose-induced inflammation and apoptosis in cardiomyocytes and the
25
26 1076 development of diabetic cardiomyopathy. *Diabetes* 63, 3497-3511.
27
28 1077 Rosenkranz, S. 2004. TGF-beta1 and angiotensin networking in cardiac remodeling.
29
30 1078 *Cardiovasc Res* 63, 423-432.
31
32 1079 Roskoski, R., Jr. 2007. Sunitinib: a VEGF and PDGF receptor protein kinase and
33
34 1080 angiogenesis inhibitor. *Biochem Biophys Res Commun* 356, 323-328.
35
36 1081 Saitoh, M., Nishitoh, H., Fujii, M., Takeda, K., Tobiume, K., Sawada, Y., Kawabata, M.,
37
38 1082 Miyazono, K. and Ichijo, H. 1998. Mammalian thioredoxin is a direct inhibitor of apoptosis
39
40 1083 signal-regulating kinase (ASK) 1. *EMBO J* 17, 2596-2606.
41
42 1084 Sandhu, H., Ansar, S. and Edvinsson, L. 2010. Comparison of MEK/ERK pathway inhibitors
43
44 1085 on the upregulation of vascular G-protein coupled receptors in rat cerebral arteries. *Eur. J.*
45
46 1086 *Pharmacol* 644, 128-137.
47
48 1087 Sandhu, H., Cooper, S., Hussain, A., Mee, C. and Maddock, H. 2017. Attenuation of
49
50 1088 Sunitinib-induced cardiotoxicity through the A3 adenosine receptor activation. *Eur J*
51
52 1089 *Pharmacol*.
53
54
55
56
57
58
59
60
61
62
63
64
65

1090 Schmidinger, M., Zielinski, C.C., Vogl, U.M., Bojic, A., Bojic, M., Schukro, C., Ruhsam, M.,
1 Hejna, M. and Schmidinger, H. 2008. Cardiac toxicity of sunitinib and sorafenib in patients
2 with metastatic renal cell carcinoma. *J. Clin. Oncol* 26, 5204-5212.
3
4 1092 Schramek, D., Kotsinas, A., Meixner, A., Wada, T., Elling, U., Pospisilik, J.A., Neely, G.G.,
5
6 1093 Zwick, R.H., Sigl, V., Forni, G., Serrano, M., Gorgoulis, V.G. and Penninger, J.M. 2011. The
7
8 stress kinase MKK7 couples oncogenic stress to p53 stability and tumor suppression. *Nat*
9 1094
10 *Genet* 43, 212-219.
11
12 1095 Shah, R.R. and Morganroth, J. 2015. Update on Cardiovascular Safety of Tyrosine Kinase
13
14 Inhibitors: With a Special Focus on QT Interval, Left Ventricular Dysfunction and Overall
15
16 Risk/Benefit. *Drug Saf* 38, 693-710.
17
18 1099 Shukla, S., Robey, R.W., Bates, S.E. and Ambudkar, S.V. 2009. Sunitinib (Sutent,
19
20 SU11248), a small-molecule receptor tyrosine kinase inhibitor, blocks function of the ATP-
21
22 binding cassette (ABC) transporters P-glycoprotein (ABCB1) and ABCG2. *Drug Metab*
23
24 *Dispos* 37, 359-365.
25
26 1101 Song, M.A., Dasgupta, C. and Zhang, L. 2015. Chronic Losartan Treatment Up-Regulates
27
28 AT1R and Increases the Heart Vulnerability to Acute Onset of Ischemia and Reperfusion
29
30 Injury in Male Rats. *PLoS One* 10, e0132712.
31
32 1104 Song, N.R., Lee, E., Byun, S., Kim, J.E., Mottamal, M., Park, J.H., Lim, S.S., Bode, A.M.,
33
34 Lee, H.J., Lee, K.W. and Dong, Z. 2013. Isoangustone A, a novel licorice compound, inhibits
35
36 cell proliferation by targeting PI3K, MKK4, and MKK7 in human melanoma. *Cancer Prev Res*
37
38 *(Phila)* 6, 1293-1303.
39
40 1108 Sucharov, C., Bristow, M.R. and Port, J.D. 2008. miRNA expression in the failing human
41
42 heart: functional correlates. *J Mol Cell Cardiol* 45, 185-192.
43
44 1110 Sundarajan, M., Boyle, D.L., Chabaud-Riou, M., Hammaker, D. and Firestein, G.S. 2003.
45
46 Expression of the MAPK kinases MKK-4 and MKK-7 in rheumatoid arthritis and their role as
47
48 key regulators of JNK. *Arthritis Rheum* 48, 2450-2460.
49
50 1111 Takeda, K., Shimozono, R., Noguchi, T., Umeda, T., Morimoto, Y., Naguro, I., Tobiume, K.,
51
52 Saitoh, M., Matsuzawa, A. and Ichijo, H. 2007. Apoptosis signal-regulating kinase (ASK) 2
53
54
55
56
57
58
59
60
61
62
63
64
65

1118 functions as a mitogen-activated protein kinase kinase kinase in a heteromeric complex with
1
2 1119 ASK1. *J Biol Chem* 282, 7522-7531.
3
4 1120 Tang, B., Du, J., Wang, J., Tan, G., Gao, Z., Wang, Z. and Wang, L. 2012. Alpinetin
5
6 1121 suppresses proliferation of human hepatoma cells by the activation of MKK7 and elevates
7
8 1122 sensitization to cis-diammined dichloridoplatium. *Oncol Rep* 27, 1090-1096.
9
10
11 1123 Taniike, M., Yamaguchi, O., Tsujimoto, I., Hikoso, S., Takeda, T., Nakai, A., Omiya, S.,
12
13 1124 Mizote, I., Nakano, Y., Higuchi, Y., Matsumura, Y., Nishida, K., Ichijo, H., Hori, M. and Otsu,
14
15 1125 K. 2008. Apoptosis signal-regulating kinase 1/p38 signaling pathway negatively regulates
16
17 1126 physiological hypertrophy. *Circulation* 117, 545-552.
18
19
20 1127 Thijs, A.M., El Messaoudi, S., Vos, J.C., Wouterse, A.C., Verweij, V., van Swieten, H., van
21
22 1128 Herpen, C.M., van der Graaf, W.T., Noyez, L. and Rongen, G.A. 2015. Sunitinib does not
23
24 1129 attenuate contractile force following a period of ischemia in isolated human cardiac muscle.
25
26 1130 *Target Oncol* 10, 439-443.
27
28
29 1131 Thum, T., Galuppo, P., Wolf, C., Fiedler, J., Kneitz, S., van Laake, L.W., Doevendans, P.A.,
30
31 1132 Mummery, C.L., Borlak, J., Haverich, A., Gross, C., Engelhardt, S., Ertl, G. and Bauersachs,
32
33 1133 J. 2007. MicroRNAs in the human heart: a clue to fetal gene reprogramming in heart failure.
34
35 1134 *Circulation* 116, 258-267.
36
37
38 1135 Tijssen, A.J., Pinto, Y.M. and Creemers, E.E. 2012. Non-cardiomyocyte microRNAs in heart
39
40 1136 failure. *Cardiovasc Res* 93, 573-582.
41
42 1137 Tobiume, K., Saitoh, M. and Ichijo, H. 2002. Activation of apoptosis signal-regulating kinase
43
44 1138 1 by the stress-induced activating phosphorylation of pre-formed oligomer. *J Cell Physiol*
45
46 1139 191, 95-104.
47
48
49 1140 Toldo, S., Breckenridge, D.G., Mezzaroma, E., Van Tassell, B.W., Shryock, J., Kannan, H.,
50
51 1141 Phan, D., Budas, G., Farkas, D., Lesnefsky, E., Voelkel, N. and Abbate, A. 2012. Inhibition
52
53 1142 of apoptosis signal-regulating kinase 1 reduces myocardial ischemia-reperfusion injury in the
54
55 1143 mouse. *J Am Heart Assoc* 1, e002360.
56
57
58
59
60
61
62
63
64
65

1144 Volynets, G.P., Chekanov, M.O., Synyugin, A.R., Golub, A.G., Kukharensko, O.P., Bdzholia,
1
2 1145 V.G. and Yarmoluk, S.M. 2011. Identification of 3H-naphtho[1,2,3-de]quinoline-2,7-diones as
3
4 1146 inhibitors of apoptosis signal-regulating kinase 1 (ASK1). *J Med Chem* 54, 2680-2686.
5
6 1147 Wang, X., Destrumont, A. and Tournier, C. 2007. Physiological roles of MKK4 and MKK7:
7
8 1148 insights from animal models. *Biochim Biophys Acta* 1773, 1349-1357.
9
10
11 1149 Wang, Y., Su, B., Sah, V.P., Brown, J.H., Han, J. and Chien, K.R. 1998. Cardiac hypertrophy
12
13 1150 induced by mitogen-activated protein kinase kinase 7, a specific activator for c-Jun NH2-
14
15 1151 terminal kinase in ventricular muscle cells. *J Biol Chem* 273, 5423-5426.
16
17
18 1152 Windak, R., Muller, J., Felley, A., Akhmedov, A., Wagner, E.F., Pedrazzini, T., Sumara, G.
19
20 1153 and Ricci, R. 2013. The AP-1 transcription factor c-Jun prevents stress-imposed maladaptive
21
22 1154 remodeling of the heart. *PLoS One* 8, e73294.
23
24
25 1155 Xiao, J., Luo, X., Lin, H., Zhang, Y., Lu, Y., Wang, N., Zhang, Y., Yang, B. and Wang, Z.
26
27 1156 2007. MicroRNA miR-133 represses HERG K⁺ channel expression contributing to QT
28
29 1157 prolongation in diabetic hearts. *J Biol Chem* 282, 12363-12367.
30
31 1158 Xu, C., Lu, Y., Pan, Z., Chu, W., Luo, X., Lin, H., Xiao, J., Shan, H., Wang, Z. and Yang, B.
32
33 1159 2007. The muscle-specific microRNAs miR-1 and miR-133 produce opposing effects on
34
35 1160 apoptosis by targeting HSP60, HSP70 and caspase-9 in cardiomyocytes. *J. Cell Sci* 120,
36
37 1161 3045-3052.
38
39
40 1162 Yamaguchi, O., Higuchi, Y., Hirotsu, S., Kashiwase, K., Nakayama, H., Hikoso, S., Takeda,
41
42 1163 T., Watanabe, T., Asahi, M., Taniike, M., Matsumura, Y., Tsujimoto, I., Hongo, K., Kusakari,
43
44 1164 Y., Kurihara, S., Nishida, K., Ichijo, H., Hori, M. and Otsu, K. 2003. Targeted deletion of
45
46 1165 apoptosis signal-regulating kinase 1 attenuates left ventricular remodeling. *Proc Natl Acad*
47
48
49 1166 *Sci U S A* 100, 15883-15888.
50
51 1167 Zhang, H., Tao, L., Jiao, X., Gao, E., Lopez, B.L., Christopher, T.A., Koch, W. and Ma, X.L.
52
53 1168 2007. Nitrate thioresoxin inactivation as a cause of enhanced myocardial
54
55 1169 ischemia/reperfusion injury in the aging heart. *Free Radic Biol Med* 43, 39-47.
56
57
58 1170 Zhang, L., Chen, J. and Fu, H. 1999. Suppression of apoptosis signal-regulating kinase 1-
59
60 1171 induced cell death by 14-3-3 proteins. *Proc Natl Acad Sci U S A* 96, 8511-8515.
61
62
63
64
65

1 **Involvement of mitogen activated kinase kinase 7 intracellular signalling pathway in**

2 **Sunitinib-induced cardiotoxicity**

3

4 Samantha Louise Cooper^{a,¶}, Hardip Sandhu^{a,¶}, Afthab Hussain^a, Christopher Mee^a, Helen
5 Maddock^{a,*}

6 ¶ shared first authorship

7

8 * Corresponding author: Prof. Helen Maddock

9 E-mail: helen.maddock@coventry.ac.uk

10 Phone: +44 2477 658 710

11

12 E-mail list:

13 Ms Samantha Louise Cooper: cooper87@uni.coventry.ac.uk

14 Dr Hardip Sandhu: hardip.sandhu@coventry.ac.uk

15 Dr Afthab Hussain: afthab.hussain@coventry.ac.uk

16 Dr Christopher Mee: christopher.mee@coventry.ac.uk

17

18 ^a Faculty Research Centre for Sport, Exercise and Life Sciences, Faculty of Health and Life
19 Sciences, Science & Health Building, 20 Whitefriars Street, Coventry, CV1 2DS, United
20 Kingdom

21

22 **Abbreviations:**

23 ASK1, apoptosis signal-regulating kinase 1; ASK2, apoptosis signal-regulating kinase 2;

24 DMSO, dimethyl sulphoxide; hERG, human ether-a-go-go-related gene; JNK, c-Jun N-

25 terminal kinase; MKK7, mitogen activated kinase kinase 7; MTT, 3-(4,5-dimethylthiazol-2-yl)-

26 2,5-diphenyltetrazolium bromide; NQDI-1, 2,7-dihydro-2,7-dioxo-3*H*-naphtho[1,2,3-

27 *de*]quinoline-1-carboxylic acid ethyl ester; TTC, 2,3,5-Triphenyl-2*H*-tetrazolium chloride.

28 **Abstract**

29 The tyrosine kinase inhibitor Sunitinib is used to treat cancer and is linked to severe adverse
30 cardiovascular events. Mitogen activated kinase kinase 7 (MKK7) is involved in the
31 development of cardiac injury and is a component of the c-Jun N-terminal kinase (JNK)
32 signal transduction pathway. Apoptosis signal-regulating kinase 1 (ASK1) is the upstream
33 activator of MKK7 and is specifically inhibited by 2,7-dihydro-2,7-dioxo-3*H*-naphtho[1,2,3-
34 *de*]quinoline-1-carboxylic acid ethyl ester (NQDI-1). This study investigates the role of ASK1,
35 MKK7 and JNK during Sunitinib-induced cardiotoxicity.

36
37 Infarct size were measured in isolated male Sprague-Dawley rat Langendorff perfused
38 hearts treated for 125 min with Sunitinib in the presence and absence of NQDI-1. Left
39 ventricular cardiac tissue samples were analysed by qRT-PCR for MKK7 mRNA expression
40 and cardiotoxicity associated microRNAs (miR-1, miR-27a, miR-133a and miR-133b) or
41 Western blot analysis to measure ASK1/MKK7/JNK phosphorylation.

42
43 Administration of Sunitinib (1 μ M) during Langendorff perfusion resulted in increased infarct
44 size, increased miR-133a expression, and decreased phosphorylation of the
45 ASK1/MKK7/JNK pathway compared to control. Co-administration of NQDI-1 (2.5 μ M)
46 attenuated the increased Sunitinib-induced infarct size, reversed miR-133a expression and
47 restored phosphorylated levels of ASK1/MKK7/JNK. These findings suggest that the
48 ASK1/MKK7/JNK intracellular signalling pathway is important in Sunitinib-induced
49 cardiotoxicity. The anti-cancer properties of Sunitinib were also assessed using the 3-(4,5-
50 dimethylthiazol-2-yl)-2,5-diphenyltetrazolium bromide (MTT) cell viability assay. Sunitinib
51 significantly decreased the cell viability of human acute myeloid leukemia 60 cell line (HL60).
52
53 The combination of Sunitinib (1 nM - 10 μ M) with NQDI-1 (2.5 μ M) enhanced the cancer-
54 fighting properties of Sunitinib. Investigations into the ASK1/MKK7/JNK transduction
55 pathway could lead to development of cardioprotective adjunct therapy, which could prevent
Sunitinib-induced cardiac injury.

56

1
2 57 **Keywords:**

- 3
4 58 – drug-induced cardiotoxicity
5
6
7 59 – tyrosine kinase inhibitor
8
9 60 – sunitinib
10
11 61 – mitogen activated kinase kinase 7
12
13
14 62 – novel adjunct therapy
15
16
17 63 – ASK1 inhibitor 2,7-dihydro-2,7-dioxo-3*H*-naphtho[1,2,3-*de*]quinoline-1-
18
19 64 carboxylic acid ethyl ester
20
21

22 65

23
24 66 **1. Introduction**

25
26 67 The tyrosine kinase inhibitor Sunitinib is used in the treatment of renal cell carcinoma and in
27
28 68 gastrointestinal stromal tumours (Faivre et al. 2007). ~~The tyrosine kinase inhibitor Sunitinib is~~
29
30
31 69 ~~used in the treatment of many soft cell cancers (Faivre et al. 2007).~~ Sunitinib prevents
32
33 70 tumour cell survival and angiogenesis by inhibiting a variety of growth factor and cytokine
34
35 71 receptors, including platelet derived growth factor receptors, vascular endothelial growth
36
37 72 factor receptors and proto-oncogenes c-Kit and RET. However, Sunitinib unfortunately is
38
39 73 also associated with a lack of kinase selectivity resulting in the cardiotoxic adverse effects
40
41 74 (Force et al. 2007). In the clinic, Sunitinib causes QT prolongation (Bello et al. 2009), left
42
43 75 ventricular dysfunction (Shah and Morganroth 2015) and heart failure (Ewer et al. 2014).
44
45 76 These findings are consistent with many other successful chemotherapy agents linked with
46
47 77 severe drug-induced cardiotoxicity (Hahn et al. 2014), including electrophysiological changes
48
49 78 and left ventricular dysfunction which can cause heart failure in some patients (Aggarwal et
50
51 79 al. 2013). Intracellular studies using animals have revealed that Sunitinib causes
52
53 80 mitochondrial injury and cardiomyocyte apoptosis through an increase in caspase-9 and
54
55 81 cytochrome C release in both mice and in cultured rat cardiomyocytes (Chu et al. 2007).
56
57
58
59
60
61
62
63
64
65

82 Other indicators of apoptosis, such as an increase in caspase-3/7, have also been detected
1
2 83 after Sunitinib treatment in rat myocytes (Hasinoff et al. 2008).

3
4 84
5
6 85 MKK7 is a member of the mitogen-activated protein kinase kinase super family, which allows
7
8 86 the cell to respond to exogenous and endogenous stimuli (Foltz et al. 1998), and furthermore
9
10 87 MKK7 has shown to demonstrate a key role in protecting the heart from hypertrophic
11
12 88 remodelling, which occurs via cardiomyocyte apoptosis and heart failure (Liu et al. 2011).

13
14
15 89 The MKK7 activation of JNK results in many cellular processes including: proliferation,
16
17 90 differentiation and apoptosis (Chang and Karin 2001; Schramek et al. 2011; Sundarajan et
18
19 91 al. 2003), and JNK signalling is vital for the maintenance and organisation of the
20
21 92 cytoskeleton and sarcomere structure in cardiomyocytes (Windak et al. 2013). Interestingly,
22
23 93 Sunitinib is an ATP analogue and competitively inhibits the ATP binding domain of its target
24
25 94 proteins (Roskoski 2007; Shukla et al. 2009). MKK7 also contains a highly conserved ATP
26
27 95 binding domain (Song et al. 2013). It is possible that Sunitinib binds as a ligand in the MKK7
28
29 96 ATP binding pocket, and thereby Sunitinib inhibits the MKK7/JNK transduction pathway, and
30
31 97 as a result this could potentially cause myocardial injury. It is important to determine the
32
33 98 relationship between MKK7 expression and Sunitinib induced cardiotoxicity by measuring
34
35 99 the alteration of MKK7 mRNA and phosphorylated MKK7 levels in the presence of Sunitinib.
36
37
38 100 Unravelling the relationship between Sunitinib and MKK7 could lead to a greater
39
40 101 understanding of its off-target mechanism of action and lead to the improvement in the
41
42 102 development of future drug discovery programmes or novel cardioprotective adjunct
43
44 103 therapies.
45
46
47
48
49
50

51 105 Short non-coding RNA microRNAs carry out the negative regulation of mRNA transcripts by
52
53 106 repressing translation (Bagga et al. 2005). Specific microRNAs expression patterns have
54
55 107 been linked to cardiomyocyte differentiation and in response to stress (Babiarz et al. 2012)
56
57 108 and have also been shown to be differentially expressed during the development of heart
58
59 109 failure (Thum et al. 2007). The microRNAs miR-1, miR-27a, miR-133a and miR-133b
60
61

110 produce differential expression patterns during the progression of heart failure (Akat et al.
111 2014; Tijssen et al. 2012). It is important to identify microRNA expression profiles in response
112 to drug-induced cardiotoxicity as similar patterns in microRNA expression to those identified
113 during heart failure may indicate the early onset of cardiotoxicity at a molecular level.

114
115 As MKK7 has no direct inhibitor, we have chosen to look at the upstream kinase ASK1
116 linked to MKK7 activation (Ichijo et al. 1997). ASK1 is activated in response to oxidative
117 stress-induced cardiac vascular endothelial growth factor suppression in the heart (Nako et
118 al. 2012). Izumiya et al. 2003 used ASK1 deficient transgenic mice to assess the role of
119 ASK1 in angiotensin II induced hypertension and cardiac hypertrophy. Both the wild type and
120 ASK1 deficient mice developed hypertension when stimulated with angiotensin II, however,
121 the ASK1 deficient mice lacked cardiac hypertrophy and remodelling and activation of ASK1,
122 p38 and JNK was severely attenuated, thus emphasising the importance of ASK1 in cardiac
123 hypertrophy and remodelling signalling (Izumiya et al. 2003). ASK1 is selectively inhibited by
124 NQDI-1 with high specificity with a K_i of 500nM and IC_{50} of 3 μ M (Volynets et al. 2011),
125 however, as this is a relatively new drug, a complete pharmacological profile has not yet
126 been fully characterised. ASK1 inhibition has previously been shown to offer protection
127 against ischemia reperfusion injury (Toldo et al. 2012) and has also been shown to suppress
128 the progression of ventricular remodelling and fibrosis in hamsters expressing severe
129 cardiomyopathy phenotypes (Hikoso et al. 2007). These findings highlight the potential of
130 NQDI-1 as a valuable asset to inhibit cardiac injury via the ASK1/MKK7/JNK pathway.

131
132 This novel study investigated the involvement of the ASK1/MKK7/JNK pathway in the
133 Sunitinib-induced cardiotoxicity via the assessment of cardiac function and infarct in
134 conjunction with relevant intracellular signalling mediators. Furthermore, we assessed the
135 anti-cancer properties of Sunitinib and determined whether co-administration of Sunitinib
136 with NQDI-1 affected the anti-cancer/apoptotic effect of Sunitinib in HL60 cells.

137

138 **2. Materials and Methods**

139 **2.1. Main reagents and kits**

140 Sunitinib malate and NQDI-1 were purchased from Sigma Aldrich (UK). Both drugs were
141 dissolved in dimethyl sulphoxide (DMSO) and stored at -20 °C. Krebs perfusate salts were
142 from either VWR International (UK) or Fisher Scientific (UK). Total ASK1 (Catalogue no
143 ab131506) was purchased from Abcam (UK). Phospho-ASK1 (Thr 845) (Catalogue no
144 3765S), Phospho-MKK7 (Ser271/Thr275) (Catalogue no 4171S), Total MKK7 (Catalogue no
145 4172S), Phospho-SAPK/JNK (Thr183/Tyr185) (Catalogue no 9251), Total SAPK/JNK rabbit
146 mAb antibody (Catalogue no 9252), anti-rabbit IgG, HRP-linked antibody and anti-biotin,
147 HRP-linked antibody were purchased from Cell signalling technologies (UK). All the
148 primary antibodies were from a rabbit host, and MKK7 and JNK were monoclonal antibodies,
149 whereas ASK1 was polyclonal (all antibodies were validated by the manufacturers). The
150 Ambion MicroPoly(A)Puris kit, Ambion mirVana miRNA Isolation Kit and Reverse
151 Transcription Kit were from Life Technologies (USA). The mRNA primers and the Applied
152 Biosystems primers assays (U6, rno-miR-1, hsa-miR-27a, hsa-miR-133a, and hsa-miR-
153 133b) were purchased from Invitrogen (UK). The iTaq Universal SYBR Green Supermix was
154 purchased from BioRad (UK). The HL60 cell line were obtained from European Collection of
155 Cell Culture (UK) (catalogue no. 98070106).

156
157 **2.2. Animals**

158 Adult male Sprague-Dawley rats (300-350 g in body weight); were purchased from Charles
159 River UK Ltd (UK) and housed suitably. They received humane care and had free access to
160 standard diet according to the Guide for the Care and Use of Laboratory Animals published
161 by the US National Institute of Health (NIH Publication No. 85-23, revised 1996). Animals
162 were selected at random for all treatment groups and the collected tissue was blinded for
163 infarct size assessment. The experiments were performed following approval of the protocol
164 by the Coventry University Ethics Committee. All efforts were made to minimise animal
165 suffering and to reduce the number of animals used in the experiments. Rats were sacrificed

166 by cervical dislocation (Schedule 1 Home Office procedure). A total of 80 animals were used
167 for this study and the data from 68 rats were included, while data from 12 rats were excluded
168 from analysis due to the established haemodynamic exclusion criteria. No animals were
169 culled due to ill health. A total of 16 animals were included for Langendorff perfusion
170 experiments per main groups (Control, Sunitinib, Sunitinib+NQDI-1, and NQDI-1, where 6 of
171 the animals were used for measurement of the area of infarct and the area of risk and the
172 left ventricular tissue from another 10 animals was used for real time PCR and Western blot
173 analysis). Furthermore, an additional 4 animals were used for Langendorff perfusion
174 experiments with Sorbitol as a positive control for p-MKK7 Western blot analysis.

2.3. Langendorff perfusion model

177 The hearts were rapidly excised after the rats were culled and placed into ice-cold Krebs
178 Henseleit buffer (118.5 mM NaCl, 25 mM NaHCO₃, 4.8 mM KCl, 1.2 mM MgSO₄, 1.2 mM
179 KH₂PO₄, 1.7 mM CaCl₂, and 12 mM glucose, pH7.4). ~~Each Langendorff study was~~
180 ~~conducted using the protocol for naïve Langendorff studies (Gharanei et al. 2013).~~The
181 hearts were mounted onto the Langendorff system and retrogradely perfused with Krebs
182 Henseleit buffer. The pH of the Krebs Henseleit buffer was maintained at 7.4 by gassing
183 continuously with 95 % O₂ and 5 % CO₂ and maintained at 37 ± 0.5 °C using a water-
184 jacketed organ chamber. Each Langendorff experiment was carried out for 145 minutes: a
185 20 minute stabilisation period and 125 minutes of drug or vehicle perfusion in normoxic
186 conditions. Hearts were included in the study with a CF between 3.5-12.0 ml/g (weight of the
187 rat heart) during the stabilisation period. Sunitinib malate (1 µM) was administered
188 throughout the perfusion period in the presence or absence of NQDI-1 (2.5 µM).

189
190 The clinically relevant dose of 1 µM Sunitinib was chosen in line with previous studies by
191 (Henderson et al. 2013). Additionally, it has been reported that the plasma concentration of
192 Sunitinib has a C_{max} in the range of 0.5–1.4µM (Doherty et al. 2013). While, the dose of 2.5
193 µM NQDI-1 was chosen following a thorough literature review (Eaton et al. 2014; Song et al.

194 2015; Volynets et al. 2011). NQDI-1 is not yet used in the clinic, therefore a clinically relevant
1
2 195 dose has not been reported.

3
4 196
5
6 197 Langendorff perfused hearts treated with vehicle were analysed as the control group. The
7
8 198 hearts were then weighed and either stored at -20 °C for 2,3,5-triphenyl-2H-tetrazolium
9
10 199 chloride (TTC) staining or the left ventricular tissue was dissected free and immersed in
11
12 200 RNAlater from Ambion (USA) for qRT-PCR or snap frozen by liquid nitrogen for Western blot
13
14 201 analysis.

15
16
17 202

18 203 **2.4. Infarct size analysis**

19
20 204 Frozen whole hearts were sliced into approximately 2 mm thick transverse sections and
21
22 205 incubated in 0.1 % TTC solution in phosphate buffer (2 ml of 100 mM NaH₂PO₄·2H₂O and 8
23
24 206 ml of 100 mM NaH₂PO₄) at 37 °C for 15 minutes and fixed in 10% formaldehyde (Fisher
25
26 207 Scientific, UK) for 4 hours. The risk zone and infarct areas were traced onto acetate sheets.
27
28 208 The tissue at risk stained red and infarct tissue appeared pale. The acetate sheet was
29
30 209 scanned and ImageTool from UTHSCSA (USA) software was used to measure the area of
31
32 210 infarct and the area of risk. A ratio of infarct to risk size was calculated as a percentage for
33
34 211 each slice. An average was taken of all of the slices from each heart to give the percentage
35
36 212 infarct size of the whole heart. The mean of infarct to risk ratio for each treatment group and
37
38 213 the mean ± SEM was plotted as a bar chart. The infarct size determination was randomised
39
40 214 and blinded.

41
42
43 215

44 216 **2.5. Analysis of microRNA expression profiles**

45
46 217 The microRNA was isolated from left ventricular tissue using the *mirVana*[™] miRNA Isolation
47
48 218 Kit from Ambion (UK). The microRNA quantity and quality was measured by NanoDrop from
49
50 219 Nanoid Technology (USA). A total of 500 ng microRNA was reverse transcribed into cDNA
51
52 220 using primers specific for housekeeping reference RNA U6 snRNA and target microRNAs:
53
54 221 hsa-miR-155, hsa-miR-15a, hsa-miR-16-1, rno-miR-1, hsa-miR-27a, hsa-miR-133a or hsa-

222 miR-133b (please note all human hsa-miR assays are compatible with rat samples) from
223 Applied Biosystems (USA) using the MicroRNA Reverse Transcription Kit from Applied
224 Biosystems (USA) according to the manufacturer's instructions. The reverse transcription
225 quantitative PCR reaction was performed with the following setup: 16 °C for 30 min, 42°C for
226 30 min and 85 °C for 5 min and ∞ at 4°C. The qRT-PCR was performed using the TaqMan
227 Universal PCR Master Mix II (no UNG) from Applied Biosystems (USA) protocol on the 7500
228 HT Real Time PCR sequence detection system from Applied Biosystems (USA). A 20µl
229 reaction mixture containing 100 ng cDNA, specific primer assays mentioned above from
230 Applied Biosystems (USA) and the TaqMan Universal PCR Master Mix was used in the qRT-
231 PCR reaction in triplicates. A non-template control was included in all experiments. The real
232 time PCR reaction was performed using the program: 1) 2 minutes at 50°C, 2) 10 minutes at
233 95°C, 3) 15 seconds at 95°C, 4) 1 minute at 60°C. Steps 3) and 4) were repeated 40 times.
234
235 Analysis of qRT-PCR data of microRNAs were performed using the Ct values for U6 snRNA
236 as reference for the comparison of the relative amount of microRNAs (rno-miR-1, hsa-miR-
237 27a, hsa-miR-133a and hsa-miR-133b). The values of each of the microRNAs were
238 calculated to compare their ratios. The formula used was $X_0/R_0=2^{CTR-CTX}$, where X_0 is the
239 original amount of target microRNA, R_0 is the original amount of U6 snRNA, CTR is the CT
240 value for U6 snRNA, and CTX is the CT value for the target microRNAs (rno-miR-1, hsa-
241 miR-27a, hsa-miR-133a and hsa-miR-133b) (Sandhu et al. 2010). Averages of the Ct values
242 for each sample group (Control and Sunitinib treated hearts) and each individual primer set
243 were calculated and bar charts were plotted with mean ± SEM. The mean of the control
244 group was set as 1 for all microRNAs.

2.6. Measurement of MKK7 mRNA expression

247 Total mRNA was extracted from left ventricular tissue using The Ambion MicroPoly(A)Purist
248 kit from Ambion (USA). Extracted mRNA was processed directly to cDNA by reverse
249 transcription using Reverse Transcription Kit from Applied Biosystems (USA) with the

250 respective primers for MKK7 (MKK7 forward primer: CCCCGTAAAATCACAAAGAAAATCC
251 and MKK7 reverse primer: GGCGGACACACACTCATAAACAGA) and GAPDH (GAPDH
252 Forward primer: GAACGGGAAGCTCACTGG and GAPDH Reverse primer:
253 GCCTGCTTCACCACCTTCT) according to the instructions from the manufacturer Invitrogen
254 (UK). The reverse transcription PCR reaction was performed with the following setup: 16 °C
255 for 30 minutes, 42°C for 30 minutes and 85 °C for 5 minutes. The qRT-PCR reactions were
256 performed with the iTaq Universal SYBR Green Supermix from BioRad (UK), GAPDH and
257 MKK7 mRNA primer sets on the 7500 HT Real Time PCR machine from Applied Biosystems
258 (USA) using the program: 1) 2 minutes at 50°C, 2) 10 minutes at 95°C, 3) 15 seconds at
259 95°C, 4) 1 minute at 60°C. Steps 3) and 4) were repeated 40 times.

261 Analysis of qRT-PCR data of MKK7 mRNA were performed using the Ct values for GAPDH
262 mRNA as reference for the comparison of the relative amount of MKK7 mRNA. The value of
263 mRNA was calculated to compare the ratios using the formula $X_0/R_0=2^{CTR-CTX}$, where X_0 is
264 the original amount of target mRNA, R_0 is the original amount of GAPDH mRNA, CTR is the
265 CT value for GAPDH mRNA, and CTX is the CT value for the MKK7 mRNA (Sandhu et al.
266 2010). Averages of the Ct values for each sample group (control and Sunitinib treated
267 hearts) and each individual primer set were calculated and bar charts were plotted with
268 mean \pm SEM. The mean of the control group was set as 1 for the MKK7 mRNA.

270 **2.7. Western blot detection of ASK1, MKK7 and JNK**

271 A total 45-55 mg of the frozen left ventricular tissue was lysed in lysis buffer (NaCl 0.1 M,
272 Tris base 10 μ M, EDTA 1 mM, sodium pyrophosphate 2 mM, NaF 2 mM, β -glycaophosphate
273 2 mM, 4-(2-Aminoethyl) benzenesulfonyl fluoride hydrochloride (0.1 mg/ml, 1/1.5 of protease
274 cocktail tablet) using a IKA Overtechnical T25homogeniser at 11,000 RPM. The
275 supernatants were measured for protein content using NanoDrop from Nanoid Technology
276 (USA). Then 80 μ g of protein was loaded to 4–15 % Mini-Protean TGX Gel from BioRad
277 (UK) and separated at 200 V for 60 minutes. After separation, the proteins were transferred

1
2
3
4
5
6
7
8
9
10
11
12
13
14
15
16
17
18
19
20
21
22
23
24
25
26
27
28
29
30
31
32
33
34
35
36
37
38
39
40
41
42
43
44
45
46
47
48
49
50
51
52
53
54
55
56
57
58
59
60
61
62
63
64
65

278 to the Bond-P polyvinylidene difluoride membrane from BioRad (UK) by using the Trans-Blot
279 Turbo transfer system from BioRad (UK) and probed for the phosphorylated forms
280 Phospho(Thr⁸⁴⁵)-ASK1 (p-ASK1), Phospho(Ser²⁷¹/Thr²⁷⁵)-MKK7 (p-MKK7) and
281 Phospho(Thr¹⁸³/Tyr¹⁸⁵) -SAPK/JNK (p-JNK), and total forms of ASK1(Thr⁸⁴⁵),
282 MKK7(Ser²⁷¹/Thr²⁷⁵) and JNK(Thr¹⁸³/Tyr¹⁸⁵). The p-MKK7 and p-JNK blots were stripped by
283 boiling and the PVDF membrane was used for total MKK7 and total JNK analysis,
284 respectively. According to recommendations from Cell signalling technologies (UK) total
285 ASK1 analysis had to be performed on a separate Western blot, as the stripping procedure
286 would remove total ASK1 protein. The relative changes in the p-ASK1, p-MKK7 and p-JNK
287 protein levels were measured and corrected for differences in protein loading as established
288 by probing for total ASK1, MKK7 and JNK respectively.

289
290 For Western blot analysis phosphorylated antibody levels were normalised to total antibody
291 levels in order to correlate for unequal loading of protein and differential blot transfer and to
292 identify the level of active vs inactive protein levels. Results were expressed as a percentage
293 of the density of phosphorylated protein relative to the density of total protein using Image
294 Lab 4.1 from BioRad (UK). The phosphorylated antibody levels determination was
295 randomised and blinded.

296 297 **2.8. MTT assay assessment of HL60 cell viability in the presence of Sunitinib with and** 298 **without NQDI-1**

299 The HL60 cell line were maintained in in RPMI 1640 medium supplemented with L-
300 Glutamine (2 mM) and 10 % heat-inactivated fetal bovine serum and antibiotics mix at 37 °C
301 in a humidified incubator under 5 % CO₂/95 % air. Cells were split in a 1:5 ratio every 2-3
302 days. Cells were incubated with Control, increasing concentrations of Sunitinib (1nM – 10
303 µM), Sunitinib (0.1 – 10 µM) + NQDI-1 (2.5 µM), or increasing concentrations of NQDI-1
304 (0.2-200 µM) for 24 h. Both Sunitinib and NQDI-1 were dissolved in DMSO. The DMSO
305 concentration was < 0.05 % (v/v) during the *in vitro* studies.

306

1
2 307 Cells were plated at a cell density of 10^5 cells/ml in 96-well plates and the above indicated
3
4 308 concentration of the drug was added. The plate was then incubated at 37°C for 24hrs. After
5
6 309 drug incubation, 50 μ l of MTT solution (5 mg MTT/ml H₂O) was added and the cells were
7
8 310 incubated for a further 24 h. Next, 50 μ l of DMSO was added to each well and mixed by
9
10
11 311 pipetting to release reduced MTT crystals from the cells. Relative cell viability was obtained
12
13 312 by scanning with an ELISA reader (Anthos Labtech AR 2001 Multiplate Reader, *Anthos*
14
15 313 *Labtec* Instruments, Austria) with a 490 nm filter. Results were expressed as a percentage of
16
17 314 viable cells relative to untreated cells/control. Experiments were performed in triplicates and
18
19 315 repeated \geq 3 times.
20
21

22 316

24 317 **2.9. Statistical analysis**

26 318 Results are presented as mean \pm standard error of the mean (SEM). Significance of all data
27
28 319 sets was measured by one-way ANOVA analysis with the Tukey post hoc test using the
29
30 320 Matlab prism program. The following groups were compared during ANOVA analysis:

33 321 Control versus Sunitinib, Control versus Sunitinib and NQDI-1, Control versus NQDI-1 (all
34
35 322 statistically significant data compared to control marked with *), and Sunitinib versus
36
37 323 Sunitinib and NQDI-1 (all statistically significant data compared to Sunitinib marked with #).
38
39 324 ~~Control versus Sunitinib (red), Control versus Sunitinib and NQDI-1 (green), Control~~
40
41 325 ~~versus NQDI-1 (blue) (all statistically significant data compared to control marked with *),~~
42
43 326 ~~and Sunitinib versus Sunitinib and NQDI-1 (all statistically significant data compared to~~
44
45 327 ~~Sunitinib marked with a purple \$).~~ For MKK7 mRNA some data was evaluated by using
46
47 328 student's t-test. P-values <0.05 were considered statistically significant.
48
49

50 329

53 330 **3. Results**

56 331 **3.1. Sunitinib treatment induces cardiac injury**

58 332 The effect of Sunitinib (1 μ M) administration on myocardial infarction development was
59
60 333 investigated by TTC staining. The hearts were stabilised for a period of 20 minutes, followed
61

334 by 125 minutes of drug perfusion. Administration of Sunitinib (1 μ M) for 125 minutes resulted
335 in a significant increase in infarct size compared with non-treated controls (Control: 7.81 \pm
336 1.16 %; Sunitinib: 41.02 \pm 1.23 %, $p < 0.001$) (Fig 1). This demonstrated that Sunitinib
337 treatment of the Langendorff perfused hearts results in a drastic increase in cardiac injury.

The infarct was globally distributed in all groups investigated in this study (i.e. Control,
Sunitinib \pm NQDI-1, and NQDI-1).

3.2. Sunitinib and NQDI-1 co-treatment alleviate cardiac injury

342 The effect of ASK1 inhibition by NQDI-1 on cardiac function and infarction was investigated.
343 Co-administration of Sunitinib (1 μ M) with NQDI-1 (2.5 μ M) significantly decreased infarct
344 size compared to Sunitinib treated hearts (Sunitinib: 41.02 \pm 1.23 %; Sunitinib + NQDI-1:
345 17.54 \pm 2.97 %, $p < 0.001$). However, administration of NQDI-1 alone for 125 minutes of
346 perfusion significantly increased infarct size compared with control hearts (Control: 7.81 \pm
347 1.16 %; NQDI-1: 16.68 \pm 2.66 %, $p < 0.05$) (Fig 1).

3.3. Sunitinib treatment modulates expression of microRNAs involved in cardiac injury

351 The expression of cardiac injury specific microRNAs during Sunitinib-induced cardiotoxicity
352 was determined by qRT-PCR assessment. The microRNAs miR-1, miR-27a, miR-133a and
353 miR-133b have been shown to produce differential expression patterns during the
354 progression of heart failure. The ratio of target microRNA normalised to U6 was set to 1 in
355 the control group for easier comparison of microRNA ratio values between the various drug
356 therapy groups. There was a significant increase in miR-133a when hearts were perfused
357 with Sunitinib (1 μ M) compared to control hearts (Ratio of target microRNA normalised to U6
358 in Sunitinib treated hearts: miR-133a: 535.78 \pm 61.27, $p < 0.001$). Co-administration of NQDI-
359 1 (2.5 μ M) along with Sunitinib reversed this miR-133a expression trend by decreasing the
360 miR-133a expression when compared to Sunitinib perfused hearts (Ratio of target microRNA
361 normalised to U6 in Sunitinib and NQDI-1 treated hearts: miR-133a: 52.76 \pm 28.30,

362 p<0.001). Hearts perfused with NQDI-1 alone showed an increase in miR-1, miR-27a and
363 miR-133b expression compared to control hearts (Ratio of target microRNA normalised to
364 U6 in NQDI-1 treated hearts: miR-1: 32.33 ± 16.47, p<0.01; miR-27a: 11.27 ± 2.86, p<0.001;
365 miR-133b: 167.85 ± 58.13, p<0.001). The expression of miR-1, miR-27a, miR-133a and
366 miR-133b was increased in the Sunitinib and NQDI-1 co-treated hearts when compared to
367 Sunitinib perfused hearts (miR-1: p<0.05; miR-27a: p<0.001; miR-133a: p<0.001; miR-133b:
368 p<0.05). (Fig 2 A-D).

369
370 The results from the microRNA qRT-PCR analysis show there is a similar expression pattern
371 for miR-1, miR-27 and miR-133b, while miR-133a has its own pattern. This indicates that the
372 cardiac injury induced by Sunitinib, which is alleviated by the ASK1 inhibitor NQDI-1, triggers
373 a complex alteration of these cardiac injury microRNAs. Further studies looking at the
374 altered expression profiles for these cardiac injury microRNAs have to be undertaken in
375 order to clarify the expression patterns. This indicates a complex alteration of these cardiac
376 injury microRNAs by Sunitinib and ASK1 specific inhibitor, NQDI-1. This indicates an
377 interaction between the ASK1/MKK7 pathway and Sunitinib in respect to expression of
378 cardiotoxicity linked microRNAs during cardiac injury.

379 380 **3.4. MKK7 mRNA expression profile is altered by ASK1 inhibitor NQDI-1**

381 As MKK7 contains an ATP binding domain (Song et al. 2013) and Sunitinib is an ATP
382 analogue and competitively inhibits the ATP binding domain of its target proteins (Roskoski
383 2007; Shukla et al. 2009). We therefore wanted to investigate the interaction between
384 Sunitinib and MKK7, and question whether Sunitinib could bind as a ligand in the ATP
385 binding pocket of MKK7. This would determine if Sunitinib might potentially have an
386 inhibitory effect on the MKK7/JNK pathway. The relationship between MKK7 expression and
387 Sunitinib-induced cardiotoxicity was assessed on transcriptional level by MKK7 mRNA qRT-
388 PCR analysis on Sunitinib (1 µM) perfused hearts, and the interaction by ASK1 specific
389 inhibitor NQDI-1 was detected to highlight if any interaction between ASK1/MKK7 and

390 Sunitinib-induced alteration of MKK7 transcription due to cardiac injury was observed to
1
2 391 impact on mRNA levels. The ratio of MKK7 mRNA normalised to GAPDH was set to 1 in the
3
4 392 control group for easier comparison of GAPDH normalised MKK7 mRNA values between the
5
6 393 various drug therapy groups. The qRT-PCR analysis of MKK7 mRNA revealed that co-
7
8 394 administration of NQDI-1 with Sunitinib caused a significant increase in MKK7 mRNA
9
10 395 expression compared to Sunitinib treatment alone ($p < 0.01$) (Ratio of MKK7 mRNA
11
12 396 normalised to GAPDH. Sunitinib: 0.12 ± 0.03 ; Sunitinib + NQDI-1: 1.18 ± 0.65) (Fig 3). The
13
14 397 decrease in MKK7 mRNA observed in the Sunitinib ($1 \mu\text{M}$) perfused hearts compared to
15
16 398 control hearts was not significant, but a clear trend was observed. If the data from groups
17
18 399 control and Sunitinib were compared using a Student's t-test the decline in MKK7 mRNA in
19
20 400 Sunitinib treated hearts was statistically significant with $p = 0.0043$.

21
22
23
24 401

25
26 402 These MKK7 mRNA qRT-PCR results clearly demonstrate that Sunitinib treatment shows a
27
28 403 tendency to decrease the MKK7 mRNA, and co-administration of ASK1 specific inhibitor
29
30 404 NQDI-1 restores the MKK7 mRNA level observed in control treated heart. This could indicate
31
32 405 a complex regulation system where Sunitinib-induced cardiac injury is directly linked with the
33
34 406 ability of Sunitinib to reduce MKK7 expression at transcriptional level, which is counteracted
35
36 407 by the ASK1 specific inhibitor NQDI-1.

37
38
39
40 408

41 409 **3.5. ASK1/MKK7/JNK pathway is involved in Sunitinib-induced cardiotoxicity**

42 410 As explained in the previous MKK7 mRNA results section we wanted to investigate the
43
44 411 interaction between Sunitinib and MKK7, as they both interact via the ATP binding pocket.
45
46 412 The key question being if Sunitinib can bind as a ligand in the ATP binding pocket of MKK7
47
48 413 and if Sunitinib is able to block the MKK7/JNK pathway. Here we investigate the role of
49
50 414 cardiotoxic Sunitinib therapy on the ASK1/MKK7/JNK pathway phosphorylation and how the
51
52 415 interaction with the cardioprotective ASK1 specific agent NQDI-1 affects the
53
54 416 ASK1/MKK7/JNK pathway phosphorylation. Following Langendorff perfusion of Sunitinib and
55
56
57
58
59
60
61
62
63
64
65

1
2 417 NQDI-1, p-ASK1, p-MKK7 and p-JNK levels were measured in the left ventricular tissue of
3 the hearts by Western blot analysis.

4 419
5
6 420 Western blot analysis showed that Sunitinib treatment decreased p-ASK1, p-MKK7 and p-
7
8 421 JNK levels significantly when compared to control (density of phosphorylated protein
9
10 422 normalised to total protein: *p-ASK1*: Control: 389.43 ± 4.18 and Sunitinib: 16.47 ± 3.56 ,
11
12 423 $p < 0.001$; *p-MKK7*: Control: 55.60 ± 4.86 and Sunitinib: 23.66 ± 4.53 , $p < 0.001$; *p-JNK*:
13
14 424 Control: 43.66 ± 2.82 and Sunitinib: 22.52 ± 2.74 , $p < 0.001$). Co-administration with NQDI-1
15
16 425 increased the p-ASK1, p-MKK7 and p-JNK levels, and these were statistically significantly
17
18 426 elevated when compared to heart treated with Sunitinib monotherapy. Co-administration with
19
20 427 NQDI-1 restored the decrease in p-ASK1, p-MKK7 and p-JNK levels and increased them
21
22 428 back to control levels (density of phosphorylated protein normalised to total protein: *p-ASK1*:
23
24 429 Sunitinib + NQDI-1: 51.17 ± 3.66 , $p < 0.001$; *p-MKK7*: Sunitinib + NQDI-1: 38.11 ± 1.87 ,
25
26 430 $p < 0.05$; *p-JNK*: 48.95 ± 2.76 , $p < 0.001$). The p-ASK1, p-MKK7 and p-JNK levels were
27
28 431 decreased in NQDI-1 treated hearts compared to control hearts (density of phosphorylated
29
30 432 protein normalised to total protein: *p-ASK1*: NQDI-1: 20.56 ± 1.99 , $p < 0.01$; *p-MKK7*: NQDI-1:
31
32 433 18.40 ± 2.98 , $p < 0.001$; *p-JNK*: 28.78 ± 3.03 , $p < 0.01$) (Fig 4A-C).
33
34
35
36
37
38
39

40 435 These Western blot results show that Sunitinib decreased the phosphorylation of the
41
42 436 ASK1/MKK7/JNK pathway. The fact that Sunitinib was able to show a strong tendency of
43
44 437 decreasing the MKK7 mRNA highlights that the decreased MKK7 phosphorylation is
45
46 438 regulated at the transcriptional level, which is then affecting the post-transcriptional MKK7
47
48 439 phosphorylation levels. However, interestingly the cardiotoxic Sunitinib is having an inhibiting
49
50 440 effect throughout all three parts of the ASK1/MKK7/JNK pathway. Co-administration of
51
52 441 NQDI-1 is counteracting the Sunitinib inhibiting effect on the phosphorylation level
53
54 442 throughout the ASK1/MKK7/JNK pathway. These results show a clear indication of Sunitinib
55
56 443 interacting with ASK1, MKK7 and JNK at post-translational level and MKK7 gene expression
57
58 444 at pre-transcriptional level.
59
60
61
62
63
64
65

445

1
2
3
4
5
6
7
8
9
10
11
12
13
14
15
16
17
18
19
20
21
22
23
24
25
26
27
28
29
30
31
32
33
34
35
36
37
38
39
40
41
42
43
44
45
46
47
48
49
50
51
52
53
54
55
56
57
58
59
60
61
62
63
64
65

3.6. Cancer cell viability in response to Sunitinib with and without NQDI-1

The effect of Sunitinib on cell viability was examined in HL60 cells. The HL60 cells were treated with Sunitinib for 24 hrs and then the level of mitochondrial metabolic-activity inhibition was measured with the MTT assay. Sunitinib showed a pronounced decrease in metabolic activity and a dose-dependent decrease in cell viability (Fig 5A). In particular, Sunitinib significantly reduces cell viability at 1 nM (82.62 ± 6.55 %, $p < 0.05$), 0.1 μ M (85.94 ± 3.80 %, $p < 0.05$), 0.5 μ M (83.94 ± 3.86 %, $p < 0.05$), 1 μ M (77.28 ± 6.58 %, $p < 0.05$), 5 μ M (58.61 ± 4.44 % $p < 0.001$) and 10 μ M (47.14 ± 6.77 %, $p < 0.001$) concentrations of Sunitinib. The IC_{50} value was 6.16 μ M. All the concentrations of Sunitinib in the absence and presence of NQDI-1 used during this study produced significant reductions in HL60 cell viability compared to vehicle treatment.

The co-administration of NQDI-1 (2.5 μ M) to increasing concentrations of Sunitinib (1 nM - 10 μ M) enhanced the inhibition of mitochondrial metabolism shown by Sunitinib (Fig 5A). Specifically, co-treatment of Sunitinib with NQDI-1 reduced cell viability at 1 μ M (59.58 ± 6.30 %, $p < 0.001$), 5 μ M (36.62 ± 6.52 %, $p < 0.001$) and 10 μ M (15.10 ± 2.31 %, $p < 0.001$) concentrations of Sunitinib compared to Sunitinib alone. The IC_{50} value for Sunitinib plus NQDI-1 was 1.76 μ M.

Interestingly, increasing concentrations of NQDI-1 alone (0.2-200 μ M) only significantly reduced cell viability at very high concentrations. Reductions in cell viability were significant at 100 μ M (55.44 ± 12.39 %, $p < 0.05$), 200 μ M (33.15 ± 9.67 %, $p < 0.001$) (Fig 5B). The IC_{50} value for NQDI-1 produced by the MTT assay was 130.8 μ M.

4. Discussion

4.1. Involvement of ASK1/MKK7/JNK in Sunitinib-induced cardiotoxicity

The occurrence heart failure associated with anti-cancer treatment has been investigated

473 extensively (Khakoo et al. 2008), however, the underlying mechanism of cardiotoxicity is still
1
2 474 unclear. Determining cellular pathways involved in Sunitinib-induced cardiotoxicity could help
3
4 475 to develop therapies which could prevent the potential development of heart failure
5
6 476 associated with Sunitinib treatment.
7

8
9 477
10
11 478 Data presented in this study confirms that Sunitinib causes drug-induced myocardial injury
12
13 479 via an increase in infarct size (Fig 1). We observed that infarct size increased from ~ 8 % in
14
15 480 Control hearts to ~ 41 % in hearts perfused with Sunitinib. This observation is in accordance
16
17 481 with our previous study, where we investigated the involvement of A3 adenosine receptor
18
19 482 activation during Sunitinib induced cardiotoxicity in perfused rat hearts (Sandhu et al. 2017).
20
21 483 Also, the injury induced by Sunitinib administration is very similar to ischemia/reperfusion
22
23 484 injury rats investigated by the same Langendorff model (Gharanei et al. 2013). The Control
24
25 485 rat hearts do suffer from minor infarct injury during the brief period it takes from sacrificing
26
27 486 the animal and perfusing the heart with the Krebs buffer during the Langendorff model. This
28
29 487 insult accounts for the ~ 8 % infarct size we observe in Control hearts. A dose of 1 μ M
30
31 488 Sunitinib increased the infarct to ~ 41 % in perfused heart, and this steady state blood
32
33 489 concentration of Sunitinib has been found in patients treated with Sunitinib (Henderson et al.
34
35 490 2013). As the rat hearts are physically much smaller than human hearts, the rat hearts may
36
37 491 have been more sensitive to the adverse effect of Sunitinib administration at the clinically
38
39 492 relevant dose of 1 μ M.
40
41
42
43
44
45
46

47 493
48 494 Other animal studies investigating Sunitinib-induced cardiotoxicity were linked to a significant
49
50 495 decrease in left ventricular function (Henderson et al. 2013; Mooney et al. 2015), and
51
52 496 interestingly left ventricular dysfunction has also been identified in patients undergoing
53
54 497 Sunitinib chemotherapy (Di Lorenzo et al. 2009). Data presented in this study confirms that
55
56 498 Sunitinib causes drug-induced myocardial injury via an increase in infarct size (Fig 1). These
57
58 499 observations are in accordance with other studies investigating Sunitinib-induced
59
60 500 cardiotoxicity linked with a significant decrease in left ventricular function in animals
61
62
63
64
65

501 ~~(Henderson et al. 2013; Mooney et al. 2015), and left ventricular dysfunction has also been~~
1
2 502 ~~identified in patients undergoing Sunitinib chemotherapy (Di Lorenzo et al. 2009).~~ Also,
3
4 503 sunitinib has also been associated with electrophysiological disturbances and an increased
5
6 504 pro-arrhythmic relative risk of developing QTc interval prolongation (Ghatalia et al. 2015;
7
8 505 Schmidinger et al. 2008). Several studies show that Sunitinib could potentially block human
9
10 ether-a-go-go-related gene (hERG) potassium channels and cause irregular contractions
11 506
12
13 507 (Doherty et al. 2013; Guo et al. 2013). The in vitro study by Thijs et al. 2015 investigated the
14
15 508 effect of Sunitinib on the contractile force measured during normal pacing or after simulated
16
17 509 ischemia on isolated human atrial trabeculae from patients awaiting coronary artery bypass
18
19 510 graft and/or aorta valve replacement. They showed that treatment with 81.3 nM Sunitinib did
20
21 511 not attenuate the recovery in contractile force of atrial cardiomyocytes after simulated
22
23 512 ischemia and reperfusion compared to vehicle treated atrial cardiomyocytes, and thus they
24
25 513 concluded that the development of heart failure in patients treated with Sunitinib could not be
26
27 514 explained by an acute cardiotoxic Sunitinib stimulation of cardiomyocytes. However, it
28
29 515 should be noted that they used a 12-times lower Sunitinib dose compared to what we have
30
31 516 used in this study, and thus they might have not used a dose of Sunitinib in the toxic range
32
33 517 (Thijs et al. 2015).
34
35
36
37
38 518

39
40 519 Modulation of ASK1 and its downstream targets MKK7 and JNK have been shown to play
41
42 520 important roles in regulating cardiomyocyte survival, apoptosis, hypertrophic remodeling and
43
44 521 intracellular signalling associated with heart failure (Mitchell et al. 2006). Therefore, we
45
46 522 hypothesised that successful modulation of the ASK1/MKK7/JNK pathway would produce an
47
48 523 effective cardioprotective treatment against Sunitinib induced cardiotoxicity.
49
50

51 524
52
53 525 As we were interested in the ASK1/MKK7/JNK signalling pathway we targeted ASK1 with
54
55 526 NQDI-1. Administration of the ASK1 specific inhibitor NQDI-1 resulted in abrogation of the
56
57 527 some cardiotoxic effects of Sunitinib. This study therefore, demonstrates the potentially
58
59 528 pivotal role that this kinase and the related pathway could play in protecting the heart from
60
61
62
63
64
65

1
2 530 Sunitinib induced cardiotoxicity. These observations are in accordance with other studies
3
4 531 that have also implicated the involvement of ASK1 in cardioprotection in other mammalian
5
6 532 models (Boehm 2015; Hao et al. 2016; He et al. 2003). Furthermore, inhibition of ASK1 with
7
8 533 thioredoxin results in reduction of infarct size compared to ischemic/reperfusion control
9
10 hearts (Gerczuk et al. 2012; Huang et al. 2015; Zhang et al. 2007).

11 534

12
13 535 ASK1 signalling pathway is facilitated through two main routes: either (i) MKK4/7 and JNK,
14
15 536 or (ii) MKK3/6 and p38 (Ichijo et al. 1997). As mentioned in the introduction the study by
16
17 537 Izumiya *et al.* 2003 showed the importance of ASK1 during angiotensin II induced
18
19 538 hypertension and cardiac hypertrophy in mice, as ASK1 knockout mice failed to develop
20
21 539 cardiac hypertrophy and remodelling through both JNK and p38 (Izumiya et al. 2003). In
22
23 540 another study by Yamaguchi *et al.* 2003 knockout of ASK1 in mice was also linked to
24
25 541 cardioprotection through the JNK pathway, as coronary artery ligation or thoracic transverse
26
27 542 aortic constriction in ASK1 deficient hearts showed no morphological or histological defects.
28
29 543 Both left ventricular end-diastolic and end-systolic ventricular dimensions were increased
30
31 544 less than wild-type mice, and the decreases in fractional shortening in both experimental
32
33 545 models ~~were~~ less when compared with wild-type mice (Yamaguchi et al. 2003). However,
34
35 546 in a study by Taniike *et al.* 2008 when ASK1 knockout mice were subjected to mechanical
36
37 547 stress it resulted in exaggerated heart growth and hypertrophy development through p38
38
39 548 pathway (Taniike et al. 2008). It is worth noting that attenuation of ASK1 by NQDI-1 during
40
41 549 normoxic conditions and Sunitinib treatment could have affected the MKK3/6 and p38
42
43 550 signalling pathway, which would have led to the conflicting results that we observe during
44
45 551 our study: ~~t~~here was a significant reduction in infarct size when Sunitinib was administered
46
47 552 in the presence of the ASK-1 inhibitor NQDI-1, however administration of NQDI-1 alone also
48
49 553 increased the infarct size. The increase in infarct size with NQDI-1 was not as profound as
50
51 554 the increase observed with Sunitinib (Fig 1).

52
53
54
55
56
57
58 555

59
60 556 NQDI-1 is a recently discovered highly specific ASK1 inhibitor. In the presence of 25 μ M
61
62
63
64
65

1 NQDI-1 the residual activity of ASK1 is reduced to 12.5 % using the γ -32P-ATP *in vitro*
2 kinase assay model. By using the same assay model Volynets and colleagues determined
3
4 559 the residual activity of the tyrosine protein kinase fibroblast growth factor receptor 1 (FGFR1)
5
6 560 which was measured to be 44 % after 25 μ M NQDI-1 exposure (Volynets et al. 2011).
7
8 561 FGFR1 as a key component involved in *in vivo* cardiomyocyte proliferation during early
9
10 562 stage heart development (Mima et al. 1995). Furthermore, FGFR1 is an essential regulator
11
12 563 of coronary vascular development through Hedgehog signalling activation, which in the adult
13
14 564 heart leads to increased coronary vessel density (Lavine et al. 2006). It is therefore possible
15
16 565 that NQDI-1 is blocking FGFR1 directly in the treated hearts of our study and thereby
17
18 566 exerting a slight increase in infarct size compared to the control.
19
20
21

22 567
23
24 568 In addition, NQDI-1's specificity towards other kinases has yet to be determined. In particular
25
26 569 its homologue apoptosis signal-regulating kinase 2 (ASK2) may potentially be inhibited by
27
28 570 NQDI-1 (Hattori et al. 2009). Both ASK1 and ASK2 is expressed in the heart (Iriyama et al.
29
30 571 2009). ASK2 is only stable and active when it forms a heteromeric complex with ASK1.
31
32 572 ASK2 mediate its stress response from the stable ASK1-ASK2 heteromeric complex
33
34 573 platform through both JNK and p38 and induce apoptosis. Furthermore, ASK1 and AS2 are
35
36 574 able to activate each other, and thus ASK1 assist~~s~~ ASK2 with ASK2 regulatory mechanisms
37
38 575 in addition to stabilising and activating ASK2 (Takeda et al. 2007). It is therefore very likely
39
40 576 that NQDI-1 will affect the ASK2 mediated signalling. Several studies by the team of Kataoka
41
42 577 have revealed the involvement of ASK2 during hypertension, cardiac hypertrophy and
43
44 578 remodelling development. They have shown that ASK2 deficient mice have a significantly
45
46 579 higher blood pressure and increased left ventricular weight then wild type mice, with an
47
48 580 underlying analysis revealing that perivascular and interstitial myocardial fibrosis was
49
50
51 581 increased (Kataoka 2008, 2009, 2010, 2011). Therefore, the relatively small adverse effect
52
53 582 of NQDI-1 administration on producing an increased infarct size could also be caused by the
54
55 583 NQDI-1 effect through attenuated ASK2 signalling. Therefore, the cardiac adverse effect of
56
57 584 NQDI-1 upon increased infarct size detected in this study could also be caused by the NQDI-
58
59
60
61
62
63
64
65

585 | ~~1-effect through attenuated ASK2 signalling.~~

586

587 Further studies are required to unravel the underlying mechanisms associated with the
588 cardiac tissue injury and haemodynamic responses observed upon NQDI-1 stimuli to assess
589 if p38, FGFR1, and/or ASK2 are involved. Also, other concentration of NQDI-1 treatment of
590 hearts should be investigated, as lower concentrations of NQDI-1 most likely would cause
591 less cardiac adverse effects.

592

593 **4.2. Profiling of cardiotoxicity linked microRNAs**

594 MicroRNAs have been shown to have important roles in tissue formation and function in
595 response to injury and disease. The microRNAs miR-1, miR-27a, miR-133a and miR-133b
596 have been shown to produce differential expression patterns during the progression of heart
597 failure (Akat et al. 2014; Tijssen et al. 2012). Here we investigate the altered expression
598 profiles of microRNAs miR-1, miR-27a, miR-133a and miR-133b after Sunitinib-induced
599 cardiotoxicity with or without the ASK1 inhibitor NQDI-1 (Fig 2A-D). To the best of our
600 knowledge there are no other studies showing a significant altered expression of miR-1,
601 miR-27a, miR-133a and miR-133b after Sunitinib treatment. A reduction in hERG potassium
602 channels expression causes the delayed myocyte repolarisation attributed to a long QT
603 interval and interestingly the 3' untranslated region of hERG potassium channel transcripts
604 have a partial complimentary miR-133a target site (Xiao et al. 2007). The current study
605 shows an increase in miR-133a expression following Sunitinib treatment, which was
606 attenuated with NQDI-1 co-administration (Fig 2C). This could imply that miR-133a
607 overexpression inhibits the hERG potassium channel, which would have a negative impact
608 on the electrophysiological response (Xu et al. 2007). Over expression of miR-133a has also
609 been shown to have negative effects on cardiomyocyte proliferation and survival (Liu et al.
610 2008), which corroborates the results from the current study.

611

1
2
3
4
5
6
7
8
9
10
11
12
13
14
15
16
17
18
19
20
21
22
23
24
25
26
27
28
29
30
31
32
33
34
35
36
37
38
39
40
41
42
43
44
45
46
47
48
49
50
51
52
53
54
55
56
57
58
59
60
61
62
63
64
65

612 In the heart miR-1 and miR-133 maintain the heart beat rhythm by regulating the cardiac
613 conduction system (Kim 2013). Furthermore, miR-1 and miR-133 are downregulated during
614 cardiac hypertrophy in both mouse and human models. *In vitro* studies have shown that the
615 overexpression of miR-133 inhibits cardiac hypertrophy, whereas inhibition of miR-133
616 induces more pronounced hypertrophy (Care et al. 2007). In addition, a decreased in cardiac
617 expression of miR-133b is sufficient to induce hypertrophic gene expression (Sucharov et al.
618 2008). In support of these studies our analysis shows that the miR-133b expression is
619 increased during NQDI-1 mono-therapy and co-administration of Sunitinib and NQDI-1 (Fig
620 2C).~~In support of these studies our analysis shows that the miR-133b expression is~~
621 ~~increased during NQDI-1 mono-therapy and co-administration hearts (Fig 2C),~~ thus
622 protecting the heart against hypotrophy/cardiac damage development, which is the same
623 pattern as we observe in the infarct to risk analysis.

624
625 The miR-27a expression has been observed to downregulate FOXO-1 protein, a
626 transcription factor which regulates genes involved in the apoptotic response, cell cycle, and
627 cellular metabolism (Guttilla and White 2009). Moreover, miR-27a is downregulated in
628 coronary sinus samples of heart failure patients (Marques et al. 2016). The increase in miR-
629 27a expression in our study during NQDI-1 mono-therapy and co-administration of Sunitinib
630 and NQDI-1.~~The increase in miR-27a expression in our study during NQDI-1 mono-therapy~~
631 ~~and co-administration hearts~~ (Fig 2B) support the findings from these studies as the link
632 increased miR-27 expression to reduced apoptosis, which is what we observe in the infarct
633 to risk analysis.

635 **4.3. Sunitinib treatment supresses the ASK1/MKK7/JNK pathway**

636 **4.3.1. ASK1**

637 Western blot assessment of Sunitinib treated hearts showed a significant decrease in p-
638 ASK1 when compared to control perfused hearts, and this decrease in p-ASK1 levels was

639 abrogated with NQDI-1 co-administration. However, in p-ASK1 levels from hearts subjected
640 to Sunitinib and NQDI-1 co-administration were compared to control hearts we did observe a
641 significant increase in p-ASK1. ~~However, if p-ASK1 levels in Sunitinib and NQDI-1 co-~~
642 ~~administration hearts were compared to control hearts we did observe a significant increase~~
643 ~~in p-ASK1.~~ Furthermore, NQDI-1 treated hearts had significantly decreased p-ASK1 levels
644 when compared to control hearts (Fig 4A).

645 ASK1 has multiple phosphorylation sites. The Akt/protein kinase B complex binds to and
646 phosphorylates Ser⁸³ of ASK1, resulting in the inhibition of ASK1-mediated apoptosis (Kim et
647 al. 2001), the 14-3-3 interacts with phosphorylated Ser⁹⁶⁷ of ASK1 to block the function of
648 ASK1 (Zhang et al. 1999), protein phosphatase 5 dephosphorylates Thr⁸⁴⁵ within the
649 activation loop of ASK1 and thereby inhibits ASK1-mediated apoptosis (Morita et al. 2001),
650 while Ser¹⁰³⁴ phosphorylation suppresses ASK1 proapoptotic function (Fujii et al. 2004).
651 ASK1 undergoes auto-phosphorylation at the Thr⁸⁴⁵ (Tobiume et al. 2002). It is possible that
652 auto-phosphorylation increased when Sunitinib was combined with NQDI-1, which led to the
653 increased levels of p-ASK1 identified by western blot analysis. In its inactive form, ASK1 is
654 complexed with thioredoxin (Saitoh et al. 1998). It has been proposed that auto-
655 phosphorylation at Thr⁸⁴⁵ is increased in response to H₂O₂ treatment, due to H₂O₂ preventing
656 thioredoxin from complexing with ASK1. This suggests that ASK1 activation is due to
657 oxidative stress (Tobiume et al. 2002). An increase in p-ASK1 could indicate increased
658 levels of oxidative stress, which potentially reduced cardiac function and generated a level of
659 infarct when NQDI-1 was administered alone compared to control.

660
661 Attenuation of ASK1 by the specific inhibitor NQDI-1 produces a protective role in the heart
662 compared to Sunitinib treatment alone. In this study we have focused on the ASK1 Thr⁸⁴⁵
663 phosphorylation site, however, in future studies it would be interesting to investigate the
664 ASK1 Ser⁹⁶⁷ phosphorylation, as phosphorylation at this site has been linked to
665 cytoprotection (Kim et al. 2009). Another interesting aspect would be to identify if NQDI-1 is

666 able to inhibit the ASK1 homologue ASK2 as indicated by Nomura *et al.* 2013 (Nomura *et al.*
667 2013) and establish the K_i and IC_{50} values are.

668
669 ASK1 is also a key mediator of apoptotic signalling (Hattori *et al.* 2009; Ichijo *et al.* 1997) and
670 the team of Huynh *et al.* 2011 investigated the expression of ASK1 in tumours lysates from
671 mice bearing 06-0606 tumours treated with 40 mg/kg/day Sunitinib for 11 days (Huynh *et al.*
672 2011). Their study showed a significant increase in total ASK1 levels after Sunitinib
673 treatment compared to vehicle treated 06-0606 tumour expressing mice, however, in our
674 study the expression of total ASK1 levels in left ventricular coronary tissue did not differ in
675 hearts perfused with Sunitinib compared to vehicle treated hearts.

676

677 **4.3.2. MKK7**

678 We assessed MKK7 expression level at both transcriptional and post-translational levels in
679 hearts treated with Sunitinib with and without the upstream ASK1 inhibitor NQDI-1. There
680 was a strong tendency for MKK7 mRNA expression to be decreased in Sunitinib perfused
681 hearts compared to control, but without significance. There was a strong tendency of
682 decreased MKK7 mRNA expression in Sunitinib perfused hearts compared to control, but
683 without significance. The expression of MKK7 mRNA was increased significantly in Sunitinib
684 and NQDI-1 co-treated hearts compared to Sunitinib perfused hearts, and NQDI-1 solo
685 treatment did not alter the MKK7 mRNA expression compared to control hearts (Fig 3). The
686 p-MKK7 level was significantly decreased in Sunitinib treated hearts when compared to
687 control, and the p-MKK7 decrease is attenuated by NQDI-1 co-administration. The p-MKK7
688 levels are significantly decreased in Sunitinib and NQDI-1 co-treatment and NQDI-1 solo-
689 treatment hearts compared to control hearts (Fig 4B). We believe that this is the first study to
690 investigate the expression of MKK7 after Sunitinib therapy.

691

692 MKK7 has a vital role in protecting the heart from hypertrophic remodelling and
693 cardiomyocytes apoptosis during stress and therefore the transition into heart failure

694 (Mitchell et al. 2006). Studies by Liu *et al.* 2011 revealed the importance of MKK7 by
1
2 695 demonstrating that deprivation of MKK7 in cardiomyocytes provokes heart failure in mice
3
4 696 when exposed to pressure overload (Liu et al. 2011). In addition to this, it has been shown
5
6 697 that inhibition and specific knockout of MKK7 increases the sensitivity of hepatocytes to
7
8 698 tumour necrosis factor alpha-induced apoptosis (Jia et al. 2015). Treatment with Sunitinib in
9
10
11 699 rat hearts in the current study down regulates both mRNA and phosphorylated protein levels
12
13 700 of MKK7. These studies suggest an important role of MKK7 in the maintenance of heart
14
15 701 homeostasis and expression of associated genes are important during cardiac hypertrophy
16
17 702 and heart failure.
18
19

20 703
21
22 704 MKK7 contains an ATP binding domain which could be inhibited by the ATP analogue,
23
24 705 Sunitinib (Roskoski 2007; Shukla et al. 2009; Song et al. 2013). It is therefore possible that
25
26 706 Sunitinib has an inhibitory effect on the MKK7/JNK signal transduction pathway. With
27
28 707 reduced MKK7 activity demonstrating both an incline towards cardiomyocyte damage and a
29
30 708 reversal of anti-tumour effects of chemotherapy, it would be interesting to assess both the
31
32 709 changes in expression levels and levels of phosphorylated MKK7 during Sunitinib treatment
33
34 710 affecting the heart in future studies. It may therefore be possible to identify a link between
35
36 711 MKK7 expression and tyrosine kinase inhibitor-induced cardiotoxicity.
37
38
39

40 712
41
42 713 Co-treatment of Sunitinib and NQDI-1 increases the level of p-MKK7 to levels compared to
43
44 714 Sunitinib treated hearts, restoring them almost back to the p-MKK7 levels observed in
45
46 715 control hearts. This could suggest that phosphorylated MKK7 is required to maintain at a
47
48 716 stable level to prevent damage to the heart. To illustrate this upregulation of transforming
49
50 717 growth factor beta has been found in compensatory hypertrophy, myocardial remodelling
51
52 718 and heart failure (Rosenkranz 2004). However, if MKK7 is removed entirely from the JNK
53
54 719 pathway cardiomyocyte damage ensues (Liu et al. 2011). Tang *et al.* 2012 demonstrated
55
56 720 that by causing an upregulation of MKK7 in hepatoma cells with the treatment with Alpinetin
57
58 721 it was possible to arrest cells in the G₀/G₁ phase of the cell cycle. However, by inhibiting
59
60
61
62
63
64
65

722 MKK7 the anti-tumour effect of the delta-opioid receptor agonist cis-diammined
1
2 723 dichloridoplatinum was reversed (Tang et al. 2012). This suggests that by agonising MKK7 it
3
4 724 may be possible to both enhance anti-cancer properties of chemotherapy agents, as well as
5
6 725 limiting apoptosis as the cell cycle is arrested.
7

8
9 726

10 11 727 **4.3.3. JNK**

12
13 728 Administration of Sunitinib decreased the p-JNK levels significantly when compared to
14
15 729 control hearts, and this decrease was abrogated with NQDI-1 co-treatment. Treatment with
16
17 730 NQDI-1 however also decreased the p-MKK7 levels when compared to control perfused
18
19 731 hearts (Fig 4C).
20

21
22 732

23
24 733 Many JNK knock out models have been used to determine the role of JNK in the
25
26 734 development of cardiac dysfunction. Kaiser *et al.* 2005 demonstrated the importance of JNK
27
28 735 in ischemia-reperfusion injury. They showed that a reduction in JNK activity in the heart
29
30 736 resulted in a reduced level of cardiac injury and cellular apoptosis. The same study
31
32 737 demonstrated an increase in JNK activity by using mouse models overexpressing MKK7 in
33
34 738 the heart, and this caused a significant protection against ischemia-reperfusion injury (Kaiser
35
36 739 *et al.* 2005). This highlights the complexity of JNK signalling. In this study, a significant
37
38 740 decrease in JNK phosphorylation was identified when hearts were treated with Sunitinib. In
39
40 741 addition, NQDI-1 treatment had a tendency to increase in JNK phosphorylation. It has been
41
42 742 established that a reduction in JNK activation is associated with cardiac hypertrophy and
43
44 743 cardiovascular dysfunction (Pan et al. 2014). The reduction in JNK activation caused by the
45
46 744 treatment of Sunitinib could also explain the increased infarct size and irregularities found in
47
48 745 the haemodynamic data.
49
50

51
52 746

53
54
55 747 Our study contradicts some previous studies, for example Wang *et al.* 1998 investigated the
56
57 748 role of MKK7 in cardiac hypertrophy in neonatal myocytes (Wang et al. 1998). Transgenic
58
59 749 neonatal rat cardiomyocytes expressing wild type MKK7 and a constitutively active mutant of
60
61

1
2
3
4
5
6
7
8
9
10
11
12
13
14
15
16
17
18
19
20
21
22
23
24
25
26
27
28
29
30
31
32
33
34
35
36
37
38
39
40
41
42
43
44
45
46
47
48
49
50
51
52
53
54
55
56
57
58
59
60
61
62
63
64
65

750 MKK7 were created. This study demonstrated JNK specific activation by MKK7 and showed
751 the key role of the JNK pathway in cardiac hypertrophy as cells infected with the
752 constitutively active form of MKK7 adopted characteristic features of myocardial stress
753 (Wang et al. 1998).

The study by Fenton et al 2010 looked at the expression of JNK in papillary cancer cells with
RET/PTC1 rearrangement treated with Sunitinib (Fenton et al. 2010). Sunitinib inhibited
proliferation of these RET/PTC1 subcloned papillary cancer cells, and furthermore inhibited
the JNK phosphorylation in the cytoplasm of the papillary cancer cells. In our study the
expression of p-JNK levels in left ventricular coronary tissue was also reduced in hearts
perfused with Sunitinib compared to vehicle treated hearts.

In summary, Sunitinib administration resulted in significant reduction in p-ASK1, p-MKK7 and
p-JNK levels, whilst NQDI-1 co-administration counteracted this increase. It is worth noting
that MKK7 is activated through phosphorylation at a special site at the C-terminal kinase
domain core called the "Domain for Versatile Docking" (DVD), which includes serine-
threonine sites (Wang et al. 2007). Sunitinib does not discriminate between inhibition of
tyrosine kinases or serine-threonine kinases (Karaman et al. 2008). Therefore, Sunitinib
might potentially inhibiting serine-threonine kinases, however, it is much more likely that
Sunitinib inhibits tyrosine kinases as expected, resulting in the downstream inhibition of
ASK1, which then results in a downstream inhibition of MKK7 and JNK. However, more
detailed investigations into the pathway involvement are required to fully elucidate the
intracellular signalling pathways. In addition, the increase in p-ASK1, p-MKK7 and p-JNK
levels that we observe in the presence of both Sunitinib and NQDI-1, when compared to
Sunitinib perfused hearts, could be due to the fact that we only assessed the
phosphorylation of ASK1 at Thr⁸⁴⁵, however, it is possible that NQDI-1 blocks both Ser⁸³ and
Thr⁸⁴⁵ of ASK1, and further investigations of phosphorylation activity at both sides could
clarify this issue. This altered pattern in ASK1/MKK7/JNK pathway phosphorylation suggests

1
2 778 ~~that Sunitinib has a direct effect on part of the ASK1/MKK7/JNK pathway. In summary,~~
3
4 779 ~~Sunitinib administration resulted in significant reduction in p-ASK1, p-MKK7 and p-JNK~~
5
6 780 ~~levels, whilst NQDI-1 co-administration counteracted this increase. It is possible that NQDI-1~~
7
8 781 ~~blocks both Ser⁸³ and Thr⁸⁴⁵, and that the increase in p-ASK1, p-MKK7 and p-JNK levels that~~
9
10 782 ~~we observe in the presence of both Sunitinib and NQDI-1 when compared to Sunitinib~~
11
12 783 ~~perfused hearts is due to fact only phosphorylation of ASK1 at Thr⁸⁴⁵ was assessed. This~~
13
14 784 altered pattern in ASK1/MKK7/JNK pathway phosphorylation suggests that Sunitinib has a
15
16 785 direct effect on part of the ASK1/MKK7/JNK pathway.
17
18 786

19 20 787 **4.4. The anti-cancer properties of Sunitinib were enhanced by NQDI-1 treatment**

21
22 788 It is well established that Sunitinib achieves anti-tumour effects by inhibiting tyrosine kinases,
23
24 789 which have been over-expressed in cancer cells (Krause and Van Etten 2005). Sunitinib has
25
26 790 previously been shown to directly inhibit the survival and proliferation of a variety of cancer
27
28 791 cells, including leukaemia cells (Ilyas 2016).
29
30

31 792
32
33 793 We demonstrated a dose dependant decline in the cell viability of HL60 cells when treated
34
35 794 with Sunitinib (Fig 5A). This produced an IC₅₀ value of 6.16 µM. Our results are in line with
36
37 795 existing data on the anti-proliferative effect of Sunitinib on HL60 cells. Sunitinib has
38
39 796 previously been shown to reduce the level of HL60 cell survival in a dose dependant manor
40
41 797 using a cell-titre blue reagent proliferation assay. This produced an IC₅₀ value of 5.7 µM after
42
43 798 48 hrs of Sunitinib treatment (Ilyas 2016). Another group performed an MTT assay on a
44
45 799 variety of acute myelogenous leukaemia cell lines and found Sunitinib to have an IC₅₀ values
46
47 800 between 0.007-13 µM (Hu et al. 2008).
48
49

50
51 801
52
53 802 To investigate the anti-proliferative effect of inhibition of the MKK7 pathway, HL60 cells were
54
55 803 treated with Sunitinib in co-treatment with NQDI-1 and NQDI-1 alone (Fig 5A-B). NQDI-1 is a
56
57 804 selective inhibitor for ASK1, the upstream regulator of MKK7. Previous studies have shown
58
59 805 ASK1 to have a crucial role in a variety of organ systems. However, ASK1 has also been
60
61

806 shown to promote tumorigenesis in gastric cancer and promote the proliferation of cancer
807 cells in skin cancer (Hayakawa et al. 2012; Iriyama et al. 2009).

808

809 Inhibition of ASK1 with compound K811 has been shown to prevent cell proliferation in
810 gastric cancer cell lines and reduce the size of xenograft tumours (Hayakawa et al. 2012).

811 Recently, Luo et al. 2016, investigated the involvement of ASK1 during proliferation in

812 pancreatic tumour cell line PANC-1 (Luo et al. 2016). The knock-down of ASK1 in mice with

813 pancreatic tumours reduced tumour growth, suggesting that ASK1 has an important role in

814 pancreatic tumorigenesis. The same group also demonstrated a dose-dependent inhibition

815 of the PANC-1 cell line when cells were treated with NQDI-1 at concentrations of 10 and 30

816 μM . However, the inhibition of ASK1 did not increase levels of apoptosis.

817

818 We have shown that increasing concentrations of NQDI-1 (0.2-200 μM) significantly reduce

819 the level of viable HL60 cells at 100 and 200 μM . This could suggest that ASK1 is expressed

820 at different levels in different cell types as a higher concentration was required in HL60 cells

821 compared to PANC-1 cells. Interestingly, the increasing concentrations of Sunitinib with 2.5

822 μM NQDI-1 enhanced the level of Sunitinib induced a reduction in HL60 cell proliferation.

823 The reason for this is not yet clear and further investigation into this is required.

824

825 As mentioned before NQDI-1 blocks FGFR-1 (Volynets et al. 2011). In cancer cells FGFR1

826 inhibitors have shown to elicit direct anti-tumour effects. The FGFR-1 inhibitors being

827 investigated in clinical trials for their anti-tumour qualities effecting various cancer types

828 include AZD4547, BGJ398, Debio-1347 and dovitinib (Katoh 2016). The apoptotic effect of

829 NQDI-1 we are observing in HL60 cells can therefore be a direct consequence of FGFR-1

830 inhibition.

831

832 In conclusion, our study demonstrates the potential of NQDI-1 as a valuable asset to cardiac

833 injury through the ASK1/MKK7/JNK transduction pathway, which could potentially lead to

1 834 development of cardioprotective adjunct therapy during drug-induced cardiac injury. NQDI-1
2 835 was observed to be cardioprotective as it reduced the Sunitinib-induced infarct size, and
3
4 836 addition it increased the apoptotic effect of Sunitinib in HL60 cells. This could indicate that
5
6 837 NQDI-1 - or an optimised derivative - could potentially be used as cardioprotective adjunct
7
8 838 therapy in e.g. Sunitinib treated leukaemia patients, which would not only protect the
9
10
11 839 patients' hearts but also boost the anti-cancer abilities of Sunitinib.
12

13 840

14
15 841
16
17
18
19
20
21
22
23
24
25
26
27
28
29
30
31
32
33
34
35
36
37
38
39
40
41
42
43
44
45
46
47
48
49
50
51
52
53
54
55
56
57
58
59
60
61
62
63
64
65

842 **Funding**

843 This research did not receive any specific grant from funding agencies in the public,
844 commercial, or non-for-profit sectors.

845

846 **Conflict of interest**

847 All authors have no conflict of interest to declare.

848

849 **Acknowledgments**

850 The assistance and support from technicians at Coventry University Mr Mark Bodycote and
851 Mrs Bethan Grist is greatly appreciated.

852

853 **Figure legends**

854 Figure 1: Infarct to whole heart ratio assessment. The hearts were drug perfused with
855 Sunitinib and/or NQDI-1 for 125 min in an isolated Langendorff heart model. This establishes
856 that Sunitinib-induced cardiotoxicity is reduced by ASK1 inhibitor NQDI-1. Groups: Control,
857 Sunitinib (1 μ M), Sunitinib (1 μ M) and NQDI-1 (2.5 μ M), and NQDI-1 (2.5 μ M) (n=6 per
858 group). Groups were assessed for statistical significance at each time point using one-way
859 ANOVA. Control versus Sunitinib (**=P<0.001), Control versus Sunitinib+NQDI-1
860 (**=P<0.01), Control versus NQDI-1 (*=P<0.05), or Sunitinib vs Sunitinib+NQDI-1
861 (###=P<0.001).

862

863 Figure 2: Cardiotoxicity linked microRNAs expression. The effect of Sunitinib (1 μ M) and the
864 co-administration of ASK1 inhibitor, NQDI-1 (2.5 μ M), on the expression of cardiotoxicity
865 linked microRNAs following 125 minute drug perfusion in an isolated heart Langendorff
866 model. The qRT-PCR results are shown as the ratio of target microRNA normalised to U6
867 with control group microRNA ratio set as 1 of microRNAs A) miR-1, B) miR-27a, C) miR-
868 133a and D) miR-133b. The ratio of target microRNA normalised to U6 is presented on a log
869 scale. Groups: Control (n=6 for miR-1, miR-27a and miR-133a; n=5 for miR-133b), Sunitinib

1
2 871 (1 μ M) (n=6 for miR-1 and miR-27a; n=5 for miR-133a and miR-133b), Sunitinib (1 μ M) and
3
4 872 NQDI-1 (2.5 μ M) (n=6 for miR-1, miR-27a, miR-133a and miR-133b), and NQDI-1 (2.5 μ M)
5
6 873 (n=4 for miR-1, miR-27a, miR-133a and miR-133b). Groups were assessed for statistical
7
8 874 significance at each time point using one-way ANOVA. Control versus Sunitinib
9
10 875 (***=P<0.001), Control versus Sunitinib+NQDI-1 (*=P<0.05, **=P<0.01), Control versus
11
12 876 NQDI-1 (**=P<0.01, ***=P<0.001), or Sunitinib vs Sunitinib+NQDI-1 (#=p<0.05,
13
14 877 ###=P<0.001).

15
16
17
18 878 **Figure 3: MKK7 mRNA expression levels. The qRT-PCR assessment of MKK7 mRNA**
19
20 879 **expression levels in an isolated heart Langendorff model. The qRT-PCR results are shown**
21
22 880 **as the ratio of MKK7 mRNA normalised to GAPDH with control group ratio set as 1. Groups:**
23
24 881 **Control (n=5), Sunitinib (1 μ M) (n=6), Sunitinib (1 μ M) and NQDI-1 (2.5 μ M) (n=3), and**
25
26 882 **NQDI-1 (2.5 μ M) (n=3). Groups were assessed for statistical significance at each time point**
27
28 883 **using one-way ANOVA. Control versus Sunitinib, Control versus Sunitinib+NQDI-1, Control**
29
30 884 **versus NQDI-1, or Sunitinib vs Sunitinib+NQDI-1 (#=p<0.05).**

31
32
33 885
34
35 886 **Figure 4: ASK1/MKK7/JNK pathway western blot assessment. A) p-ASK1, B) p-MKK7, and**
36
37 887 **C) p-JNK phosphorylation levels in an isolated heart Langendorff model. Sorbitol was**
38
39 888 **included as a positive control in p-MKK7 Western blot analysis (n=4). Groups: Control (n=6**
40
41 889 **for p-ASK1; n=4 for p-MKK7 and p-JNK), Sunitinib (1 μ M) (n=5 for p-ASK1; n=4 for p-MKK7**
42
43 890 **and p-JNK), Sunitinib (1 μ M) and NQDI-1 (2.5 μ M) (n=6 for p-ASK1; n=4 for p-MKK7 and p-**
44
45 891 **JNK) and NQDI-1 (2.5 μ M) (n=5 for p-ASK1; n=4 for p-MKK7 and p-JNK). Groups were**
46
47 892 **assessed for statistical significance at each time point using one-way ANOVA. Control**
48
49 893 **versus Sunitinib (***=P<0.001), Control versus Sunitinib+NQDI-1 (*=p<0.05), Control versus**
50
51 894 **NQDI-1 (**=P<0.01; ***=P<0.001), or Sunitinib vs Sunitinib+NQDI-1 (#=p<0.05;**
52
53 895 **###=P<0.001).**

897 **Figure 5:** HL60 cell viability. HL60 cells (10^5 cells/ml) were incubated for 24 hours with
1
2 898 control or with increasing concentrations of A) Sunitinib (0.1 – 10 μ M) or Sunitinib (0.1 – 10
3
4 899 μ M) + NQDI-1 (2.5 μ M) or B) NQDI-1 (0.2 μ M – 200 μ M). Groups were assessed for
5
6 900 statistical significance at each time point using one-way ANOVA. Control versus Sunitinib
7
8 901 (*= P <0.05 and ***= P <0.001), Control versus NQDI-1 (*= P <0.05 and ***= P <0.001), or
9
10 902 Sunitinib vs Sunitinib+NQDI-1 (###= p <0.001). **Figure 1:** Infarct to whole heart ratio
11
12 903 assessment. The hearts were drug perfused with Sunitinib and/or NQDI-1 for 125 min in an
13
14 904 isolated Langendorff heart model. This establishes that Sunitinib-induced cardiotoxicity is
15
16 905 reduced by ASK1 inhibitor NQDI-1. Groups: Control, Sunitinib (1 μ M), Sunitinib (1 μ M) and
17
18 906 NQDI-1 (2.5 μ M), and NQDI-1 (2.5 μ M) (n=6 per group). Groups were assessed for
19
20 907 statistical significance at each time point using one-way ANOVA. Control versus Sunitinib
21
22 908 (red ***= P <0.001), Control versus Sunitinib+NQDI-1 (green **= P <0.01), Control versus
23
24 909 NQDI-1 (blue *= P <0.05), or Sunitinib vs Sunitinib+NQDI-1 (purple \$\$\$= P <0.001).
25
26
27
28
29
30

31 911 **Figure 2:** Cardiotoxicity linked microRNAs expression. The effect of Sunitinib (1 μ M) and the
32
33 912 co-administration of ASK1 inhibitor, NQDI-1 (2.5 μ M), on the expression of cardiotoxicity
34
35 913 linked microRNAs following 125 minute drug perfusion in an isolated heart Langendorff
36
37 914 model. The qRT-PCR results are shown as the ratio of target microRNA normalised to U6
38
39 915 with control group microRNA ratio set as 1 of microRNAs A) miR-1, B) miR-27a, C) miR-
40
41 916 133a and D) miR-133b. The ratio of target microRNA normalised to U6 is presented on a log
42
43 917 scale. Groups: Control (n=6 for miR-1, miR-27a and miR-133a; n=5 for miR-133b), Sunitinib
44
45 918 (1 μ M) (n=6 for miR-1 and miR-27a; n=5 for miR-133a and miR-133b), Sunitinib (1 μ M) and
46
47 919 NQDI-1 (2.5 μ M) (n=6 for miR-1, miR-27a, miR-133a and miR-133b), and NQDI-1 (2.5 μ M)
48
49 920 (n=4 for miR-1, miR-27a, miR-133a and miR-133b). Groups were assessed for statistical
50
51 921 significance at each time point using one-way ANOVA. Control versus Sunitinib (red
52
53 922 ***= P <0.001), Control versus Sunitinib+NQDI-1 (green *= P <0.05, **= P <0.01), Control versus
54
55 923 NQDI-1 (blue **= P <0.01, ***= P <0.001), or Sunitinib vs Sunitinib+NQDI-1 (purple \$= p <0.05,
56
57 924 \$\$\$= P <0.001).
58
59
60
61
62
63
64
65

925

926

927

Figure 3: MKK7 mRNA expression levels. The qRT-PCR assessment of MKK7 mRNA

928

expression levels in an isolated heart Langendorff model. The qRT-PCR results are shown

929

as the ratio of MKK7 mRNA normalised to GAPDH with control group ratio set as 1. Groups:

930

Control (n=5), Sunitinib (1 μ M) (n=6), Sunitinib (1 μ M) and NQDI-1 (2.5 μ M) (n=3), and

931

NQDI-1 (2.5 μ M) (n=3). Groups were assessed for statistical significance at each time point

932

using one-way ANOVA. Control versus Sunitinib, Control versus Sunitinib+NQDI-1, Control

933

versus NQDI-1, or Sunitinib vs Sunitinib+NQDI-1 (purple $\$=p<0.05$).

934

935

Figure 4: ASK1/MKK7/JNK pathway western blot assessment. A) p-ASK1, B) p-MKK7, and

936

C) p-JNK phosphorylation levels in an isolated heart Langendorff model. Sorbitol was

937

included as a positive control in p-MKK7 Western blot analysis (n=4). Groups: Control (n=6

938

for p-ASK1; n=4 for p-MKK7 and p-JNK), Sunitinib (1 μ M) (n=5 for p-ASK1; n=4 for p-MKK7

939

and p-JNK), Sunitinib (1 μ M) and NQDI-1 (2.5 μ M) (n=6 for p-ASK1; n=4 for p-MKK7 and p-

940

JNK) and NQDI-1 (2.5 μ M) (n=5 for p-ASK1; n=4 for p-MKK7 and p-JNK). Groups were

941

assessed for statistical significance at each time point using one-way ANOVA. Control

942

versus Sunitinib (red $***=P<0.001$), Control versus Sunitinib+NQDI-1 (green $*=p<0.05$),

943

Control versus NQDI-1 (blue $**=P<0.01$; $***=P<0.001$), or Sunitinib vs Sunitinib+NQDI-1

944

(purple $\$=p<0.05$; $$$$=P<0.001$).

945

946

Figure 5: HL60 cell viability. HL60 cells (10^5 cells/ml) were incubated for 24 hours with

947

control or with increasing concentrations of A) Sunitinib (0.1—10 μ M) or Sunitinib (0.1—10

948

μ M) + NQDI-1 (2.5 μ M) or B) NQDI-1 (0.2 μ M—200 μ M). Groups were assessed for

949

statistical significance at each time point using one-way ANOVA. Control versus Sunitinib

950

(red $*=P<0.05$ and $***=P<0.001$), Control versus NQDI-1 (blue $*=P<0.05$ and $***=P<0.001$),

951

or Sunitinib vs Sunitinib+NQDI-1 (purple $$$$=p<0.001$).

952

- 1
- 2
- 3
- 4
- 5
- 6
- 7
- 8
- 9
- 10
- 11
- 12
- 13
- 14
- 15
- 16
- 17
- 18
- 19
- 20
- 21
- 22
- 23
- 24
- 25
- 26
- 27
- 28
- 29
- 30
- 31
- 32
- 33
- 34
- 35
- 36
- 37
- 38
- 39
- 40
- 41
- 42
- 43
- 44
- 45
- 46
- 47
- 48
- 49
- 50
- 51
- 52
- 53
- 54
- 55
- 56
- 57
- 58
- 59
- 60
- 61
- 62
- 63
- 64
- 65

References

954

1

955

2

956 Aggarwal, S., Kamboj, J. and Arora, R. 2013. Chemotherapy-related cardiotoxicity. *Ther Adv*

3

957 *Cardiovasc Dis* 7, 87-98.

4

5

6

958 Akat, K.M., Moore-McGriff, D., Morozov, P., Brown, M., Gogakos, T., Correa Da Rosa, J.,

7

8

959 Mihailovic, A., Sauer, M., Ji, R., Ramarathnam, A., Totary-Jain, H., Williams, Z., Tuschl, T.

9

10

960 and Schulze, P.C. 2014. Comparative RNA-sequencing analysis of myocardial and

11

12

961 circulating small RNAs in human heart failure and their utility as biomarkers. *Proc Natl Acad*

13

14

962 *Sci U S A* 111, 11151-11156.

15

16

17

963 Babiarz, J.E., Ravon, M., Sridhar, S., Ravindran, P., Swanson, B., Bitter, H., Weiser, T.,

18

19

964 Chiao, E., Certa, U. and Kolaja, K.L. 2012. Determination of the human cardiomyocyte

20

21

965 mRNA and miRNA differentiation network by fine-scale profiling. *Stem Cells Dev* 21, 1956-

22

23

966 1965.

24

25

26

967 Bagga, S., Bracht, J., Hunter, S., Massirer, K., Holtz, J., Eachus, R. and Pasquinelli, A.E.

27

28

968 2005. Regulation by let-7 and lin-4 miRNAs results in target mRNA degradation. *Cell* 122,

29

30

969 553-563.

31

32

970 Bello, C.L., Mulay, M., Huang, X., Patyna, S., Dinolfo, M., Levine, S., Van Vugt, A., Toh, M.,

33

34

971 Baum, C. and Rosen, L. 2009. Electrocardiographic characterization of the QTc interval in

35

36

972 patients with advanced solid tumors: pharmacokinetic- pharmacodynamic evaluation of

37

38

973 sunitinib. *Clin Cancer Res* 15, 7045-7052.

39

40

41

974 Boehm, M., Kojonazarov, B., Ghofrani, H. A., Grimminger, F., Weissmann, N., Liles, J. T.,

42

43

975 Budas, G. R., Seeger, W., and Schermuly, R. T. . 2015. Effects of Apoptosis Signal-

44

45

976 Regulating Kinase 1 (ASK1) Inhibition in Experimental Pressure Overload-Induced Right

46

47

977 Ventricular Dysfunction. *European Respiratory Journal* 46, PA4913.

48

49

978 Care, A., Catalucci, D., Felicetti, F., Bonci, D., Addario, A., Gallo, P., Bang, M.L., Segnalini,

50

51

979 P., Gu, Y., Dalton, N.D., Elia, L., Latronico, M.V., Hoydal, M., Autore, C., Russo, M.A., Dorn,

52

53

980 G.W., Ellingsen, O., Ruiz-Lozano, P., Peterson, K.L., Croce, C.M., Peschle, C. and

54

55

981 Condorelli, G. 2007. MicroRNA-133 controls cardiac hypertrophy. *Nat. Med* 13, 613-618.

56

57

58

59

60

61

62

63

64

65

1 982 Chang, L. and Karin, M. 2001. Mammalian MAP kinase signalling cascades. *Nature* 410, 37-
2 983 40.
3
4 984 Chu, T.F., Rupnick, M.A., Kerkela, R., Dallabrida, S.M., Zurakowski, D., Nguyen, L., Woulfe,
5
6 985 K., Pravda, E., Cassiola, F., Desai, J., George, S., Morgan, J.A., Harris, D.M., Ismail, N.S.,
7
8 986 Chen, J.H., Schoen, F.J., Van den Abbeele, A.D., Demetri, G.D., Force, T. and Chen, M.H.
9
10 987 2007. Cardiotoxicity associated with tyrosine kinase inhibitor sunitinib. *Lancet* 370, 2011-
11
12 988 2019.
13
14 989 Di Lorenzo, G., Autorino, R., Bruni, G., Carteni, G., Ricevuto, E., Tudini, M., Ficorella, C.,
15
16 990 Romano, C., Aieta, M., Giordano, A., Giuliano, M., Gonnella, A., De Nunzio, C., Rizzo, M.,
17
18 991 Montesarchio, V., Ewer, M. and De Placido, S. 2009. Cardiovascular toxicity following
19
20 992 sunitinib therapy in metastatic renal cell carcinoma: a multicenter analysis. *Ann Oncol* 20,
21
22 993 1535-1542.
23
24 994 Doherty, K.R., Wappel, R.L., Talbert, D.R., Trusk, P.B., Moran, D.M., Kramer, J.W., Brown,
25
26 995 A.M., Shell, S.A. and Bacus, S. 2013. Multi-parameter in vitro toxicity testing of crizotinib,
27
28 996 sunitinib, erlotinib, and nilotinib in human cardiomyocytes. *Toxicol Appl Pharmacol* 272, 245-
29
30 997 255.
31
32 998 Eaton, G.J., Zhang, Q.S., Diallo, C., Matsuzawa, A., Ichijo, H., Steinbeck, M.J. and Freeman,
33
34 999 T.A. 2014. Inhibition of apoptosis signal-regulating kinase 1 enhances endochondral bone
35
36 1000 formation by increasing chondrocyte survival. *Cell Death Dis* 5, e1522.
37
38 1001 Ewer, M.S., Suter, T.M., Lenihan, D.J., Niculescu, L., Breazna, A., Demetri, G.D. and
39
40 1002 Motzer, R.J. 2014. Cardiovascular events among 1090 cancer patients treated with sunitinib,
41
42 1003 interferon, or placebo: a comprehensive adjudicated database analysis demonstrating
43
44 1004 clinically meaningful reversibility of cardiac events. *Eur J Cancer* 50, 2162-2170.
45
46 1005 Faivre, S., Demetri, G., Sargent, W. and Raymond, E. 2007. Molecular basis for sunitinib
47
48 1006 efficacy and future clinical development. *Nat Rev Drug Discov* 6, 734-745.
49
50 1007 Fenton, M.S., Marion, K.M., Salem, A.K., Hogen, R., Naeim, F. and Hershman, J.M. 2010.
51
52 1008 Sunitinib inhibits MEK/ERK and SAPK/JNK pathways and increases sodium/iodide
53
54 1009 symporter expression in papillary thyroid cancer. *Thyroid* 20, 965-974.
55
56
57
58
59
60
61
62
63
64
65

1010 Foltz, I.N., Gerl, R.E., Wieler, J.S., Luckach, M., Salmon, R.A. and Schrader, J.W. 1998.
1
2 1011 Human mitogen-activated protein kinase kinase 7 (MKK7) is a highly conserved c-Jun N-
3
4 1012 terminal kinase/stress-activated protein kinase (JNK/SAPK) activated by environmental
5
6 1013 stresses and physiological stimuli. *J Biol Chem* 273, 9344-9351.
7
8
9 1014 Force, T., Krause, D.S. and Van Etten, R.A. 2007. Molecular mechanisms of cardiotoxicity of
10
11 1015 tyrosine kinase inhibition. *Nat. Rev. Cancer* 7, 332-344.
12
13 1016 Fujii, K., Goldman, E.H., Park, H.R., Zhang, L., Chen, J. and Fu, H. 2004. Negative control of
14
15 1017 apoptosis signal-regulating kinase 1 through phosphorylation of Ser-1034. *Oncogene* 23,
16
17 1018 5099-5104.
18
19
20 1019 Gerczuk, P.Z., Breckenridge, D.G., Liles, J.T., Budas, G.R., Shryock, J.C., Belardinelli, L.,
21
22 1020 Kloner, R.A. and Dai, W. 2012. An apoptosis signal-regulating kinase 1 inhibitor reduces
23
24 1021 cardiomyocyte apoptosis and infarct size in a rat ischemia-reperfusion model. *J Cardiovasc*
25
26 1022 *Pharmacol* 60, 276-282.
27
28
29 1023 Gharanei, M., Hussain, A., Janneh, O. and Maddock, H. 2013. Attenuation of doxorubicin-
30
31 1024 induced cardiotoxicity by mdivi-1: a mitochondrial division/mitophagy inhibitor. *PLoS One* 8,
32
33 1025 e77713.
34
35
36 1026 Ghatalia, P., Je, Y., Kaymakcalan, M.D., Sonpavde, G. and Choueiri, T.K. 2015. QTc interval
37
38 1027 prolongation with vascular endothelial growth factor receptor tyrosine kinase inhibitors. *Br J*
39
40 1028 *Cancer* 112, 296-305.
41
42 1029 Guo, L., Coyle, L., Abrams, R.M., Kemper, R., Chiao, E.T. and Kolaja, K.L. 2013. Refining
43
44 1030 the human iPSC-cardiomyocyte arrhythmic risk assessment model. *Toxicol Sci* 136, 581-
45
46 1031 594.
47
48
49 1032 Guttilla, I.K. and White, B.A. 2009. Coordinate regulation of FOXO1 by miR-27a, miR-96,
50
51 1033 and miR-182 in breast cancer cells. *J Biol Chem* 284, 23204-23216.
52
53 1034 Hahn, V.S., Lenihan, D.J. and Ky, B. 2014. Cancer therapy-induced cardiotoxicity: basic
54
55 1035 mechanisms and potential cardioprotective therapies. *J Am Heart Assoc* 3, e000665.
56
57
58
59
60
61
62
63
64
65

1036 Hao, H., Li, S., Tang, H., Liu, B., Cai, Y., Shi, C. and Xiao, X. 2016. NQDI-1, an inhibitor of
1
2 1037 ASK1 attenuates acute perinatal hypoxic-ischemic cerebral injury by modulating cell death.
3
4 1038 Mol Med Rep 13, 4585-4592.
5
6 1039 Hasinoff, B.B., Patel, D. and O'Hara, K.A. 2008. Mechanisms of myocyte cytotoxicity
7
8 1040 induced by the multiple receptor tyrosine kinase inhibitor sunitinib. Mol. Pharmacol 74, 1722-
9
10 1041 1728.
11
12
13 1042 Hattori, K., Naguro, I., Runchel, C. and Ichijo, H. 2009. The roles of ASK family proteins in
14
15 1043 stress responses and diseases. Cell Commun Signal 7, 9.
16
17
18 1044 Hayakawa, Y., Hirata, Y., Sakitani, K., Nakagawa, H., Nakata, W., Kinoshita, H., Takahashi,
19
20 1045 R., Takeda, K., Ichijo, H., Maeda, S. and Koike, K. 2012. Apoptosis signal-regulating kinase-
21
22 1046 1 inhibitor as a potent therapeutic drug for the treatment of gastric cancer. Cancer Sci 103,
23
24 1047 2181-2185.
25
26
27 1048 He, X., Liu, Y., Sharma, V., Dirksen, R.T., Waugh, R., Sheu, S.S. and Min, W. 2003. ASK1
28
29 1049 associates with troponin T and induces troponin T phosphorylation and contractile
30
31 1050 dysfunction in cardiomyocytes. Am J Pathol 163, 243-251.
32
33 1051 Henderson, K.A., Borders, R.B., Ross, J.B., Huwar, T.B., Travis, C.O., Wood, B.J., Ma, Z.J.,
34
35 1052 Hong, S.P., Vinci, T.M. and Roche, B.M. 2013. Effects of tyrosine kinase inhibitors on rat
36
37 1053 isolated heart function and protein biomarkers indicative of toxicity. J. Pharmacol. Toxicol.
38
39 1054 Methods 68, 150-159.
40
41
42 1055 Hikoso, S., Ikeda, Y., Yamaguchi, O., Takeda, T., Higuchi, Y., Hirotsu, S., Kashiwase, K.,
43
44 1056 Yamada, M., Asahi, M., Matsumura, Y., Nishida, K., Matsuzaki, M., Hori, M. and Otsu, K.
45
46 1057 2007. Progression of heart failure was suppressed by inhibition of apoptosis signal-
47
48 1058 regulating kinase 1 via transcortical gene transfer. J Am Coll Cardiol 50, 453-462.
49
50
51 1059 Hu, S., Niu, H., Minkin, P., Orwick, S., Shimada, A., Inaba, H., Dahl, G.V., Rubnitz, J. and
52
53 1060 Baker, S.D. 2008. Comparison of antitumor effects of multitargeted tyrosine kinase inhibitors
54
55 1061 in acute myelogenous leukemia. Mol Cancer Ther 7, 1110-1120.
56
57
58 1062 Huang, Q., Zhou, H.J., Zhang, H., Huang, Y., Hinojosa-Kirschenbaum, F., Fan, P., Yao, L.,
59
60 1063 Belardinelli, L., Tellides, G., Giordano, F.J., Budas, G.R. and Min, W. 2015. Thioredoxin-2
61
62
63
64
65

1064 inhibits mitochondrial reactive oxygen species generation and apoptosis stress kinase-1
1
2 1065 activity to maintain cardiac function. *Circulation* 131, 1082-1097.
3
4 1066 Huynh, H., Choo, S.P., Toh, H.C., Tai, W.M., Chung, A.Y., Chow, P.K., Ong, R. and Soo,
5
6 1067 K.C. 2011. Comparing the efficacy of sunitinib with sorafenib in xenograft models of human
7
8 1068 hepatocellular carcinoma: mechanistic explanation. *Curr Cancer Drug Targets* 11, 944-953.
9
10
11 1069 Ichijo, H., Nishida, E., Irie, K., ten Dijke, P., Saitoh, M., Moriguchi, T., Takagi, M.,
12
13 1070 Matsumoto, K., Miyazono, K. and Gotoh, Y. 1997. Induction of apoptosis by ASK1, a
14
15 1071 mammalian MAPKKK that activates SAPK/JNK and p38 signaling pathways. *Science* 275,
16
17 1072 90-94.
18
19
20 1073 Ilyas, A.M., Ahmed, Y., Gari, M., Alqahtani, M. H., Kumosani, T. A., Al-Malki, A. L.,
21
22 1074 Abualnaja, K. O., Albohairy, S. H., Chaudhary, A. G., and Ahmed, F. . 2016. Sunitinib
23
24 1075 Reduces Acute Myeloid Leukemia Clonogenic Cells in Vitro and has Potent Inhibitory Effect
25
26 1076 on Sorted AML ALDH Cells. . *Open Journal of Blood Diseases* 6, 9.
27
28
29 1077 Iriyama, T., Takeda, K., Nakamura, H., Morimoto, Y., Kuroiwa, T., Mizukami, J., Umeda, T.,
30
31 1078 Noguchi, T., Naguro, I., Nishitoh, H., Saegusa, K., Tobiume, K., Homma, T., Shimada, Y.,
32
33 1079 Tsuda, H., Aiko, S., Imoto, I., Inazawa, J., Chida, K., Kamei, Y., Kozuma, S., Taketani, Y.,
34
35 1080 Matsuzawa, A. and Ichijo, H. 2009. ASK1 and ASK2 differentially regulate the counteracting
36
37 1081 roles of apoptosis and inflammation in tumorigenesis. *EMBO J* 28, 843-853.
38
39
40 1082 Izumiya, Y., Kim, S., Izumi, Y., Yoshida, K., Yoshiyama, M., Matsuzawa, A., Ichijo, H. and
41
42 1083 Iwao, H. 2003. Apoptosis signal-regulating kinase 1 plays a pivotal role in angiotensin II-
43
44 1084 induced cardiac hypertrophy and remodeling. *Circ Res* 93, 874-883.
45
46
47 1085 Jia, B., Guo, M., Li, G., Yu, D., Zhang, X., Lan, K. and Deng, Q. 2015. Hepatitis B virus core
48
49 1086 protein sensitizes hepatocytes to tumor necrosis factor-induced apoptosis by suppression of
50
51 1087 the phosphorylation of mitogen-activated protein kinase kinase 7. *J Virol* 89, 2041-2051.
52
53 1088 Kaiser, R.A., Liang, Q., Bueno, O., Huang, Y., Lackey, T., Klevitsky, R., Hewett, T.E. and
54
55 1089 Molkenstin, J.D. 2005. Genetic inhibition or activation of JNK1/2 protects the myocardium
56
57 1090 from ischemia-reperfusion-induced cell death in vivo. *J Biol Chem* 280, 32602-32608.
58
59
60
61
62
63
64
65

1091 Kataoka, K., Koibuchi, N., Toyama, K., Sueta, D., Dong, Y., Ogawa, H., Kim-Mitsuyama, S.
1
2 1092 2011. ASK2 is a Novel Factor Associated with Salt-Sensitive Hypertension. *Circulation* 124,
3
4 1093 A9386.
5
6 1094 Kataoka, K., Nakamura, T., Dong, Y., Fukuda, M., Nako, H., Toyama, K., Sueta, D., Ogawa,
7
8 1095 H., Kim-Mitsuyama, S. 2010. ASK2 Deficiency Causes Hypertension and Cardiac Fibrosis
9
10 1096 Independently of the Presence of ASK1 ~ Investigation with ASK1/2 Double Deficient Mice.
11
12 1097 *Circulation* 122, A13837.
13
14 1098 Kataoka, K., Nakamura, T., Fukuda, M., Nako, H., Dong, Y., Liu, R., Tokutomi, Y., Ogawa,
15
16 1099 H., Kim-Mitsuyama, S. 2009. Apoptosis Signal-Regulating Kinase (ASK) 2 Deficient Mice
17
18 1100 Have Salt-Resistant Hypertension With Cardiac Hypertrophy. *Circulation* 120, S1112.
19
20 1101 Kataoka, K., Tokutomi, Y., Yamamoto, E., Nakamura, T., Fukuda, M., Dong, Y., Ogawa, H.,
21
22 1102 Kim-Mitsuyama, S. 2008. ASK2 Deficient Mice Have Elevated Blood Pressures with Cardiac
23
24 1103 Hypertrophy and Remodeling. *Circulation* 118, S_384.
25
26 1104 Kato, M. 2016. FGFR inhibitors: Effects on cancer cells, tumor microenvironment and
27
28 1105 whole-body homeostasis (Review). *Int J Mol Med* 38, 3-15.
29
30 1106 Khakoo, A.Y., Kassiotis, C.M., Tannir, N., Plana, J.C., Halushka, M., Bickford, C., Trent, J.,
31
32 1107 Champion, J.C., Durand, J.B. and Lenihan, D.J. 2008. Heart failure associated with sunitinib
33
34 1108 malate: a multitargeted receptor tyrosine kinase inhibitor. *Cancer* 112, 2500-2508.
35
36 1109 Kim, A.H., Khursigara, G., Sun, X., Franke, T.F. and Chao, M.V. 2001. Akt phosphorylates
37
38 1110 and negatively regulates apoptosis signal-regulating kinase 1. *Mol Cell Biol* 21, 893-901.
39
40 1111 Kim, G.H. 2013. MicroRNA regulation of cardiac conduction and arrhythmias. *Transl Res*
41
42 1112 161, 381-392.
43
44 1113 Kim, I., Shu, C.W., Xu, W., Shiau, C.W., Grant, D., Vasile, S., Cosford, N.D. and Reed, J.C.
45
46 1114 2009. Chemical biology investigation of cell death pathways activated by endoplasmic
47
48 1115 reticulum stress reveals cytoprotective modulators of ASK1. *J Biol Chem* 284, 1593-1603.
49
50 1116 Krause, D.S. and Van Etten, R.A. 2005. Tyrosine kinases as targets for cancer therapy. *N.*
51
52 1117 *Engl. J Med* 353, 172-187.
53
54
55
56
57
58
59
60
61
62
63
64
65

1118 Lavine, K.J., White, A.C., Park, C., Smith, C.S., Choi, K., Long, F., Hui, C.C. and Ornitz,
1
2 1119 D.M. 2006. Fibroblast growth factor signals regulate a wave of Hedgehog activation that is
3
4 1120 essential for coronary vascular development. *Genes Dev* 20, 1651-1666.
5
6 1121 Liu, N., Bezprozvannaya, S., Williams, A.H., Qi, X., Richardson, J.A., Bassel-Duby, R. and
7
8 1122 Olson, E.N. 2008. microRNA-133a regulates cardiomyocyte proliferation and suppresses
9
10
11 1123 smooth muscle gene expression in the heart. *Genes Dev* 22, 3242-3254.
12
13 1124 Liu, W., Zi, M., Chi, H., Jin, J., Prehar, S., Neyses, L., Cartwright, E.J., Flavell, R.A., Davis,
14
15 1125 R.J. and Wang, X. 2011. Deprivation of MKK7 in cardiomyocytes provokes heart failure in
16
17 1126 mice when exposed to pressure overload. *J Mol Cell Cardiol* 50, 702-711.
18
19
20 1127 Luo, Y., Gao, S., Hao, Z., Yang, Y., Xie, S., Li, D., Liu, M. and Zhou, J. 2016. Apoptosis
21
22 1128 signal-regulating kinase 1 exhibits oncogenic activity in pancreatic cancer. *Oncotarget* 7,
23
24 1129 75155-75164.
25
26 1130 Marques, F.Z., Vizi, D., Khammy, O., Mariani, J.A. and Kaye, D.M. 2016. The transcardiac
27
28 1131 gradient of cardio-microRNAs in the failing heart. *Eur J Heart Fail* 18, 1000-1008.
29
30
31 1132 Mima, T., Ueno, H., Fischman, D.A., Williams, L.T. and Mikawa, T. 1995. Fibroblast growth
32
33 1133 factor receptor is required for in vivo cardiac myocyte proliferation at early embryonic stages
34
35 1134 of heart development. *Proc Natl Acad Sci U S A* 92, 467-471.
36
37 1135 Mitchell, S., Ota, A., Foster, W., Zhang, B., Fang, Z., Patel, S., Nelson, S.F., Horvath, S. and
38
39 1136 Wang, Y. 2006. Distinct gene expression profiles in adult mouse heart following targeted
40
41 1137 MAP kinase activation. *Physiol Genomics* 25, 50-59.
42
43 1138 Mooney, L., Skinner, M., Coker, S.J. and Currie, S. 2015. Effects of acute and chronic
44
45 1139 sunitinib treatment on cardiac function and calcium/calmodulin-dependent protein kinase II.
46
47 1140 *Br J Pharmacol* 172, 4342-4354.
48
49
50
51 1141 Morita, K., Saitoh, M., Tobiume, K., Matsuura, H., Enomoto, S., Nishitoh, H. and Ichijo, H.
52
53 1142 2001. Negative feedback regulation of ASK1 by protein phosphatase 5 (PP5) in response to
54
55 1143 oxidative stress. *EMBO J* 20, 6028-6036.
56
57 1144 Nako, H., Kataoka, K., Koibuchi, N., Dong, Y.F., Toyama, K., Yamamoto, E., Yasuda, O.,
58
59 1145 Ichijo, H., Ogawa, H. and Kim-Mitsuyama, S. 2012. Novel mechanism of angiotensin II-

1146 induced cardiac injury in hypertensive rats: the critical role of ASK1 and VEGF. *Hypertens*
1
2 1147 *Res* 35, 194-200.
3
4 1148 Nomura, K., Lee, M., Banks, C., Lee, G. and Morris, B.J. 2013. An ASK1-p38 signalling
5
6 1149 pathway mediates hydrogen peroxide-induced toxicity in NG108-15 neuronal cells. *Neurosci*
7
8 1150 *Lett* 549, 163-167.
9
10
11 1151 Pan, Y., Wang, Y., Zhao, Y., Peng, K., Li, W., Wang, Y., Zhang, J., Zhou, S., Liu, Q., Li, X.,
12
13 1152 Cai, L. and Liang, G. 2014. Inhibition of JNK phosphorylation by a novel curcumin analog
14
15 1153 prevents high glucose-induced inflammation and apoptosis in cardiomyocytes and the
16
17 1154 development of diabetic cardiomyopathy. *Diabetes* 63, 3497-3511.
18
19
20 1155 Rosenkranz, S. 2004. TGF-beta1 and angiotensin networking in cardiac remodeling.
21
22 1156 *Cardiovasc Res* 63, 423-432.
23
24 1157 Roskoski, R., Jr. 2007. Sunitinib: a VEGF and PDGF receptor protein kinase and
25
26 1158 angiogenesis inhibitor. *Biochem Biophys Res Commun* 356, 323-328.
27
28
29 1159 Saitoh, M., Nishitoh, H., Fujii, M., Takeda, K., Tobiume, K., Sawada, Y., Kawabata, M.,
30
31 1160 Miyazono, K. and Ichijo, H. 1998. Mammalian thioredoxin is a direct inhibitor of apoptosis
32
33 1161 signal-regulating kinase (ASK) 1. *EMBO J* 17, 2596-2606.
34
35 1162 Sandhu, H., Ansar, S. and Edvinsson, L. 2010. Comparison of MEK/ERK pathway inhibitors
36
37 1163 on the upregulation of vascular G-protein coupled receptors in rat cerebral arteries. *Eur. J.*
38
39 1164 *Pharmacol* 644, 128-137.
40
41
42 1165 Sandhu, H., Cooper, S., Hussain, A., Mee, C. and Maddock, H. 2017. Attenuation of
43
44 1166 Sunitinib-induced cardiotoxicity through the A3 adenosine receptor activation. *Eur J*
45
46 1167 *Pharmacol*.
47
48
49 1168 Schmidinger, M., Zielinski, C.C., Vogl, U.M., Bojic, A., Bojic, M., Schukro, C., Ruhsam, M.,
50
51 1169 Hejna, M. and Schmidinger, H. 2008. Cardiac toxicity of sunitinib and sorafenib in patients
52
53 1170 with metastatic renal cell carcinoma. *J. Clin. Oncol* 26, 5204-5212.
54
55 1171 Schramek, D., Kotsinas, A., Meixner, A., Wada, T., Elling, U., Pospisilik, J.A., Neely, G.G.,
56
57 1172 Zwick, R.H., Sigl, V., Forni, G., Serrano, M., Gorgoulis, V.G. and Penninger, J.M. 2011. The
58
59
60
61
62
63
64
65

1173 stress kinase MKK7 couples oncogenic stress to p53 stability and tumor suppression. Nat
1
2 1174 Genet 43, 212-219.
3
4 1175 Shah, R.R. and Morganroth, J. 2015. Update on Cardiovascular Safety of Tyrosine Kinase
5
6 1176 Inhibitors: With a Special Focus on QT Interval, Left Ventricular Dysfunction and Overall
7
8 1177 Risk/Benefit. Drug Saf 38, 693-710.
9
10
11 1178 Shukla, S., Robey, R.W., Bates, S.E. and Ambudkar, S.V. 2009. Sunitinib (Sutent,
12
13 1179 SU11248), a small-molecule receptor tyrosine kinase inhibitor, blocks function of the ATP-
14
15 1180 binding cassette (ABC) transporters P-glycoprotein (ABCB1) and ABCG2. Drug Metab
16
17 1181 Dispos 37, 359-365.
18
19
20 1182 Song, M.A., Dasgupta, C. and Zhang, L. 2015. Chronic Losartan Treatment Up-Regulates
21
22 1183 AT1R and Increases the Heart Vulnerability to Acute Onset of Ischemia and Reperfusion
23
24 1184 Injury in Male Rats. PLoS One 10, e0132712.
25
26
27 1185 Song, N.R., Lee, E., Byun, S., Kim, J.E., Mottamal, M., Park, J.H., Lim, S.S., Bode, A.M.,
28
29 1186 Lee, H.J., Lee, K.W. and Dong, Z. 2013. Isoangustone A, a novel licorice compound, inhibits
30
31 1187 cell proliferation by targeting PI3K, MKK4, and MKK7 in human melanoma. Cancer Prev Res
32
33 1188 (Phila) 6, 1293-1303.
34
35
36 1189 Sucharov, C., Bristow, M.R. and Port, J.D. 2008. miRNA expression in the failing human
37
38 1190 heart: functional correlates. J Mol Cell Cardiol 45, 185-192.
39
40 1191 Sundarajan, M., Boyle, D.L., Chabaud-Riou, M., Hammaker, D. and Firestein, G.S. 2003.
41
42 1192 Expression of the MAPK kinases MKK-4 and MKK-7 in rheumatoid arthritis and their role as
43
44 1193 key regulators of JNK. Arthritis Rheum 48, 2450-2460.
45
46
47 1194 Takeda, K., Shimosono, R., Noguchi, T., Umeda, T., Morimoto, Y., Naguro, I., Tobiume, K.,
48
49 1195 Saitoh, M., Matsuzawa, A. and Ichijo, H. 2007. Apoptosis signal-regulating kinase (ASK) 2
50
51 1196 functions as a mitogen-activated protein kinase kinase kinase in a heteromeric complex with
52
53 1197 ASK1. J Biol Chem 282, 7522-7531.
54
55
56 1198 Tang, B., Du, J., Wang, J., Tan, G., Gao, Z., Wang, Z. and Wang, L. 2012. Alpinetin
57
58 1199 suppresses proliferation of human hepatoma cells by the activation of MKK7 and elevates
59
60 1200 sensitization to cis-diammined dichloridoplatium. Oncol Rep 27, 1090-1096.
61
62
63
64
65

1201 Taniike, M., Yamaguchi, O., Tsujimoto, I., Hikoso, S., Takeda, T., Nakai, A., Omiya, S.,
1
2 1202 Mizote, I., Nakano, Y., Higuchi, Y., Matsumura, Y., Nishida, K., Ichijo, H., Hori, M. and Otsu,
3
4 1203 K. 2008. Apoptosis signal-regulating kinase 1/p38 signaling pathway negatively regulates
5
6 1204 physiological hypertrophy. *Circulation* 117, 545-552.
7
8
9 1205 Thijs, A.M., El Messaoudi, S., Vos, J.C., Wouterse, A.C., Verweij, V., van Swieten, H., van
10
11 1206 Herpen, C.M., van der Graaf, W.T., Noyez, L. and Rongen, G.A. 2015. Sunitinib does not
12
13 1207 attenuate contractile force following a period of ischemia in isolated human cardiac muscle.
14
15 1208 *Target Oncol* 10, 439-443.
16
17
18 1209 Thum, T., Galuppo, P., Wolf, C., Fiedler, J., Kneitz, S., van Laake, L.W., Doevendans, P.A.,
19
20 1210 Mummery, C.L., Borlak, J., Haverich, A., Gross, C., Engelhardt, S., Ertl, G. and Bauersachs,
21
22 1211 J. 2007. MicroRNAs in the human heart: a clue to fetal gene reprogramming in heart failure.
23
24 1212 *Circulation* 116, 258-267.
25
26
27 1213 Tijssen, A.J., Pinto, Y.M. and Creemers, E.E. 2012. Non-cardiomyocyte microRNAs in heart
28
29 1214 failure. *Cardiovasc Res* 93, 573-582.
30
31 1215 Tobiume, K., Saitoh, M. and Ichijo, H. 2002. Activation of apoptosis signal-regulating kinase
32
33 1216 1 by the stress-induced activating phosphorylation of pre-formed oligomer. *J Cell Physiol*
34
35 1217 191, 95-104.
36
37
38 1218 Toldo, S., Breckenridge, D.G., Mezzaroma, E., Van Tassell, B.W., Shryock, J., Kannan, H.,
39
40 1219 Phan, D., Budas, G., Farkas, D., Lesnefsky, E., Voelkel, N. and Abbate, A. 2012. Inhibition
41
42 1220 of apoptosis signal-regulating kinase 1 reduces myocardial ischemia-reperfusion injury in the
43
44 1221 mouse. *J Am Heart Assoc* 1, e002360.
45
46
47 1222 Volynets, G.P., Chekanov, M.O., Synyugin, A.R., Golub, A.G., Kukharensko, O.P., Bdzhola,
48
49 1223 V.G. and Yarmoluk, S.M. 2011. Identification of 3H-naphtho[1,2,3-de]quinoline-2,7-diones as
50
51 1224 inhibitors of apoptosis signal-regulating kinase 1 (ASK1). *J Med Chem* 54, 2680-2686.
52
53
54 1225 Wang, X., Destrumont, A. and Tournier, C. 2007. Physiological roles of MKK4 and MKK7:
55
56 1226 insights from animal models. *Biochim Biophys Acta* 1773, 1349-1357.
57
58
59
60
61
62
63
64
65

1227 Wang, Y., Su, B., Sah, V.P., Brown, J.H., Han, J. and Chien, K.R. 1998. Cardiac hypertrophy
1 induced by mitogen-activated protein kinase kinase 7, a specific activator for c-Jun NH2-
2 1228 terminal kinase in ventricular muscle cells. *J Biol Chem* 273, 5423-5426.
3
4 1229
5
6 1230 Windak, R., Muller, J., Felley, A., Akhmedov, A., Wagner, E.F., Pedrazzini, T., Sumara, G.
7
8 1231 and Ricci, R. 2013. The AP-1 transcription factor c-Jun prevents stress-imposed maladaptive
9
10 remodeling of the heart. *PLoS One* 8, e73294.
11 1232
12
13 1233 Xiao, J., Luo, X., Lin, H., Zhang, Y., Lu, Y., Wang, N., Zhang, Y., Yang, B. and Wang, Z.
14
15 1234 2007. MicroRNA miR-133 represses HERG K⁺ channel expression contributing to QT
16
17 1235 prolongation in diabetic hearts. *J Biol Chem* 282, 12363-12367.
18
19
20 1236 Xu, C., Lu, Y., Pan, Z., Chu, W., Luo, X., Lin, H., Xiao, J., Shan, H., Wang, Z. and Yang, B.
21
22 1237 2007. The muscle-specific microRNAs miR-1 and miR-133 produce opposing effects on
23
24 1238 apoptosis by targeting HSP60, HSP70 and caspase-9 in cardiomyocytes. *J. Cell Sci* 120,
25
26 1239 3045-3052.
27
28
29 1240 Yamaguchi, O., Higuchi, Y., Hirotsu, S., Kashiwase, K., Nakayama, H., Hikoso, S., Takeda,
30
31 1241 T., Watanabe, T., Asahi, M., Taniike, M., Matsumura, Y., Tsujimoto, I., Hongo, K., Kusakari,
32
33 1242 Y., Kurihara, S., Nishida, K., Ichijo, H., Hori, M. and Otsu, K. 2003. Targeted deletion of
34
35 1243 apoptosis signal-regulating kinase 1 attenuates left ventricular remodeling. *Proc Natl Acad*
36
37 1244 *Sci U S A* 100, 15883-15888.
38
39
40 1245 Zhang, H., Tao, L., Jiao, X., Gao, E., Lopez, B.L., Christopher, T.A., Koch, W. and Ma, X.L.
41
42 1246 2007. Nitrate thioresoxin inactivation as a cause of enhanced myocardial
43
44 1247 ischemia/reperfusion injury in the aging heart. *Free Radic Biol Med* 43, 39-47.
45
46
47 1248 Zhang, L., Chen, J. and Fu, H. 1999. Suppression of apoptosis signal-regulating kinase 1-
48
49 1249 induced cell death by 14-3-3 proteins. *Proc Natl Acad Sci U S A* 96, 8511-8515.
50
51
52 1250
53
54
55
56
57
58
59
60
61
62
63
64
65

Figure 1
[Click here to download high resolution image](#)

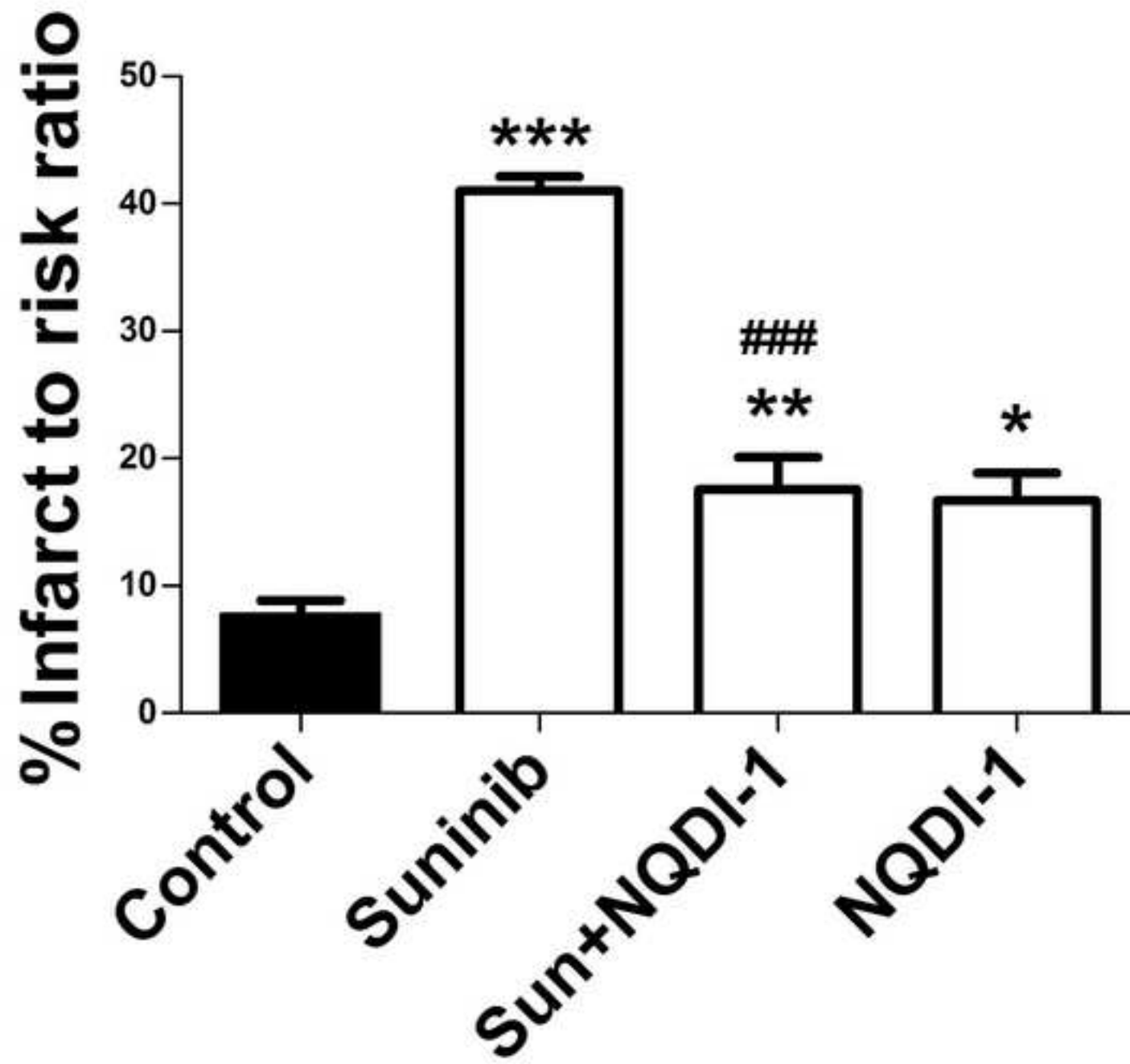


Figure 2A
[Click here to download high resolution image](#)

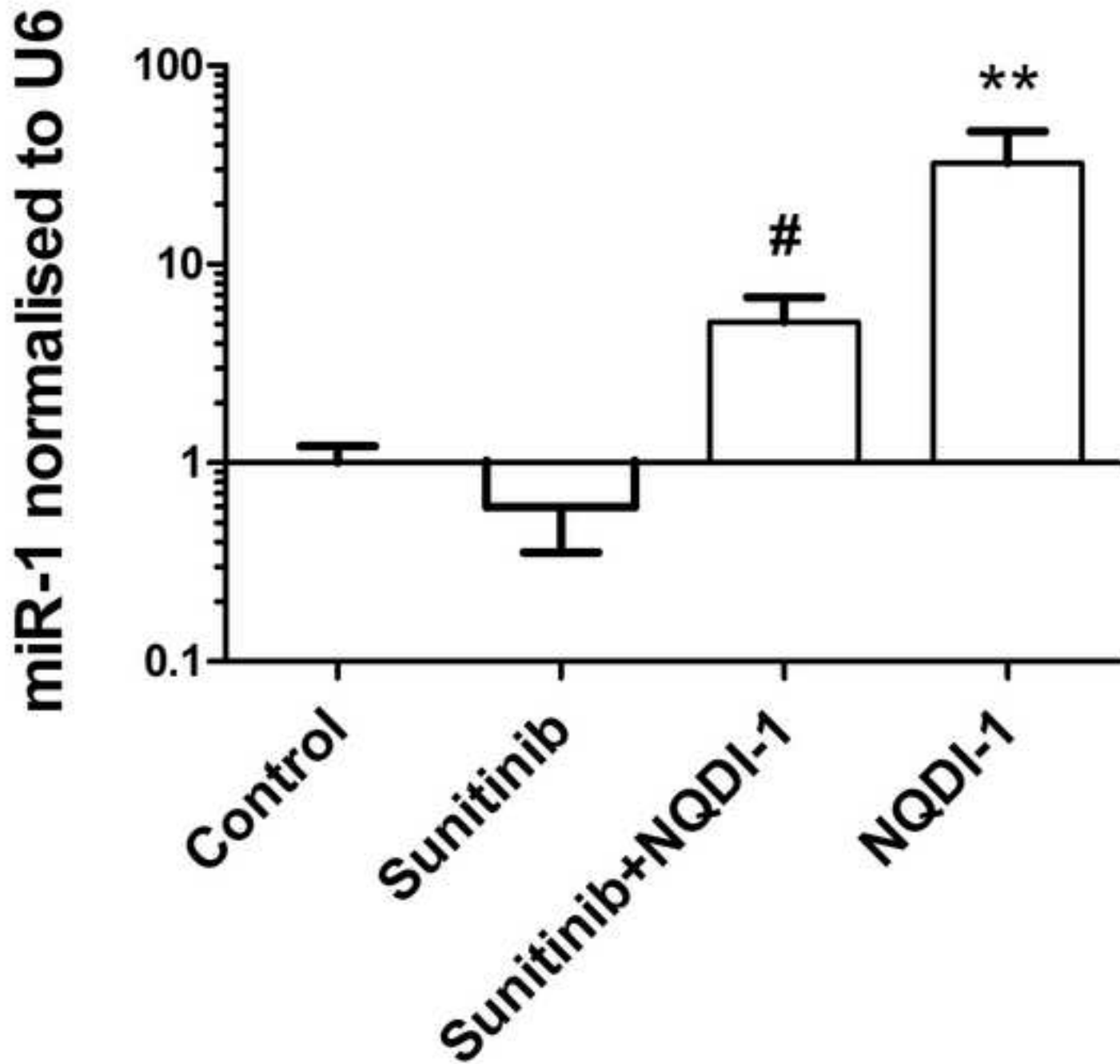


Figure 2B
[Click here to download high resolution image](#)

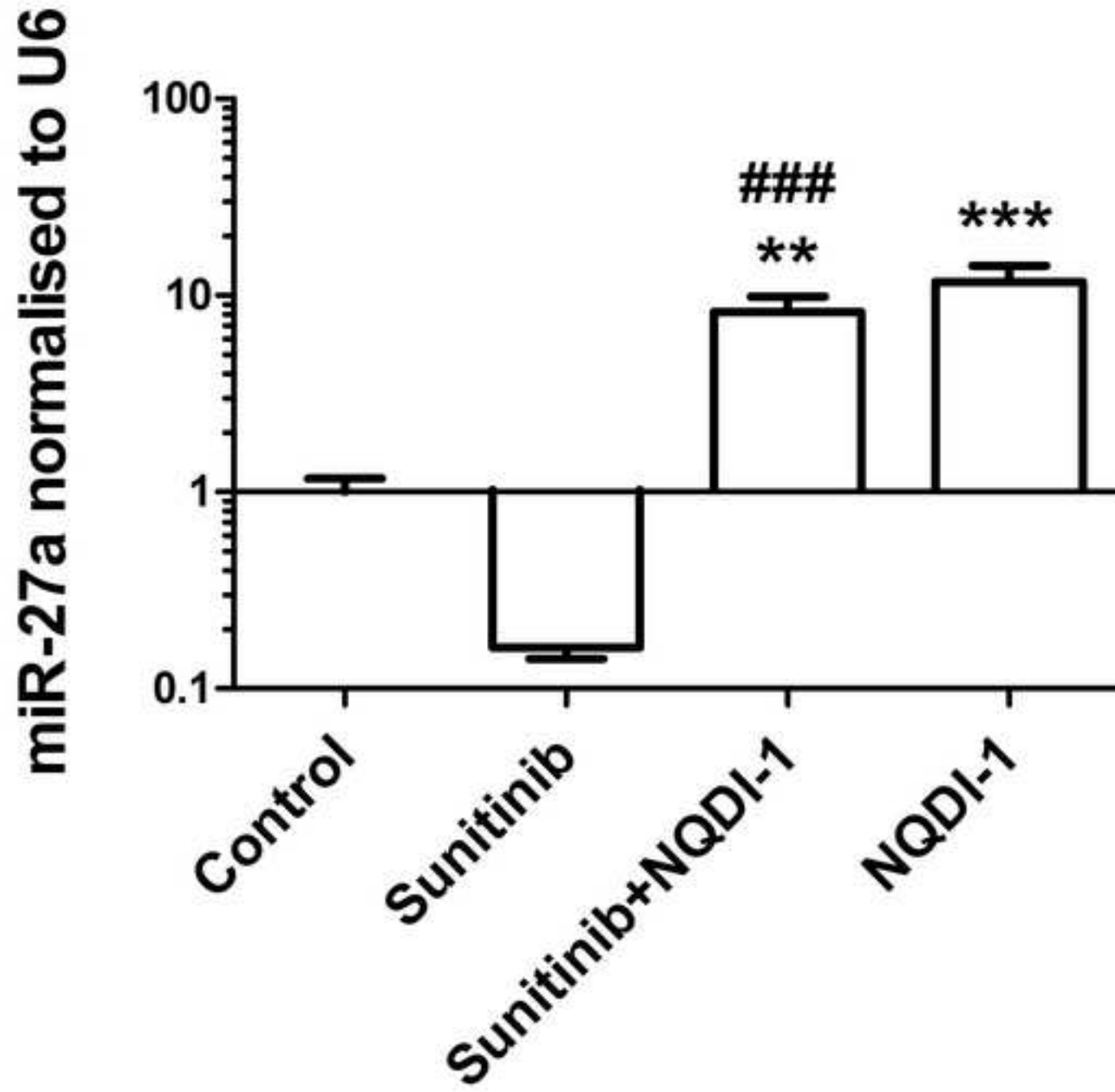


Figure 2C
[Click here to download high resolution image](#)

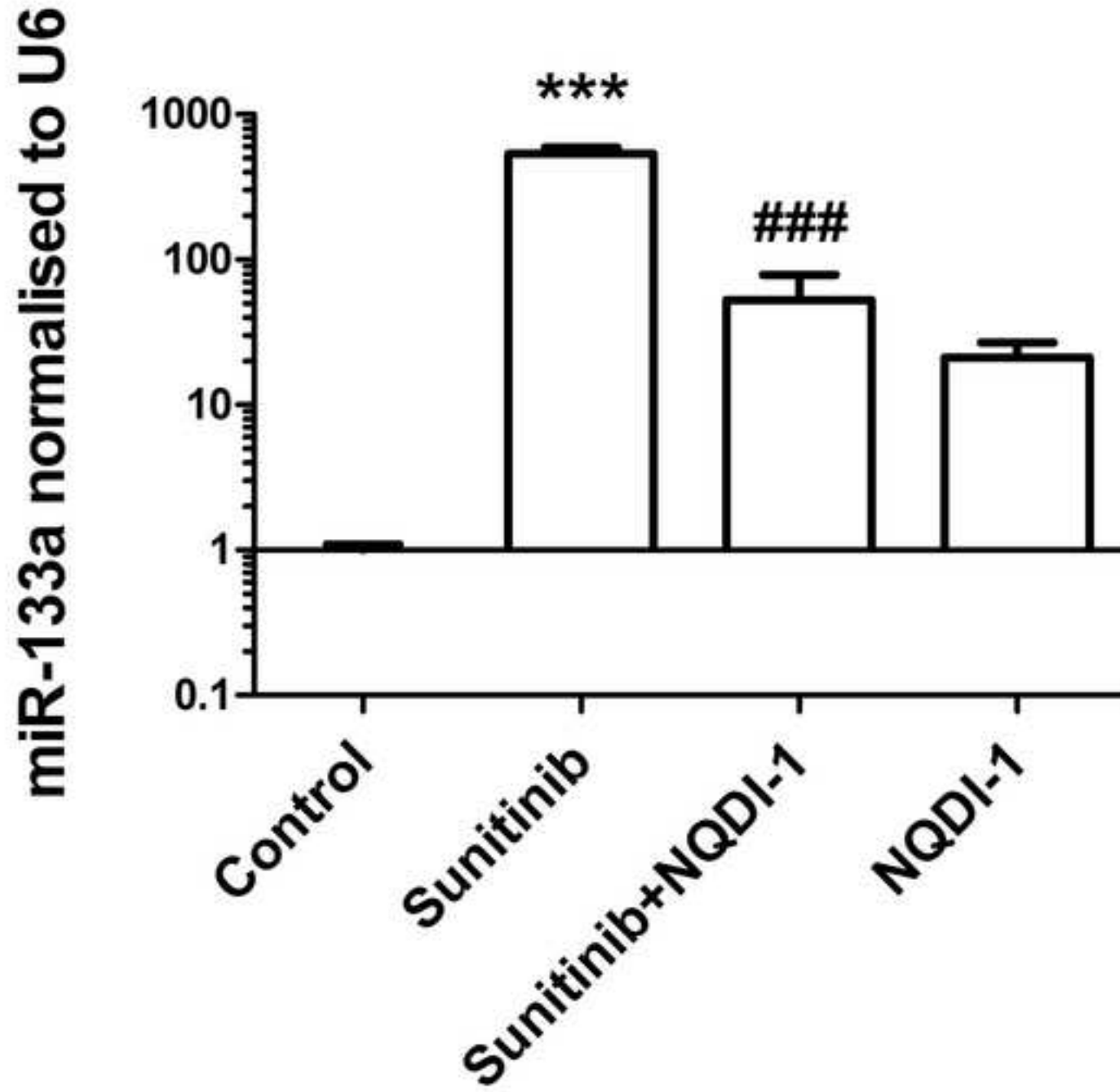


Figure 2D
[Click here to download high resolution image](#)

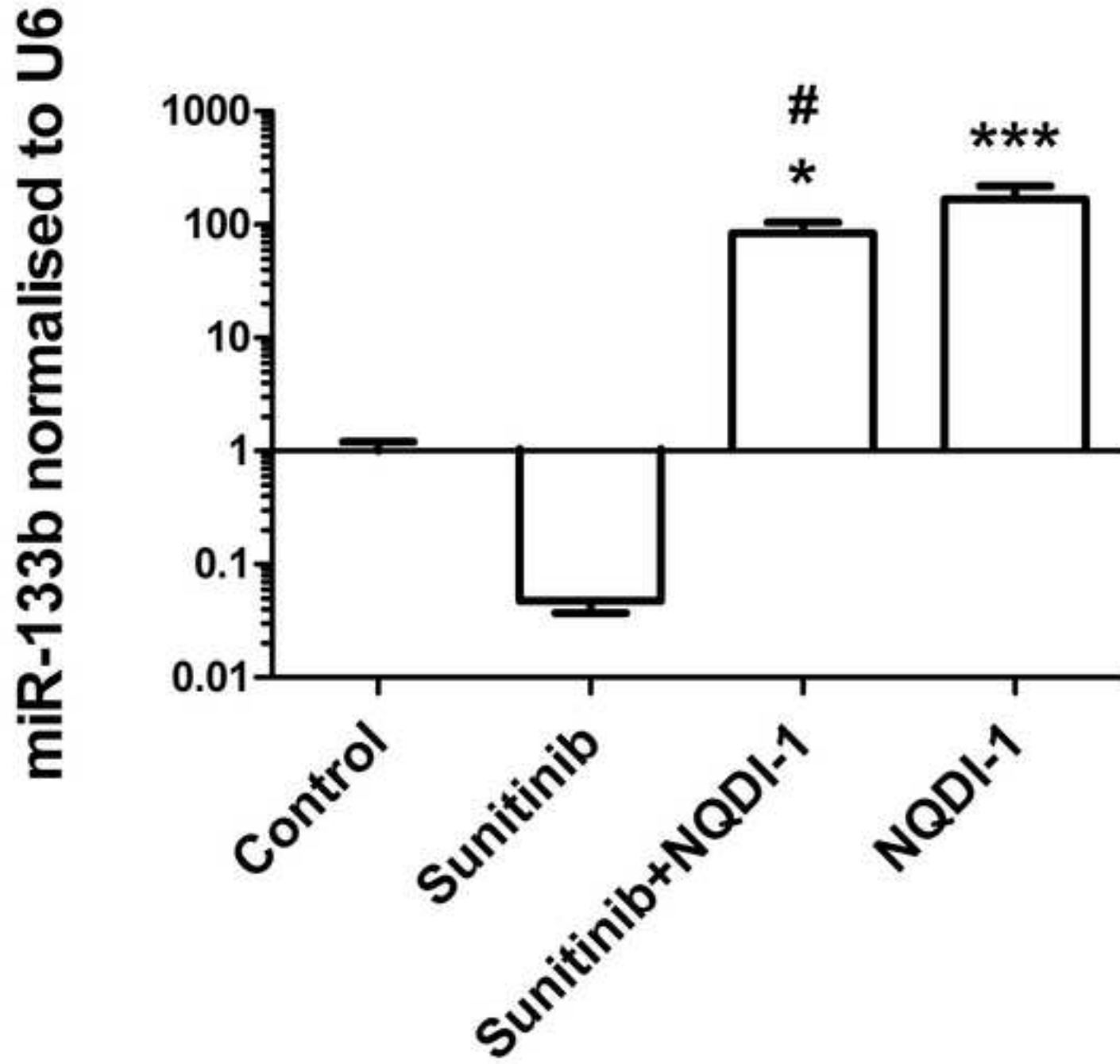
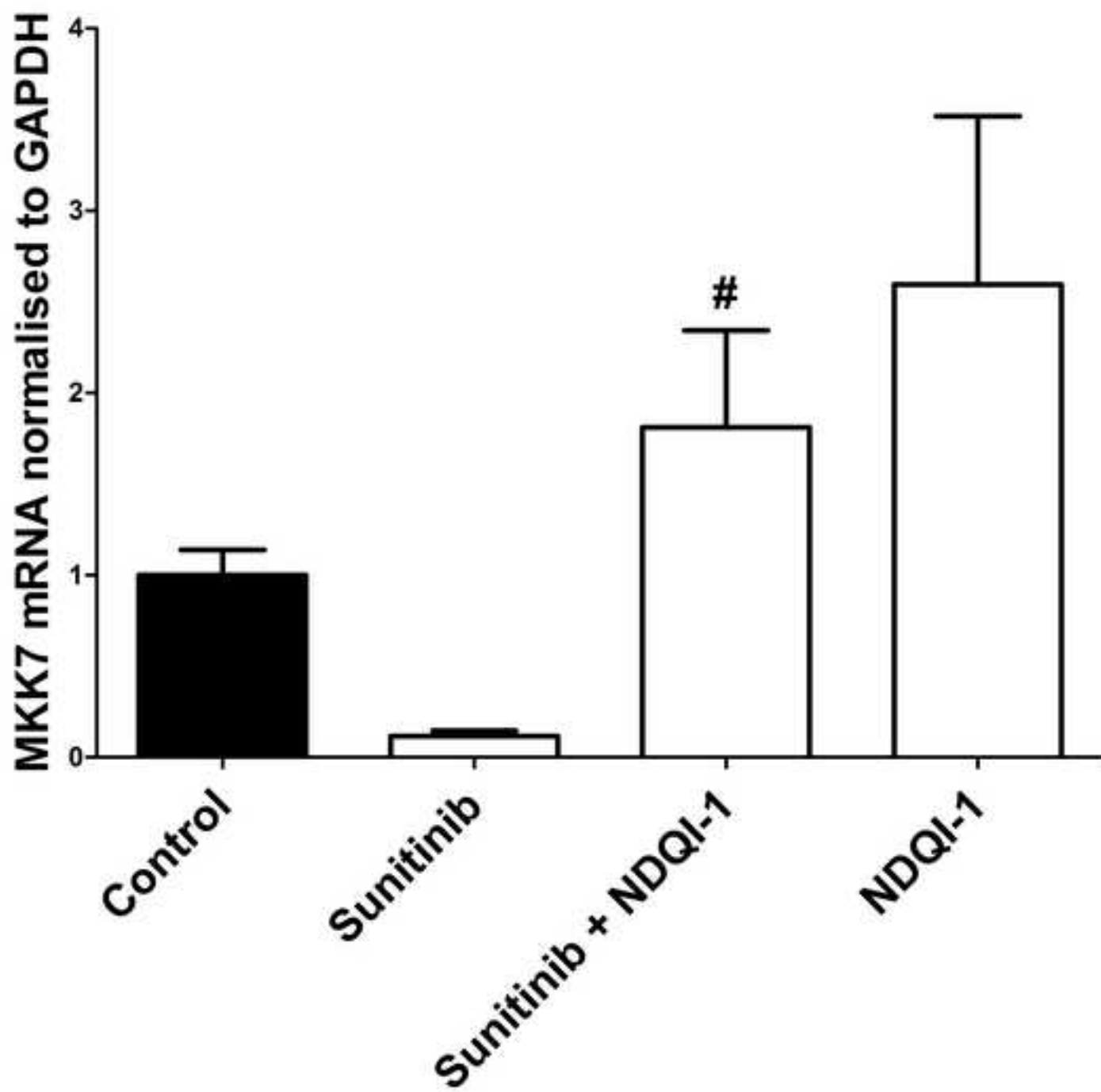


Figure 3
[Click here to download high resolution image](#)



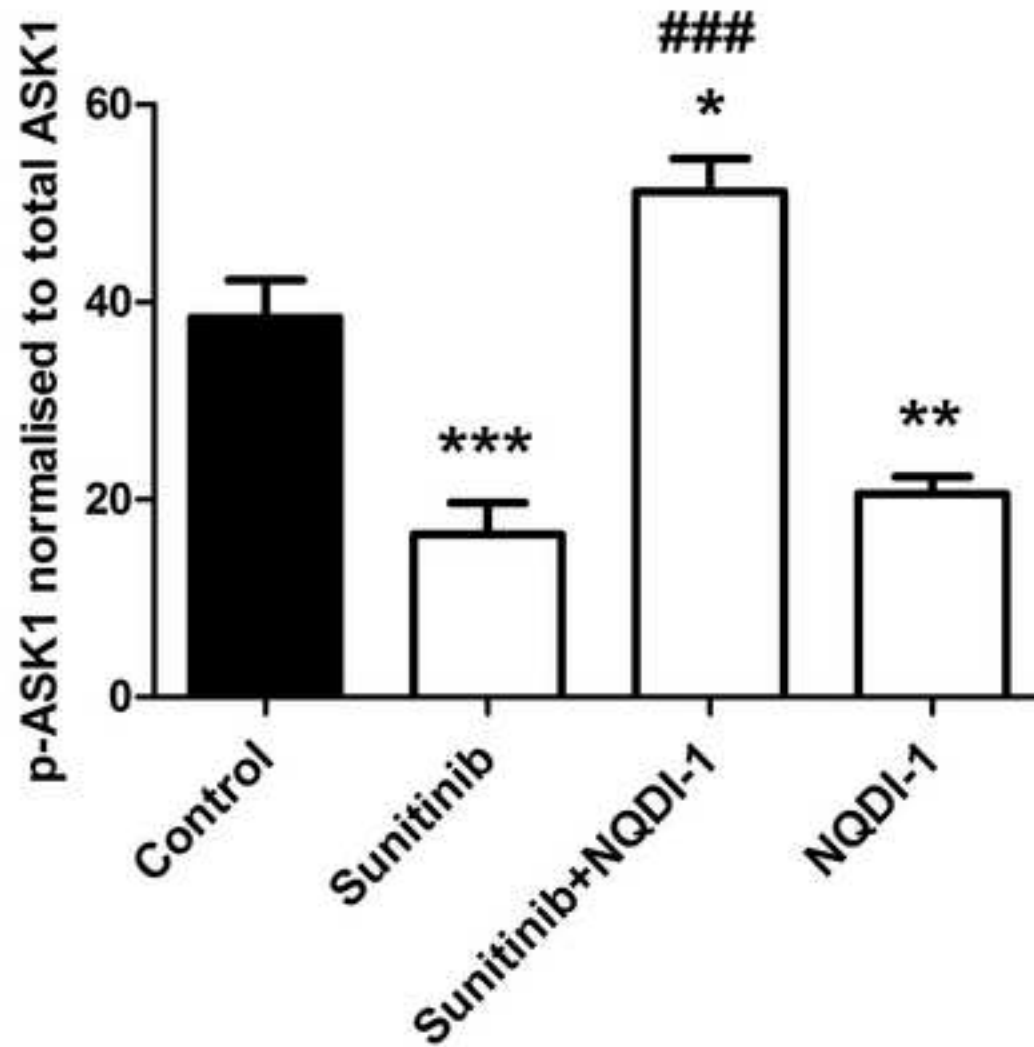
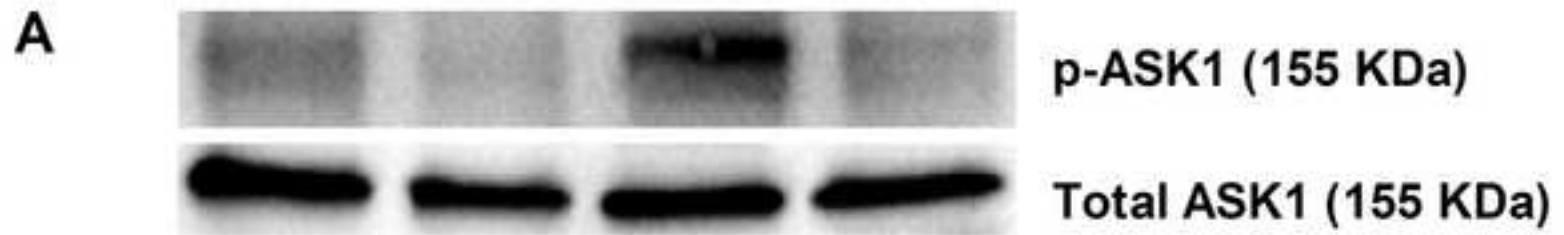
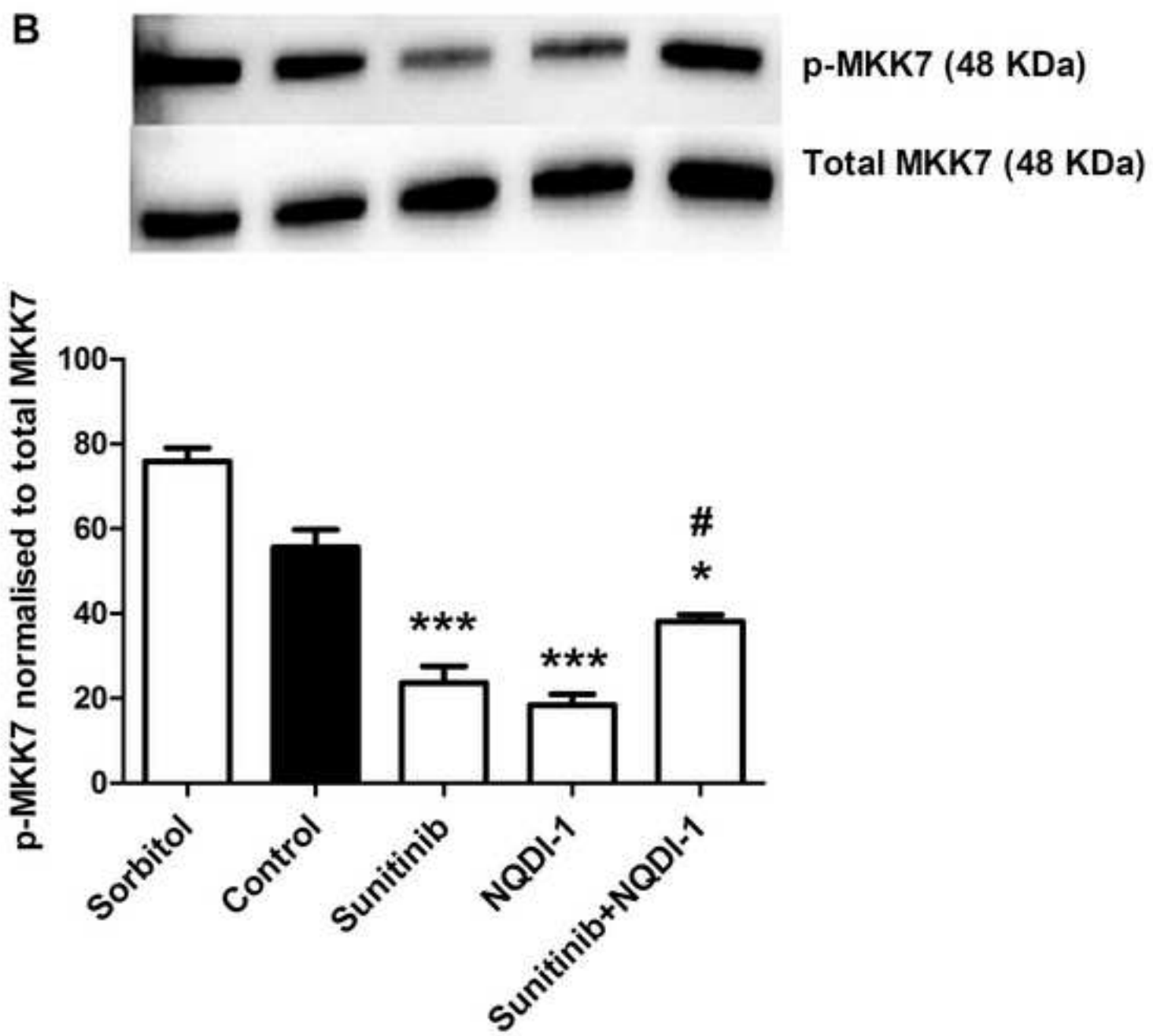


Figure 4B
[Click here to download high resolution image](#)



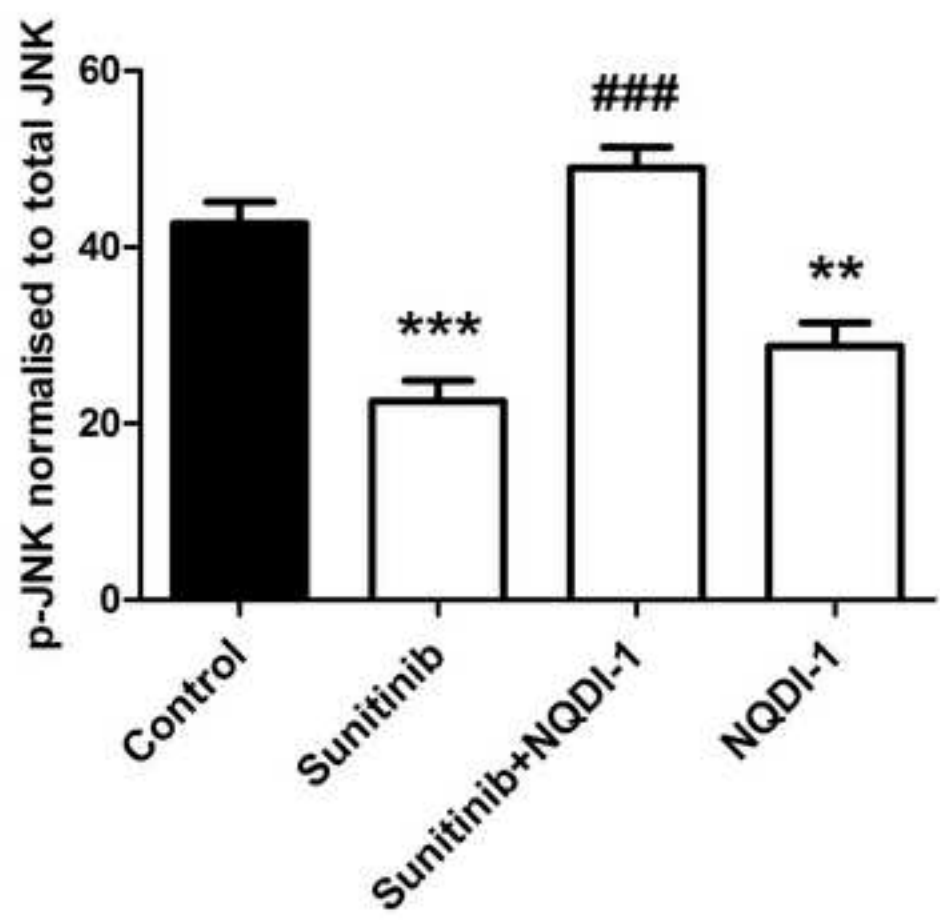
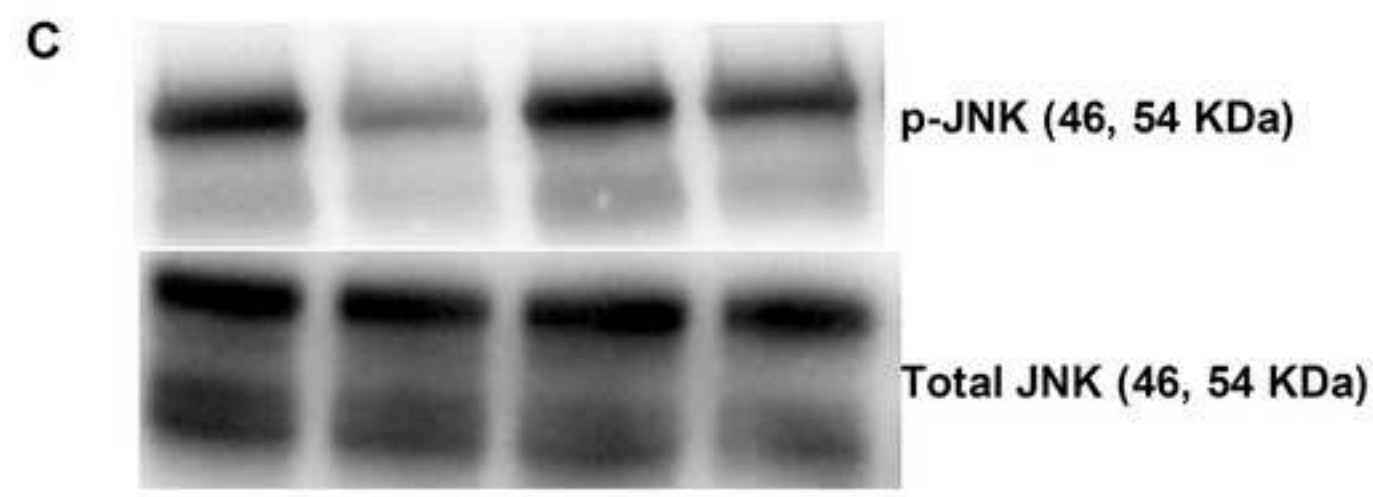


Figure 5A
[Click here to download high resolution image](#)

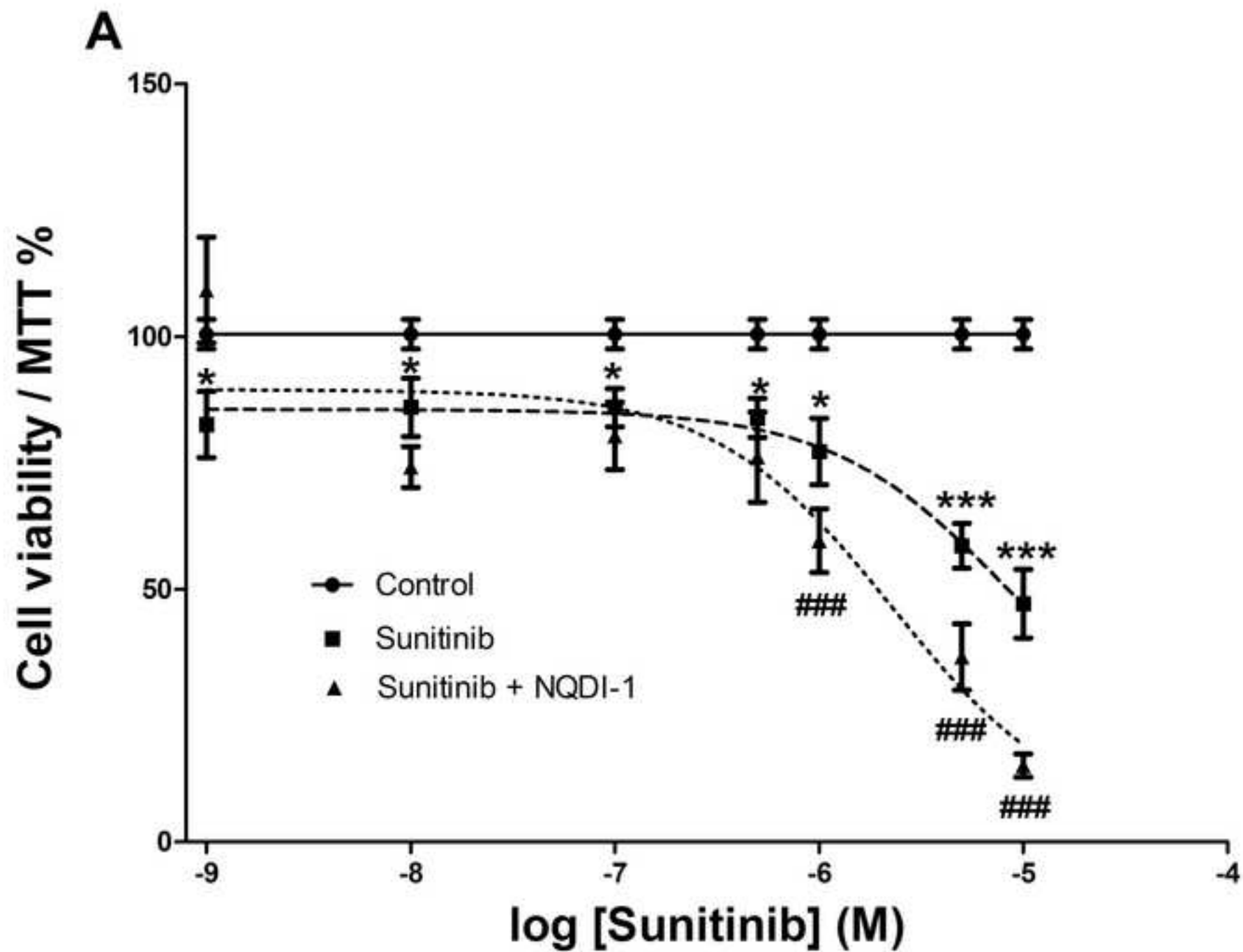
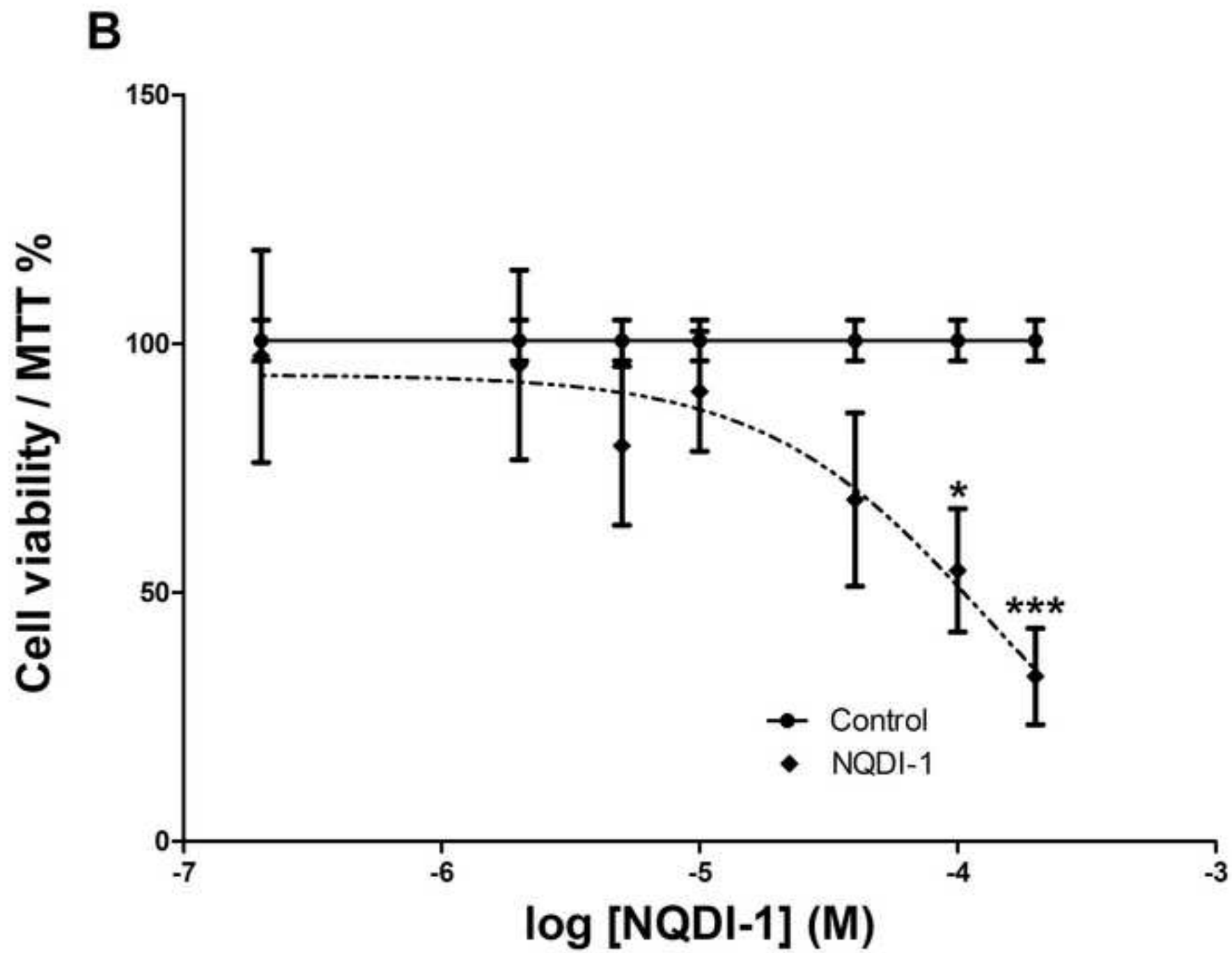


Figure 5B
[Click here to download high resolution image](#)



***Conflict of Interest Statements (per author)**

[Click here to download Conflict of Interest Statements \(per author\): Corresponding_Author_TOX-signed HM.pdf](#)